

Spring 5-2013

Polymers for DNA Binding

Sue Yuan Li

Follow this and additional works at: <https://scholarship.shu.edu/dissertations>

 Part of the [Analytical Chemistry Commons](#), and the [Polymer Chemistry Commons](#)

Recommended Citation

Li, Sue Yuan, "Polymers for DNA Binding" (2013). *Seton Hall University Dissertations and Theses (ETDs)*. 1850.
<https://scholarship.shu.edu/dissertations/1850>

Polymers for DNA Binding

*This dissertation is submitted to the faculty of the Department of
Chemistry and Biochemistry in the Graduate School of Arts and
Science in partial fulfillment of requirements*

for the degree of

Doctor of Philosophy

At

SETON HALL UNIVERSITY

400 South Orange Avenue

By

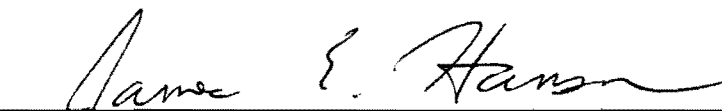
Sue Yuan Li

May 2013


CERTIFICATION

We certify that we have read this thesis and that in our opinion it is adequate in scientific scope and quality as a dissertation for the degree of Doctor of Philosophy.


APPROVED



James Hanson, PhD. Research Advisor



Wyatt R. Murphy Jr., PhD.



Yufeng Wei, PhD.



Steven Kelty, PhD
Chairman, Seton Hall University Department of Chemistry and Biochemistry

DEDICATION

This dissertation is dedicated to my parents for their unconditional love to me.

ACKNOWLEDGEMENTS

It has been a long journey for me to complete this study. There are many people who played an important role and accompany me through this journey.

First, I would like to thank GOD –for HIS unending love which provides me the strength, persistence and endurance to run for the finish line.

I would like to give my sincere thanks to my mentor Dr. James Hanson. This dissertation would not have been possible without his help, guidance and supervision. My special thanks go to Dr. Rory Murphy, Dr. Yufeng Wei for their time, help and assistance in reviewing my dissertation and suggestion in scientific discussions. I would also like to take this opportunity to thank Dr. Wei for his help in NMR studies. I thank Dr. Cecilia Marzabadi and Dr. Cosimo Antonacci for their invaluable discussions, suggestions and help in many ways. Special thank for Rose Mercadante for her love, friendships and encouragement. I thank all people from Dr. Hanson's group for their help, discussions, sharing and warm friendships when I worked in the laboratory. Last but not the least, my deepest gratitude and thanks are due to the Chemistry and Biochemistry faculty and staff for their assistance in needs.

Most importantly, I wish to share this accomplishment to my parents for their support, understanding, encouragement and prayers during the time of my study and working. I also want to thank my sister and brothers for their concern and support over many years.

Finally, I would like to thank all my friends for their friendships and prayers whenever I need it. I would like to extend my gratitude to Fr. Lawrence Frizzell for his guidance and friendship since I studied in Seton Hall University.

TABLE OF CONTENTS

Dedication	iii
Acknowledgements	iv
Abstract	1
1. Introduction	5
1.1 Polymers as non-viral nucleic acid vehicles	5
1.2 Polymers and Quadruplex DNA Interaction	7
2. Historical	10
2.1 Polymers.....	10
2.1.1 Neutral polymers	10
2.1.2 Cationic Polymers	13
2.1.3 Polyethylenimine (PEI).....	14
2.1.4 Cross-Linking.....	18
2.1.5 Cross-Linking Polymers	18
2.1.6 Amine-Aldehyde Reaction	19
2.1.7 Pre-Screening Polymer Candidates for Nucleic Acid Delivery System.....	19
2.2 DNA Structure and Function	20
2.2.1 Nitrogen Bases, Nucleosides, and Nucleotides	20
2.2.2 Deoxyribonucleic Acid (DNA)	23
2.2.2.1 History of the DNA	23
2.2.2.2 Base Pairing Role in Nucleic Acid Structures	24
2.2.2.3 Tautomerization of DNA Bases	27
2.2.3 DNA Structure	30
2.2.3.1 Alternative DNA Conformation	31
2.3 DNA, Telomeres and Telomerase.....	37
2.3.1 Mechanism of Gene Delivery System	37
2.3.2 DNA Replication.....	39
2.3.3 Telomeres and Telomerase	41
2.3.4 Telomerase and Aging	43
2.3.5 Telomerase and Cancer	43
2.3.6 Quadruplex DNA	44
2.3.7 Quadruplex Structure	45
2.3.8 G-Quadruplex Architectures	47

2.3.9	The Stability of Quadruplex Structures-----	56
2.3.10	The Biological Role of the G-quadruplex DNA-----	57
2.3.11	Porphyrim Chemistry -----	58
3	Instrumentations -----	61
3.1	Spectroscopy -----	61
3.1.1	Quasi-Elastic Light Scattering / Dynamic Light Scattering -----	62
3.1.2	Theory-----	63
3.2	Nuclear magnetic resonance (NMR) -----	69
3.2.1	³¹ P NMR and ¹ H NMR-----	69
3.2.2	Diffusion NMR -----	70
3.2.3	¹ H NMR: Diffusion Experiment-----	71
3.2.4	Nuclear Overhauser Effect Spectroscopy (NOESY) -----	74
3.3	Ultraviolet-Visible Spectroscopy (UV/Vis) -----	75
3.4	Circular Dichroism (CD) -----	78
3.4.1	Basic Theory -----	78
4	Material and Methods-----	83
4.1	Materials -----	83
4.1.1	Buffer Solutions -----	84
4.2	Methods -----	85
4.2.1	DNA Preparation -----	85
4.2.1.1	Dialysis Procedure-----	85
4.2.1.2	Quadruplex DNA Preparation -----	85
4.2.2	Polyethylenimine Intra-Molecular Cross-Linking -----	87
4.2.2.1	Intra-molecular cross-linking (in solution) -----	87
4.2.3	Cross-Linking Examined by NMR Experiment -----	87
4.2.4	<i>In Situ</i> Study-----	87
4.2.5	Identify the Intra- Molecular Cross-Linking by Organic Solvent Extraction and Examined by UV-Vis -----	88
4.2.5.1	UV-Vis Experiment-----	88
4.2.5.2	Intermolecular Cross-Linked PEI: bulk preparation-----	89
4.2.6	Characterization of Particle Size by Light Scattering (QELS) -----	89
4.2.7	PEI / Quadruplex DNA Circular Dichroism Study -----	90
4.2.8	Polymers Screen Using UV-Vis Spectroscopy Studies -----	92
4.2.9	³¹ P NMR Study: Binding Interaction of Quadruplex DNA / Polymer -----	93
4.2.10	Diffusion NMR Experiment -----	93
4.2.10.1	Sample preparation -----	93
4.2.10.2	Experiment condition -----	94
4.2.11	PEI and Quadruplex DNA Complex Structural Transition Study by CD -----	95

5	Results and Discussion -----	96
5.1	Molecular Cross-Linking Studies -----	96
5.1.1	¹ H NMR investigates PEI cross-linking-----	96
5.1.2	UV-Vis/Extraction Experiments to Identify the Cross-linking Reaction -----	99
5.2	Light Scattering Analysis of Aggregation Behavior -----	106
5.2.1	Cross-Linking Hydrodynamic Radius Measurement by QELS-----	107
5.3	Binding Study of Polyethylenimine/ Quadruplex DNA -----	111
5.3.1	Circular Dichroism (CD) Titration Experiments -----	113
5.4	Porphyrin/ Quadruplex T ₄ G ₄ DNA / Polymers Interaction Study by UV-Vis--	118
5.5	³¹ P NMR Polymer - Quadruplex DNA Binding Study-----	124
5.6	DOSY: Diffusion NMR Experiments -----	127
5.7	PEI Induced Conformational Change in Quadruplex DNA T ₄ G ₄ : 2D NOESY NMR and CD Experiments-----	135
5.8	Circular Dichroism Experiment of the PEI and quadruplex (T ₄ G ₄) DNA: Structural Transition Investigation -----	142
6.	Summary, Conclusion and Further Study -----	148
6.1	Summary and Conclusion-----	148
6.2	Suggested Further Studies -----	152
	Reference -----	153

LIST OF ABBREVIATION

1. CD	Circular Dichroism
2. DNA	Deoxyribonucleic Acid contain nucleobases G, A, T, C
3. RNA	Ribonucleic Acid contain nucleobases G, A, U, C
4. GC, AT	DNA base pairing, nucleobases (G, C and A, T)
5. A-DNA	A Form DNA
6. B- DNA	B Form DNA
7. Z-DNA	Z-form DNA
8. PEI	Polyethylenimine
9. KPBS	Potassium phosphate buffer solution
10. 10X KPBS	10 times concentrate Potassium phosphate buffer solution
11. NMR	Nuclear magnetic resonance
12. ³¹ P NMR	31 Phosphorus NMR
13. ¹ H NMR	Proton NMR
14. NOESY	Nuclear Overhauser Effect Spectroscopy
15. DOSY	Diffusion Ordered Spectroscopy
16. UV/Vis	Ultraviolet-Visible Spectroscopy
17. MWCO	Molecular weight cut off
18. T ₄ G ₄	TTTTGGGG
19. TMPyP ₄	meso-5-10-15-20-Tetrakis (N-methyl-4-pyridyl) porphyrin
20. PVC	Poly (vinyl chloride)
21. PVP	Polyvinylpyrrolidone
22. PVPP	Polyvinylpolypyrrolidone
23. PVP _y NO	Poly(4-vinylpyridine-N- oxide)
24. PVMP Br	Poly(4-vinyl-1-methylpyridinium) bromide
25. PEG	Polyethylene glycol
26. FDA	Food and Drug Administration
27. M _w 22K, 25 K	Molecular weight 22,000 and 25,000
28. λ _{max}	Maximum wavelength
29. D ₂ O	Deuterium oxide
30. DLS	Dynamic Light Scattering
31. QELS	Quasi-Elastic Light Scattering
32. D	Diffusion coefficient
33. 2-D NMR	Two-dimensional nuclear magnetic resonance spectroscopy
34. PGSE	Pulsed Gradient Spin Echo
35. PFG-SSE	Pulsed Field Gradient Stimulated Spin Echo
36. BPP-LED	Bipolar pulse longitudinal eddy current delay

LIST OF TABLE

Table 1: A-Form, B-Form and Z-Form Geometry Comparison-----	33
Table 2: Potassium Phosphate Buffer (KPBS) 10 X Stock Solution -----	84
Table 3: Summary of the PEI/ Isophthalaldehyde Cross-linking Reaction -----	97
Table 4: Summary the pre-extraction of PEI / Isophthalaldehyde from 1:1 to 16:1 (Isophthalaldehyde $\lambda_{\text{max}}= 294\text{nm}$) -----	101
Table 5: Summary of the UV-Vis absorption for Isophthalaldehyde extracted by Dichloromethane at different PEI / isophthalaldehyde -----	105
Table 6: Percentage Remaining of Isophthalaldehyde: the mixture of PEI and Isophthalaldehyde after extraction by the dichloromethane -----	105
Table 7: Polyethylenimine (in water) Hydrodynamic Radius as a function of the Concentration -----	106
Table 8: Low concentration of PEI (0.1M) Titrated with Isophthalaldehyde (0.004M) in Phosphate Buffer pH7.0 -----	109
Table 9: High Concentration of PEI (1.8M) Titrated with Isophthalaldehyde (0.004M) (in phosphate buffer, pH 7.0) -----	110
Table 10: Parallel Quadruplex DNA (T ₄ G ₄) (250 μ L) Titrated with Pre-Mixed (PEI/10x DNA), A positive maximum peak in the vicinity of 265-270nm---	116
Table 11: Porphyrin Probe Screening of Candidate Polymers -----	123

LIST OF FIGURE

Chapter2

Figure 2.1:	Chemical Structure of the Polyvinylpyrrolidone-----	11
Figure 2.2:	Structure of Portion Polymers in the Study-----	12
Figure 2.3:	Chemical Structure of Poly (4-vinyl-1-methylpyridinium) bromide and Polyethylene glycol (PEG) -----	14
Figure 2.4:	General Structure of PEI with Primary, Secondary and Tertiary Amines--	17
Figure 2.5:	Branched Polyethylenimine -----	17
Figure 2.6:	Condensation of Anionic DNA with Cationic PEI -----	17
Figure 2.7:	Major Purine and Pyrimidine Bases -----	21
Figure 2.8:	The Formation of Polynucleotide -----	23
Figure 2.9:	Watson-Crick Base Pairing-----	26
Figure 2.10:	Difference between Watson –Crick and Hoogsteen Base Pairing -----	27
Figure 2.11:	Tautomers of Nucleobases-----	29
Figure 2.12:	Typical Double Strand Formation -----	31
Figure 2.13:	B-DNA Base Angle Orientation-----	32
Figure 2.14:	B and Z Form DNA Double Helix Conformations -----	35
Figure 2.15:	Triplex DNA-----	36
Figure 2.16:	Cellular Uptake via an Endocytic Pathway-----	37
Figure 2.17:	DNA Replication Fork-----	39
Figure 2.18:	The Steps of the DNA Replication -----	41
Figure 2.19:	G-tetrads and G-Quadruplex Structure -----	46
Figure 2.20:	Examples of Various Strand Stoichiometries of G-Quadruplex Structures-	48
Figure 2.21:	Unimolecular: Different way of Strand Loop Connectivity for Guanine Tetrad Structure (A, B, C) -----	49

Figure 2.22: Bimolecular: Strand Loop Connectivity to form Various Guanines Tetrad Structures (A, B, C, D, E) A-DNA, B-DNA and Z-DNA-----	49
Figure 2.23: Strand Polarity Arrangements in G-Quadruplex Structures -----	50
Figure 2.24: Example of the Syn/Anti Conformation Structure by the Rotation of the Glycosidic Bond-----	51
Figure 2.25: Depiction of the G-Quadruplex DNA Structures: Example of the Parallel and Anti- Parallel-----	52
Figure 2.26: Two Pairs of Adjacent Parallel Strands-Create two Medium Grooves-----	53
Figure 2.27: The Alternating Anti-Parallel Strands: Generate two Medium and two Narrow Grooves-----	53
Figure 2.28: Structures of G-Quadruplexes. Schematic Representation of G-Quadruplex Structure-----	54
Figure 2.29: Examples of Inter- and Intramolecular Quadruplex DNA Conformation --	55
Figure 2.30: The Chemical Structure Porphyrin and Derivate -----	60
Chapter 3	
Figure 3.1: Electromagnetic Spectrum-----	61
Figure 3.2: Schematic Diagram of a Conventional, 90 ⁰ Dynamic Light Scattering Instruments-----	64
Figure 3.3: Example of Autocorrelation Function of the Scattered Light-----	68
Figure 3.4: Example of the ¹ H NMR: Diffusion Experiment-----	72
Figure 3.5: Diagram of Visible Spectrum Wavelength (400nm -800nm) -----	76
Figure 3.6: Diagram of the electron transition between the bonding, non-bonding and anti-bonding -----	76
Figure 3.7: A Diagram of a Double Beam Spectrometer -----	78
Figure 3.8: Elliptical Polarization -----	80
Figure 3.9: Example of the Left-Handed and Right-Handed Ellipticity (θ) -----	81
Figure 3.10: Example of Typical Reference Spectra of Single Strand and Duplex	

DNA -----	82
Figure 3.11: Typical Reference Spectra of Parallel and Anti-Parallel Quadruplex DNA-----	82

Chapter5

Figure 5.1: ¹ H NMR of Isophthalaldehyde -----	98
Figure 5.2: ¹ H NMR of Polyethylenimine-----	98
Figure 5.3: ¹ H NMR of Isophthalaldehyde and Polyethylenimine immediately after Mixing-----	99
Figure 5.4: ¹ H NMR of Isophthalaldehyde and Polyethylenimine -Two hours Time Point-----	99
Figure 5.5: PEI/ Isophthalaldehyde in Variety Ratio Study by UV-Vis-----	102
Figure5.6: Polyethylenimine and Isophthalaldehyde extracted by Dichloromethane-----	104
Figure 5.7: Polyethylenimine (in water) Radius in different Concentration-----	107
Figure 5.8: Isophthalaldehyde (0.004M) Titrated into Low Concentration of Polyethylenimine (0.1M) -----	110
Figure 5.9: Isophthalaldehyde (0.004M) Titrated into 1.8M PEI (both prepare in Phosphate Buffer Solution at pH 7.0)-----	111
Figure 5.10: CD Spectrum of Quadruplex T ₄ G ₄ DNA (Parallel) -----	112
Figure 5.11: CD Spectrum of the Polyethylenimine -----	112
Figure 5.12: 10x PEI/Quadruplex DNA pre-mixed Solution with 1 μL each addition titrated into T ₄ G ₄ Quadruplex DNA Solution (250 μL) -----	114
Figure 5.13: Pre-mixed (T ₄ G ₄) ₄ /PEI Titrated into Quadruplex DNA (250μL) -----	115
Figure 5.14: Quadruplex (T ₄ G ₄) DNA/PEI Solution Stability -----	117
Figure 5.15: Polyethylenimine interaction with Porphyrin-Quadruplex DNA Complex-----	119
Figure 5.16: Cross-linked Polyethylenimine interaction with Porphyrin-Quadruplex DNA Complex -----	120

Figure 5.17: Poly (4-Vinyl-1-Methylpyridinium Bromide) interaction with Porphyrin/Quadruplex DNA Complex -----	120
Figure 5.18: Polyethylene Glycol (PEG) interaction with Porphyrin/Quadruplex DNA Complex -----	121
Figure 5.19: Poly (N-vinylpyrrolidone) interaction with Porphyrin- Quadruplex DNA Complex -----	121
Figure 5.20: Poly(4-vinylpyridine N-oxide) interaction with Porphyrin-Quadruplex DNA Complex -----	122
Figure 5.21: ³¹ P NMR Spectra of (TTTTGGGG) ₄ , free and in the presence of Poly(4-Vinylpyridine N- oxide), Polyethylenimine and Poly (N-vinylpyrrolidone) -----	126
Figure 5.22: ³¹ P NMR Spectra of (TTTTGGGG) ₄ , and with Poly(4-Vinylpyridine N-oxide), Polyethylenimine and Poly(N-Vinylpyrrolidone) with increased Concentration of Poly(N-Vinylpyrrolidone) and Poly(4-Vinylpyridine – N–Oxide) -----	127
Figure 5.23: DOSY NMR Experiment Study Binding Relationship of Quadruplex (T ₄ G ₄) DNA alone (black) and with Poly (N-Vinylpyrrolidone) (PVP) at the ratio of 1:1 (blue), 1:5 (red) and 1:10 (green) -----	129
Figure 5.24: ³¹ P Diffusion DOSY Experiment of Quadruplex T ₄ G ₄ alone (black) and with Poly (Vinylpyridine N-Oxide) (PVNO) (red) -----	130
Figure 5.25: ³¹ P DOSY Experiment for Quadruplex DNA, (T ₄ G ₄) ₄ / PVNO at 1 to 5 ratio and (T ₄ G ₄) ₄ /PEG at 1 to 5 ratio-----	132
Figure 5.26: ¹ H DOSY Experiment for Quadruplex DNA (T ₄ G ₄) alone (black) and DNA/PEI at Ratio of 1:5 (blue) -----	134
Figure 5.27: A 2D NOESY Spectrum of G-Quadruplex T ₄ G ₄ Parallel Structure -----	136
Figure 5.28: 2D NOESY spectrum of G-Quadruplex (T ₄ G ₄) DNA and PEI at 1 to1 Molar Ratio -----	137
Figure 5.29: 2D NOESY Spectrum of G-Quadruplex T ₄ G ₄ DNA and PEI at 1 to 5 Molar Ratio -----	138
Figure 5.30: Imino-imino and Imino-amino regions of the NOESY Spectra for Parallel T ₄ G ₄ Quadruplex DNA (A) and T ₄ G ₄ DNA with PEI 1:5 (B) -----	139

Figure 5.31: Aromatic H6/H8 to sugar H1' region of the NOESY Spectra for Parallel T ₄ G ₄ Quadruplex DNA (A) and T ₄ G ₄ DNA with PEI 1:5 (B) -----	141
Figure 5.32: Aromatic H6/H8 to thymine methyl region of the NOESY Spectra for Parallel T ₄ G ₄ Quadruplex DNA (A) and T ₄ G ₄ DNA with PEI 1:5 (B) ---	142
Figure 5.33: CD Spectra of the Quadruplex DNA alone and with PEI at 1 to 1 and 1 to 5 Molar Ratio at the initial Time Point -----	143
Figure 5.34: CD Spectra of the PEI/Quadruplex DNA (5 to 1 molar ratio) Structural Transition Profile in Different Time Point -----	145
Figure 5.35: CD Spectra of Hybrid G-Quadruplex DNA in the presence of the Potassium, Sodium and Ammonium Cation -----	145
Figure 5.36: CD Spectra of the Transition from the Antiparallel to the Parallel G-quadruplex -----	146

LIST OF EQUATION

Equation 1:	Autocorrelation Function -----	65
Equation 2:	Decay of Autocorrelation Function -----	65
Equation 3:	Monodisperse Particles: Correlation Function -----	65
Equation 4:	Polydisperse Particles: Correlation Function -----	66
Equation 5:	Decay Constant -----	66
Equation 6:	Diffusion coefficient (D) -----	66
Equation 7:	Frequency of the scattering light -----	67
Equation 8:	Stokes-Einstein equation -----	67
Equation 9:	Diffusion Coefficient $D=KT/f$ -----	72
Equation 10:	Friction Coefficient $f=6\pi \eta R_D$ -----	73
Equation 11:	Attenuated Signal (A) -----	74
Equation 12:	$-\ln (A/A_0) =G^2g^2d^2 (T-d/3) D$ -----	74
Equation 13:	Beer –Lambert law -----	77

ABSTRACT

The main goal of this study was to discover polymer candidates which can cross-link and as an imprinted template with quadruplex structures for nucleic acid applications such as recognition and transfection. Nucleic acids are classified as macro-biopolymers which are central to the functioning of organisms. Nucleic acid polymers have many applications in different fields such as biotechnology, medicine and nanomaterials. One application, gene therapy, can provide great opportunities for treating diseases from genetic disorders to cancer. Polymers are one non-viral delivery vector for gene therapy. Cationic polymers have advantages in gene delivery and appear to have promising potential in the treatment of diseases.

Polyethylenimine (PEI), a commercial cationic polymer, is available in bulk quantities. PEI has been widely used for non-viral transfection *in vitro* and *in vivo* and also been proven to be an efficient vector for use in gene delivery and other biological areas. Isophthalaldehyde, a cross-linker, was found to be effective in use with PEI. In an attempt to make cross-linked PEI nanoparticles for nucleic acid gene delivery, we cross-linked branched (25K) PEI with isophthalaldehyde. *In situ* ^1H NMR, QELS light scattering and UV-Vis data are in agreement with the cross-linking of polyethylenimine with isophthalaldehyde and could form either inter- or intra-molecular cross-links. In a relatively dilute solution, the cross-linking reaction condenses the polymer molecules only by intra-molecular cross-linking.

There are growing interests in quadruplex DNA research. Quadruplex DNA is a higher order DNA structure found in guanine rich chromosome end (telomere) regions and in promoter regions. Interest in quadruplex DNA has advanced considerably due to its utilization in cancer treatments. We looked for polymers which can bind to quadruplex DNA without disrupting the quadruplex structure. The d(T₄G₄) repeated sequence can fold into quadruplex structure in its telomere region and has been found in a living organism (*stylonychia*). The synthetic DNA sequence of (TTTTGGGG)₄, (32-bps), was used in this study. We have studied the interaction of PEI with quadruplex T₄G₄ DNA by circular dichroism, UV, and NMR.

It is known that the PEIs (cationic polymers) were shown to interact with quadruplex DNA. Our CD spectroscopy results suggested that PEI might disrupt the quadruplex DNA and converted it into a hybrid or unknown structure. However, it is currently unclear what the structure of the quadruplex DNA was.

Our ultimate aim is to be able to find the suitable polymer for our imprinted model in DNA researches. Porphyrins are known to successfully bind to quadruplex structures. Toward this goal, we have used cationic tetrapyrrolyl porphyrin (TMPyP₄) as a probe to screen the interaction of the quadruplex DNA with different categories of polymers.

Here, we have found that the UV-Vis binding interaction of porphyrin, polymers and quadruplex DNA have shown that the Soret bands of the porphyrins changed drastically upon addition of quadruplex DNA, with bathochromic shifts (to longer wavelength). By addition of polymers into porphyrin / quadruplex complex, the Soret band was observed to shift to different position as a function of polymer structure.

Our UV-Vis data have revealed that the cationic polymer (e.g. PEI) might disrupt quadruplexes DNA or alter it to an unknown or hybrid structures; the neutral polymers might associate with quadruplex DNA without structural disruption. However, the ^{31}P NMR studied showed only a weak binding or non-binding interaction for poly (4-vinylpyridine N-oxide) and poly (N-vinylpyrrolidone) with quadruplex DNA. These results motivate us for further investigation of the neutral polymers.

Dissertation Structure

This dissertation is organized in the following order: An introduction to the research is presented in Chapter 1; an historical overview is given in Chapter 2; the theory of the methodologies are given in Chapter 3; materials and experimental methods are in Chapter 4, results and discussion are given in Chapter 5; and Chapter 6 is comprised of the conclusion and possible future work, followed by references.

CHAPTER 1 INTRODUCTION

1.1 Polymers as non-viral nucleic acid vehicles

Cancer has become the number one killer in developing countries and is moving toward being the number one cause of death in industrialized countries.¹ Because of the aggressive growth of tumor cells, and the complex mechanism in cancer developments, standard treatments are not sufficiently effective in many cases.² Therefore, the search for new anticancer strategies becomes urgently required. In this regard, a better understanding of the relationship between growing cancer cells and genes led researchers to search for new approaches for treatments. The growing interest in gene therapy has become an attractive concept in recent years because it provides a promising tool for treating the tumor cells.³⁻⁴

In past decades, gene therapy has emerged as a powerful, new therapeutic intervention for gene-related diseases and has gained increasing attention in medicine, biotechnology and the pharmaceutical sciences.⁵ DNA is the hereditary material in all living organisms. An efficient gene carrier is required to be able to deliver the genetic material into target cells. The efficiency and safety for a specific delivery of therapeutic genes remains an important bottleneck for the development of gene therapy. To date, developing a stable and efficient delivery system is still a major challenge. The key considerations for the development of gene therapy strategies are to improve the efficiency and safety of genes after their administration into the body. Gene delivery systems are currently under investigation for both viral and non-viral carriers.⁶

The limitations of viral vectors and cellular barriers (extracellular/ intracellular) are the critical issues for gene delivery. There is a need for development of an appropriate

delivery system to enhance efficiency.⁷⁻⁹ The viral carriers can produce efficient gene expression but have high immunogenicity issues.¹⁰ The virus gene carrier also has drawbacks in the size capacity of therapeutic DNA and difficulty in targeting specific cell types. Although virus carriers are efficient gene delivery agents, a high death toll in clinical trials has been reported over the past decades.¹¹⁻¹² The attempt to achieve successful gene therapy has led to the evaluation and development of alternative vectors.

Synthetic non-viral systems have showed an interesting pharmaceutical profile with potential advantages for certain applications.¹³⁻¹⁸ The non-viral delivery systems have become one of the alternative methods because of their favorable gene delivery characteristics such as low immunogenicity, less size limitation, increased cost efficiency and facility of modification.¹⁹

Non-viral carriers are mainly found in three categories: naked DNA delivery, lipid-based delivery, and polymer-based delivery.²⁰ A wide range of polymeric vectors, most of a cationic nature, have been utilized to deliver therapeutic genes *in vivo*.²¹⁻²² The cationic polymers have been used as possible alternative vectors for viral and liposomal carriers in a gene delivery system.²³⁻²⁴ The advantage of using cationic polymers is that cationic polymers have many different structural elements which can self-assemble with negatively charged nucleic acids via electrostatic interactions to condense the string-like nucleic acids into compact nanoparticles.²⁵

DNA molecules are large domains which can have a wormlike random coil structure. The DNA condensation will decrease the size of the DNA chains into compact, orderly structures by which the genetic information is packaged and protected. DNA

condensation processes enable DNA easily to transfer into the target cells for gene therapy applications. The dominant forces of the DNA condensation are attractive (counterion, cross-linking) forces, hydration forces and repulsion (electrostatics) forces.

The multivalent cation condensation process can provide the free energy which can then stabilize the condensed state of DNA molecules.²⁶ The electrostatic attraction between positively charged cationic polymers and negatively charged DNA results in the formation of the polyplex. In summary, the cationic polymers are known to receive the most attention as potential non-viral gene carriers.

1.2 Polymers and Quadruplex DNA Interaction

James Watson and Francis Crick were the first to discover right-handed double helical DNA structures.²⁷ After a few decades, more polymorphic natural DNA structures have been reported. There is an increasing interest in a number of other DNA forms and their role in biological activities. Four-stranded helical guanine-rich DNA structures, joined by hydrogen bonds through Hoogsteen base pairing to form a planar structure, are of particular interest among the various DNA structures.²⁸

The human telomere with a long 3' overhang of a G-rich strand can adopt an unusual four-stranded structure called a G- quadruplex.²⁹ This quadruplex DNA displays a significant role in the regulation of telomerase activity; due to the inhibition of the enzyme telomerase, the G- quadruplex structures have been considered as a target design for anticancer drugs.³⁰⁻³³

Monovalent cations play an important role in the formation of the quadruplex structures. G-quadruplex formation varies with the cation species. The binding preference

of monovalent cations for G-quadruplex structures is $K^+ > Na^+ > Cs^+ > Li^+$.³⁴ Potassium has significant binding preference over other alkali metal ions due to the following reasons: (A) Ionic radius: potassium has an ionic radius of approximately 1.3 Å which fits well in the guanine tetrads' cavities. (B) Physiological concentrations: physiological conditions provide optimal stability for potassium ions. The potassium ion can induce the formation of the G-quadruplex structure by a slow unfolding reaction.³⁵

The original concept of this research was designed to investigate the possibility for applying polymers using an imprinting model. Traditionally, a polymerization in the presence of a cross-linker is performed to prepare this architecture. This was done by cross-linking the polymer to form a template which interacts with the nucleic acid (DNA) and formed a complex. The imprinted template is removed from the polymer by melting or dialysis of the DNA and leaves behind the specific binding site to serve as a “lock and key”.³⁶⁻³⁷

Cationic polymers are well documented in many studies for binding to anionic DNA to provide the control release of DNA polyplexes.³⁸⁻⁴⁰ We examined polycationic polymers as potential candidates because the electrostatic interactions between the negative charge of the nucleic acid and positive charge of the polycation will attract each other. Our interest has focused on one of the cationic polymers- polyethylenimine (PEI). PEI has been used as a non-viral gene delivery system for many years.⁴¹

Our experiments identified that one of the cross-linkers, isophthalaldehyde (an aromatic dialdehyde), was able to cross-link with PEI to form nanoparticles. The interaction between polymers and DNA has been studied by many researchers.^{37-38, 42} We are interested in how the polyethylenimine condensed with the quadruplex DNA, and

any conformational changes of the DNA induced by the interaction with the quadruplex DNA.

Structure of Isophthalaldehyde



Cationic porphyrins have been noted for their ability to bind and to stabilize the G-quadruplex DNA.⁴³ We utilized cationic porphyrins as a probe to screen the interaction of the quadruplex DNA with different categories of polymers. The aim in this research is to explore the information of the potential polymer candidates which can be used for the DNA binding and apply the resulting information in nucleic acid research.

CHAPTER 2 HISTORICAL

2.1 Polymers

Polymers are molecules that are composed of a large number of repeated units (monomers) which are linked by covalent bonds to form macromolecules. The large number of different building blocks of monomers can be constituted into a wide variety of macromolecules which allows for a great diversity of macromolecules. These structures can lead to a wide range of properties, allowing polymers to play an essential role in everyday life.⁴⁴

The types of polymers range from synthetic plastics (thermoplastic or thermoset), films, and elastomers to natural biopolymers. The varieties of natural biopolymers include carbohydrates, lipids, proteins and nucleic acids which are composed of different monomers and serve different functions. Synthetic polymers are one of the largest fields in materials science including synthetic rubber, nylon, PVC, polystyrene, polypropylene, etc.⁴⁵ There are three classes of organic synthetic polymers by charge; these are cationic polymers, anionic polymers and neutral polymers. In the present study, we attempted to investigate some of the neutral and cationic polymers for their interaction with the G-quadruplex DNA.

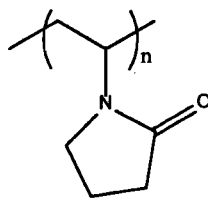
2.1.1 Neutral polymers

Some neutral polymers have shown the ability to interact or bind with DNA.⁴⁶ There are many non-ionic neutral polymers including polyvinylpyrrolidone (PVP), polyvinylpolypyrrolidone (PVPP) and poly (4-vinylpyridine-N-oxide) which are able to interact with DNA through non-condensing mechanisms.

Polyvinylpyrrolidone (PVP) is a water- soluble homopolymer made from the monomer N-vinyl pyrrolidone. PVP is a non-compacting but interactive polymer which is used in many applications such as excipients or solubilizers in the pharmaceutical industry. The interaction between DNA and PVP is based on hydrogen bonding with the base-pair in the DNA major groove. Unlike polycationic polymers, PVP is a non-condensing polymer which does not condense DNA into a polyplex.⁴⁷ PVP binds to DNA through hydrogen bonding between DNA and PVP, which makes the DNA/PVP complex have less negative charge density, shielding the charged DNA from the aqueous environment, and becoming more hydrophobic than DNA alone. The formation of DNA/PVP complexes may lead to improved cellular uptake of DNA and enhance the transfection efficiency.⁴⁸

Figure 2.1: Chemical Structure of the Polyvinylpyrrolidone

Poly (N-Vinylpyrrolidone)

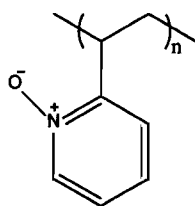


Polyvinylpolypyrrolidone (PVPP), a cross-linked form of PVP, is a water-insoluble polymer. PVPP is considered as a non-condensing agent which can be used in biochemical techniques such as DNA extraction.

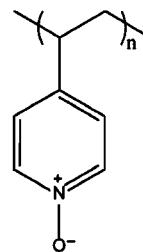
Poly (4-vinylpyridine-N- oxide) (PVP_yNO), the N oxidation product of poly (vinylpyridine), is a water soluble polymer. Poly (4-vinylpyridine-N-oxide) has a charge separation across the N⁺→O⁻ bond with a large dipole moment which can form a partial complex with water to transform the N-O group into a weak acid. Holt presented evidence suggesting that poly (4-vinylpyridine-N-oxide) and other non-ionic polymers are able to inhibit cytotoxic activity in cell cultures.⁴⁹ Figure 2.2 shows the structure of some polymers which are covered in the study.

Figure 2.2: Structure of Polymers in the Study

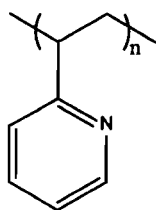
Poly (2-vinylpyridine-N-oxide)



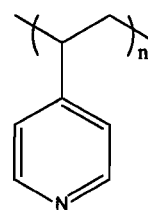
Poly (4-vinylpyridine-N-oxide)



Poly (2-vinylpyridine)



Poly (4-vinylpyridine)



2.1.2 Cationic Polymers

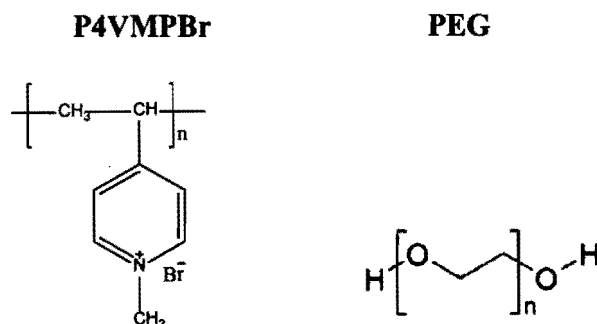
There are examples of polyanion/polycation interactions in many biological systems. The cationic polymers have been investigated intensively as non-viral gene delivery systems.⁵⁰ Due to their ease of modification, ready synthesis, and robust properties, cationic polymers have proven to be more efficient gene delivery systems than other cationic vectors (such as cationic lipids).

Although many cationic polymers can condense DNA spontaneously, they still have limited efficiency for *in vitro* and *in vivo* gene delivery.⁵¹ The chemical modification of polymers and the use of specific cell-targeting ligands may be alternative solutions for improving transfection efficiency and gene expression. Many chemically different cationic polymers have been investigated.²² However, most polymeric vectors have lower gene transfer efficiency than viral carriers. To improve the efficiency, there is a need for a better understanding of the intracellular trafficking and polymer structure/activity relationships in order to design an optimal polymer with virus-like qualities for gene delivery.⁵²

Poly (4-vinyl-1-methylpyridinium bromide) (PVMP Br) is a cationic water soluble polymer with ion-exchange properties. Polyethylene glycol (PEG), a polyether compound, is a low-toxicity hydrophilic polymer with unique physicochemical properties such as high water-solubility, high flexibility and large exclusion volume. PEG can be used in many areas from industrial to medicinal and is also FDA-approved as a component of various pharmaceutical formulations. PEG conjugates with other (cationic) polymers have been demonstrated to have the ability to improve the transfection efficiency.⁵³⁻⁵⁴

Poly (4-vinyl-1-methylpyridinium) bromide and PEG are among the polymers included in this investigation.

Figure 2.3: Chemical Structure of Poly(4-Vinyl-1-methylpyridiniumbromide) and Polyethylene glycol (PEG)



2.1.3 Polyethylenimine (PEI)

Among the various synthetic polycationic vectors, polyethylenimines have shown particular advantages in delivery system applications. Polyethylenimine (PEI), one of the cationic polymers, has been investigated and widely employed for the design of non-viral gene delivery vectors by many researchers for decades.⁵⁵⁻⁵⁷ The benefits of using polyethylenimine (PEI) as a non-viral transfection system are due to the fact that it has strong DNA compaction capacity with an intrinsic endosomolytic activity.⁵⁸⁻⁵⁹

The structurally different PEIs are categorized into linear or branched types with a wide range of molecular masses. Different molecular weights and degrees of branching of PEIs have been synthesized and evaluated for their *in vitro* or *in vivo* use.

Branched PEI is made from an acid-catalyzed aziridine ring opening reaction. Commercially available branched PEI with molecular masses around 25 kDa is the most

frequently study polymers. The linear PEI polymers are made by the hydrolysis of poly (2-ethyl-2-oxazoline). Most of the amines in linear PEI are secondary amines, only the terminal groups are primary amines. In the recent revision by the van Harpe group, they have updated the previous information about the ratio of the primary, secondary and tertiary amino groups in branched PEIs from the ratio of 1:2:1 (previous information) to closer to 1:1:1.⁶⁰ Boussif *et al* reported that non-protonated amino groups in PEI provided a high buffering capacity.⁴¹ The significant buffering capacity of the PEIs makes an attractive feature for proton sponge applications.

The phenomenon known as the “proton sponge effect” is the binding of cationic polymers to lipid groups on surface membranes, which then enter an endosome resulting in large buffering capacity. Once these cationic nanoparticles enter into an acidifying lysosomal compartment, the non-protonated amino groups (proton acceptor) are capable of sequestering protons that are supplied by a proton pump enzyme in the membrane. As protons enter the endosome, this process keeps the pump functioning and leads to the retention of one Cl⁻ ion and one water molecule per proton. This influx of water causes the endosome to burst, releasing the delivery vectors into the cytosolic space.

PEI is considered one of the most densely charged polymers due to the primary, secondary and tertiary amino groups, which exhibit this protonation property. Every third or fourth nitrogen atom carries a positive charge at physiological pH conditions therefore the nitrogens are able to buffer the relatively large number of protons in the endocytotic vesicles and keep the acidic lysosome balanced in pH.

The buffering capacity of PEI leads to osmotic swelling and rupture of endosomes, resulting in the release of the vector into the cytoplasm. Researchers also found that

linear (PEI-22K) and branched (PEI-25K) resulted in similar transfection efficiencies but a different effect with liposome complexes.⁶⁰ The transfection efficiency of PEI depends on both buffering sponge effects and molecular weight.⁶¹⁻⁶² Generally, both branched and linear PEIs are considered good candidates for non-viral vectors *in vitro* and *in vivo*.⁶³ The interaction between the positively charged polymer backbone and negatively charged DNA leads to the formation of polyplexes.⁶⁴

The positive charges of PEI are balanced by an influx of counter ions, which will protect DNA from degradation, such as osmotic swelling, bursting, and release into cytoplasm. PEIs show excellent transfection efficiency in many types of cells.⁶⁵ With a strong DNA condensation capacity and intrinsic endosomolytic activity, PEI is considered one of the most effective polymer-based non-viral gene carriers over other polycations.⁶⁶⁻⁶⁸

Studies on the interaction between quadruplex DNA and polycationic polymers have attracted much attention in the past decades.⁶⁹ Sun and co-workers⁷⁰ have reported that PEI can be used with G-quadruplex ligands, which could stabilize and regulate intramolecular G-quadruplexes and condense DNA to form a compact structure.⁷¹⁻⁷²

Figure 2. 4 shows the structure of the polyethylenimine, denoting the primary, secondary and tertiary amine sites. Figure 2.5 shows the branched PEI structure.

2.1.4 Cross-Linking

Cross-linking, one of the useful techniques for polymer structure modification, is a process by which long chains of polymers are linked together (usually at random sites in the middle of the chains), increasing the molecular mass and forming network polymers. Cross-linking reactions may occur by chemical or physical processes which are possible in natural or synthetic polymers. Physical cross-linking is a reversible reaction and occurs on the surface of the polymers. Chemical cross-linking, an irreversible and typically stable reaction, can be done by joining the chemically reactive groups within the polymer structure to form cross-links with other polymer molecules.

For the chemically reactive groups, specific chemical processes are the basic elements for the cross-linking reaction. Amine, carboxyl, sulfhydryl, aldehyde or hydroxyl groups are some of the typical chemical reactive groups which are required for cross-linking. Covalent bonds, ionic bonds or hydrogen-bonds can all be used in the formation of cross-links.

The properties of the polymer can be modified by the degree of cross-linking. For example, polymers with a higher degree of cross-linking will produce stiffer and more rigid materials which will increase the polymer strength, improve the resistance to chemicals, etc.

2.1.5 Cross-Linking Polymers

High molecular weight cationic polymers possess low gene transfection efficiency and often high cytotoxicities.⁷³⁻⁷⁴ In the efforts to develop a safe and efficient polymeric gene vector, modification of the polymeric vectors has been widely used.⁷⁵⁻⁷⁶ Cross-

linking, copolymerization, grafting and conjugation are common practices of the polymer modification processes which can be applied to polymers to improve the gene delivery system for higher gene transfection efficiency and lower toxicity.^{5,77-78}

2.1.6 Amine-Aldehyde Reaction

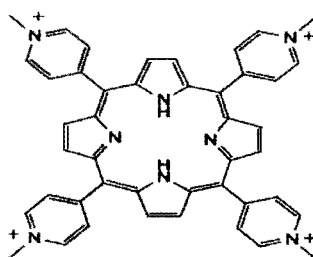
Isophthalaldehyde has two carbonyl groups which can react with the primary amine (from PEI) to form cross-links. The primary amines ($R-NH_2$ or $ArNH_2$), can undergo nucleophilic addition in which the carbonyls can react with primary amines to form stable imine bonds, creating cross-linked nanoparticles. Aromatic aldehydes, such as isophthalaldehyde, usually make stable imines with either aliphatic or aromatic amines, unlike aliphatic aldehydes, where the imines readily hydrolyze in water.

2.1.7 Pre-Screening Polymer Candidates for Nucleic Acid Delivery System

Cationic porphyrins are known to have a high affinity for binding to quadruplex DNA by intercalation or outside stacking to DNA.⁷⁹ In the present work; we used porphyrins as a probe to investigate the binding interaction between DNA and polymers. The porphyrin contains four pyrrole rings with conjugated double bonds and four methyl pyridinium groups at the meso positions. This metal-free tetra-cationic porphyrin structure has similar molecular dimensions as the G- tetrad; thus it has a good fit for intercalation or stacking with the quadruplex structure.⁸⁰⁻⁸¹ Porphyrins are also known to bind and stabilize different types of G-quadruplex structures and form DNA-porphyrin complexes.⁸²⁻⁸⁷ Electronic spectroscopy is used to evaluate the binding of porphyrin to quadruplex DNA with selected polymers. Free porphyrin has a Soret band with a λ_{max} of 422 nm; in the presence of quadruplex DNA, the porphyrin binds and the Soret

absorption maximum shifts to longer wavelength ($\lambda_{\text{max}}=433$ nm). When binding of DNA and porphyrin is disrupted – by stronger binding between quadruplex DNA and polymers, for example - the Soret λ_{max} will shift back to the free porphyrin wavelength. This data can provide us with information on strength and mode of binding by the polymer candidates.

Structure of Porphyrin



2.2 DNA Structure and Function

2.2.1 Nitrogen Bases, Nucleosides, and Nucleotides

Purine and pyrimidine derivatives are the nucleobases which are required for formation of nucleosides and nucleotides. Purine is a bicyclic base which consists of a six-membered and a five-membered nitrogen containing rings fused together, with four nitrogens in the position of 1, 3, 7, and 9. The naturally occurring purine bases are adenine (A) and guanine (G). The monocyclic bases are pyrimidines. Thymine (T), uracil (U), and cytosine (C) are the most common pyrimidine bases. Uracil has a structure similar to thymine but lacks a methyl group—uracil is found in RNA, thymine is in DNA.

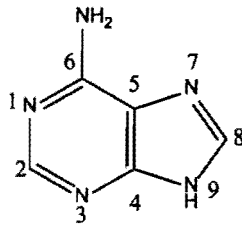
Pyrimidine and purine bases have at least one N-H position which can be linked to a sugar to form the basic building blocks for nucleic acids. In the nucleic acids and

polymers, the adenine and guanine (purine bases) are complementary with thymine/uracil and cytosine (pyrimidine bases) to form different structures.⁸⁸⁻⁹⁰

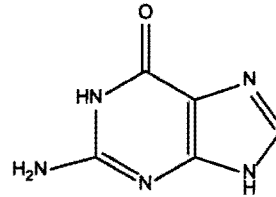
Figure 2.7: Major Purine and Pyrimidine Bases

Purine Base

Adenine (A)
6-amino urine

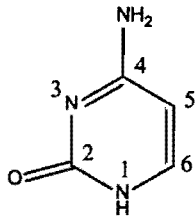


Guanine (G)
2-amino-6-oxy urine

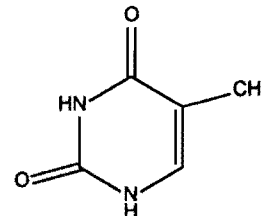


Pyrimidine Base

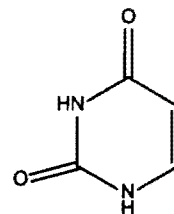
Cytosine (C)
(2-oxy-4-amino pyrimidine)



Thymine (T)
(2, 4-dioxy-5-methyl pyrimidine)

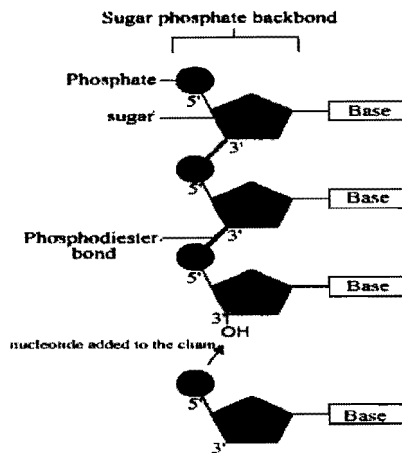
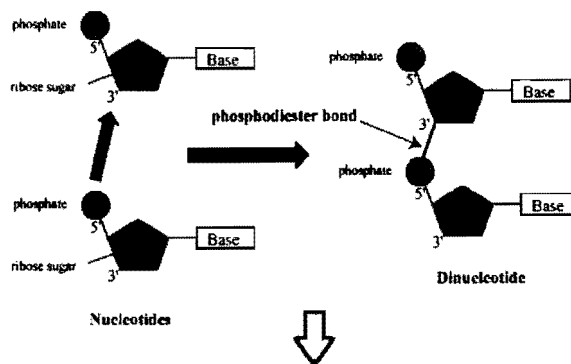


Uracil (U)
(2, 4-dioxy pyrimidine)



Nucleosides are glycosylamines consisting of the sugar (ribose or deoxyribose) and nitrogenous base. The nitrogen base joins together with sugar component via a β -glycosidic linkage which is attached to the N-9 position of a purine base or to the N-1 position of a pyrimidine base. Nucleotides are the basic monomer building blocks which, when joined together, make up the structural units of nucleic acids. The only difference between the nucleosides and the nucleotides is that the nucleotide contains one or more phosphates linked to carbon 5' of the sugar through a phosphate ester linkage. The alternating sugar and phosphate groups link together in a long chain to form the backbone of a nucleic acid. Figure 2.8 shows the formation of a polynucleotide.

Figure 2.8: The Formation of Polynucleotide



Adapted from www.click4biology.info: DNA Structure

2.2.2 Deoxyribonucleic Acid (DNA)

2.2.2.1 History of the DNA

Nucleic acids are polynucleotides, a polymeric compound, consisting of a number of nucleotide monomers covalently bonded in a chain. DNA (deoxyribonucleic acid) and RNA (ribonucleic acid) are the most common polynucleotides. Deoxyribonucleic acid

(DNA) is the unit of heredity which is associated with the transmission of genetic information in almost all activities of cells.

In 1869, scientist Johann Friedrich Miescher was the first person who isolated DNA. In 1919, the major components of DNA were identified by a Russian-American biochemist, Phoebus Levene.⁹¹⁻⁹² The first DNA sequences were confirmed by William Astbury, who used X-ray diffraction to disclose DNA patterns in 1937.⁹³ The fact that DNA carried genetic information was proved in 1952 by Alfred Hershey.⁹⁴ James Watson and Francis Crick applied Chargaff's rule to modeling the DNA structure; the famous DNA double helix structure was proposed in 1953.⁹⁵

2.2.2.2 Base Pairing Role in Nucleic Acid Structures

Nucleic acid base pairings are very important for the formation of a variety of DNA structures. The structure of DNA depends upon the nitrogen bases which join together through hydrogen bonds. Nucleotide base pairing follows rules during replication, transcription, and translation. Base pairings are important in sequence-specific recognition for nucleic acid. Hydrogen bonding plays a role in maintaining the stability of the molecular structure. The base-pairing rules govern the appropriate geometry relationships for hydrogen bonding which allow only the correct pairs to form in a stable structure. For example: DNA structures with high GC content are more stable than structures with less GC content. Adenine and guanine (the purine bicyclic molecules) pairs are energetically unfavorable since the larger rings are too close to each other which lead to molecular overlapping and repulsion. The cytosine and thymine (also uracil) have a single-ring (pyrimidine) small molecular structure. Cytosine and thymine pairs or

pairing with uracil are also an energetically unfavorable due to the two bases being too far apart. The only favorable pairings are the GC pairings or AT (AU) pairings which are energetically favorable for a stable molecular structure.

The G·C pairing and A·T pairing are usually arranged in “Watson–Crick” base pairing where maximally three hydrogen bonds are formed between G·C pair and two hydrogen bonds are formed between A·T pair. (Figure 2.9) These conformations are involved in the *cis* hydrogen bonding pattern and is symmetrical to the C1'---C1' vector of the two bases. ⁹⁶

Some other alternate hydrogen bonding patterns between base pairs can also occur in the nucleic acids, such as the wobble base pair and Hoogsteen base pair. Base pairing is a mechanism which can provide messages for molecular recognition. The Hoogsteen base-pairing model is different from the Watson and Crick model, using the N7 atom of the purine instead of the N1 atom to form the hydrogen bonding. Figure 2.10 show the difference between Watson-Crick and Hoogsteen base pairing models.

Figure 2.9: Watson-Crick Base Pairing- A: T and G: C formed by hydrogen bonding A-T base pairing form two hydrogen bonds and G-C base pairing forms three hydrogen bonds.

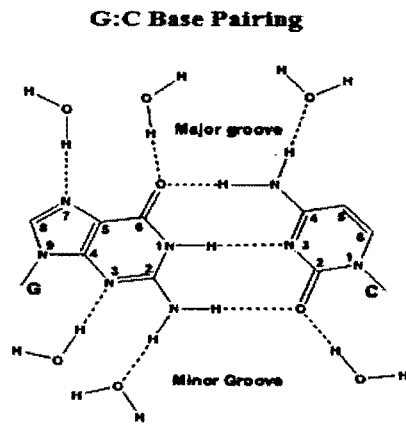
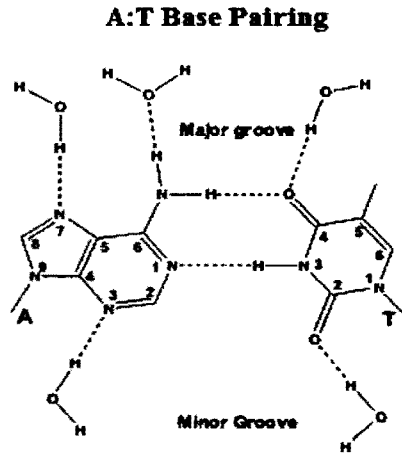
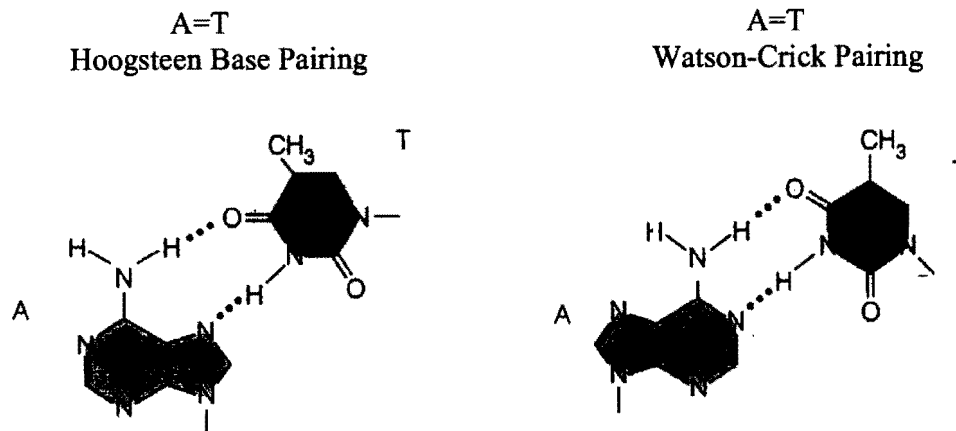


Figure 2.10: Difference between Watson –Crick and Hoogsteen Base Pairing



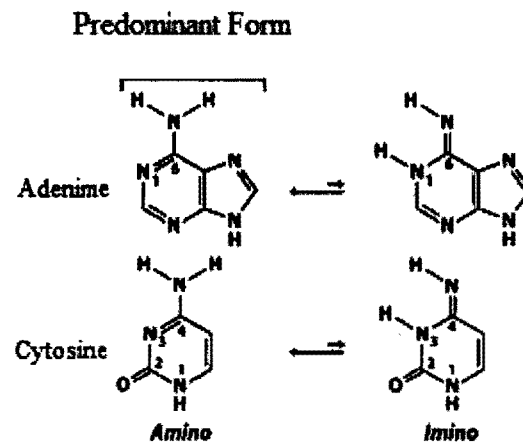
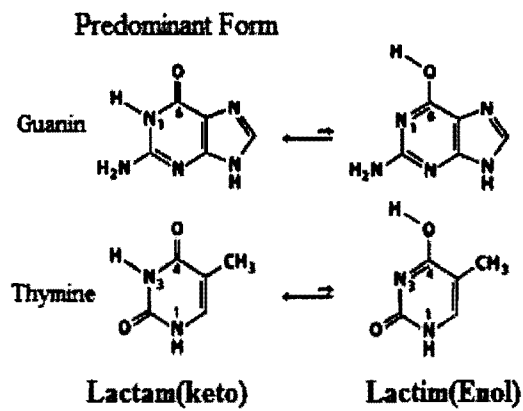
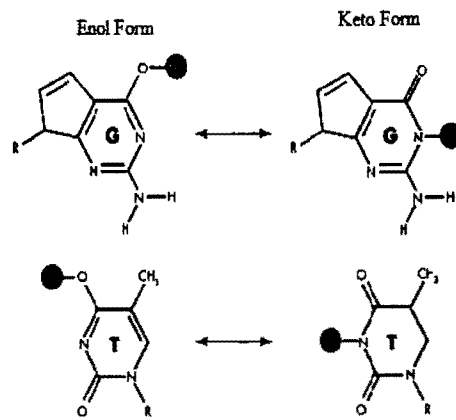
Adapted from Mathews, C.K.; Van Holde, K.E., *Biochemistry* 2/e. 1990, The Benjamin/Cummings Publishing Co., Inc.

2.2.2.3 Tautomerization of DNA Bases

The four DNA bases are all polyfunctional bases, and may exist in tautomeric forms. Tautomers are isomers of organic compounds that interconvert by a chemical reaction (tautomerization) usually migration of a proton and the shifting of bonding electrons. Tautomerism, the equilibrium between two such different structures, can play an important role in non-canonical base pairing in nucleic acids and might have biological significance. In DNA, the nucleotide bases normally are in the keto form. However, the keto and enol forms exist in dynamic equilibrium. Adenine and cytosine are cyclic amidines which exist in either amino or imino forms. Guanine and thymine can have alternate molecular structures based on different locations of a particular proton. The cyclic amide structures of guanine and thymine can exist in either lactam (keto) or lactim (enol) tautomeric forms. The keto form occurs when the proton bonds to a nitrogen atom

in the ring. An enol form occurs when the proton bonds to the exocyclic oxygen. Both guanine and thymine can switch easily between tautomers. The tautomeric forms change shape which can affect the three-dimensional structure of the molecule. The tautomeric forms exist in equilibrium but the amino and lactam tautomers are more stable and therefore predominate inside most cells under physiological conditions.⁹⁷ Figure 2.11 shows the tautomers of nucleobases (A, C, G, T) in imino or lactim form.

Figure 2.11: Tautomers of Nucleobases

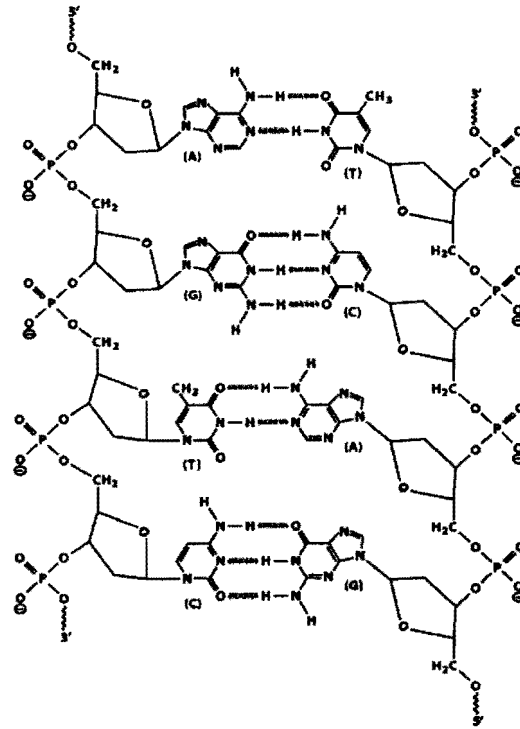


Adapted from Horton, R.A., *Principle of Biochemistry*, 4/e, 2006, Pearson Prentice Hall, Inc.

2.2.3 DNA Structure

DNA is a highly polymorphic molecule. The structures of DNA have a variety of conformation and structural motifs, including primary, secondary, tertiary and other higher order structures. The terms primary, secondary, tertiary, and quaternary structure were first defined in 1951 by Kaj Ulrik Linderstrøm-Lang, a Danish protein scientist.⁹⁸ Primary structure is the raw sequence of nucleotide bases in each of the complementary DNA strands. The secondary structure is how the strands of DNA are arranged. This can involve two or more strands, hydrogen-bonding in a highly specific way determined by the primary structure. Most of the DNA in cells occurs in double helix structures. However, other arrangements are also possible in the genome. The double helix DNA under certain conditions can accommodate a third strand in its major groove to form a triple helix structure (such as Hoogsteen triplexes). The three-stranded helical DNA has been observed and studied by some researchers.⁹⁹ In addition to three-stranded DNA, the four-stranded tetraplex structures also have been shown to exist; they have been found in some of the multiple folded protein or coiling protein molecules in a multi-subunit complex or in higher order DNA structures. Quadruplex DNA has been found in a variety of organisms particularly in telomeric repeats units.

Figure 2.12: Typical Double Strand Formation- The two strands are anti-parallel (one strand is 5' to 3' direction, the other strand is 3' to 5' in opposite direction).



Adapted from Horton, R.A., *Principles of Biochemistry*, 4/e, 2006 Pearson Prentice Hall, Inc.

2.2.3.1 Alternative DNA Conformation

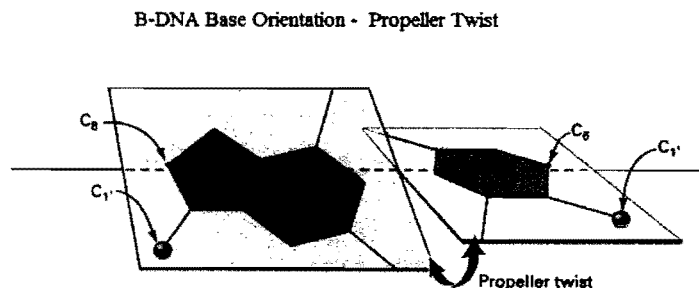
DNA is usually a double helix with the two strands running in opposite directions. DNA can adopt other secondary structures which form various possible conformations and shapes. Each structural conformation is found to be dependent on the specific base sequence patterns in which each plays its different biological role.¹⁰⁰ Under different applied forces such as twists or hydration conditions, DNA duplex can adopt many helical conformations that include the well-known A-DNA, B-DNA and Z-DNA, although this does not cover all conformations. Only B-DNA and Z-DNA have been directly observed in functional organisms. Z-DNA has been difficult to study because it

does not exist as a stable feature of the double helix structures. Instead, it is a transient structure that is occasionally induced by biological activity and then quickly disappears.¹⁰¹ Z-DNA occurs in a dynamic state, forming transitions between left-handed Z-DNA (during the physiological processes) and right-handed B-DNA (relaxing state) with the formation of the BZ-junctions.¹⁰²

B Form DNA

The most common DNA double helix structure in solution is known as B-DNA. B form DNA is a right-hand double helix structure which usually occurs in a high humidity and low salt condition. In this structure, two single strands are antiparallel and intertwined together to form a helix. The B-DNA structures are very similar to Watson and Crick's model. However, there are still numerous variations in the structure and the individual base pairs. Many bases are not exactly planar but are slightly twisted (propeller twist) in B-DNA.

Figure 2.13: B-DNA Base Angle Orientation



Adapted from www.biochem.arizona.edu

B-form DNA has all its bases in the anti-conformation; the intertwined strands are organized with the bases which create two grooves in different size: a major (wider) groove and a minor (narrow) groove. The wider major groove is easily accessed by proteins. The stability of the B-DNA double helix is determined by hydrophobic base-stacking interactions (van der Waals forces) between adjacent base pairs and hydrogen bonds forming between the base-pairs and grooves.¹⁰³⁻¹⁰⁴

A Form DNA

A-DNA occurs only in a dehydrated condition and usually is observed in RNA and RNA-DNA duplexes. When B- DNA undergoes an applied force such as a high salt or alcohol solutions, the DNA structure may change to A- DNA. A-DNA is a right-handed compact structure; its helix is shorter and wider than B-DNA. A-DNA has a deep and narrow major groove so it is not easily accessible to proteins. However, the wide and shallow minor groove allows proteins to stack inside.¹⁰⁵

Z Form DNA

It was not until 1970s, that the first single- crystal x-ray revealed the structures of the left-handed double helix DNA fragment. The alternating pyrimidine-purine sequences (especially poly (dG)₂) in alcohol or high salt solutions tend to have Z form structure. Transition from the right-handed B form to the left-handed Z form is due to the upside-down flip of the base pairs through a rotation of every other purine from the anti to the syn conformation. The two anti-parallel chains wind to the left which causes the backbone to form a zigzag pattern by Watson-Crick base pairs.¹⁰⁶ Z-DNA has a

narrower, more elongated helix than A form or B form DNA. Z-DNA can form a junction with B-DNA in a structure which involves the extrusion of a base pair.¹⁰⁷

Z-DNA is a higher energy form of the double helix structure which is stabilized by negative supercoiling.¹⁰⁸

It has been proposed that A- form DNA (low humidity) is considered to be more hydrophobic and results in the different packing modes of DNA.¹⁰⁹⁻¹¹⁰ Table 1 is the list of comparison of the A, B, Z forms of DNA.

Table 1: A-Form, B-Form and Z-Form Geometry Comparison

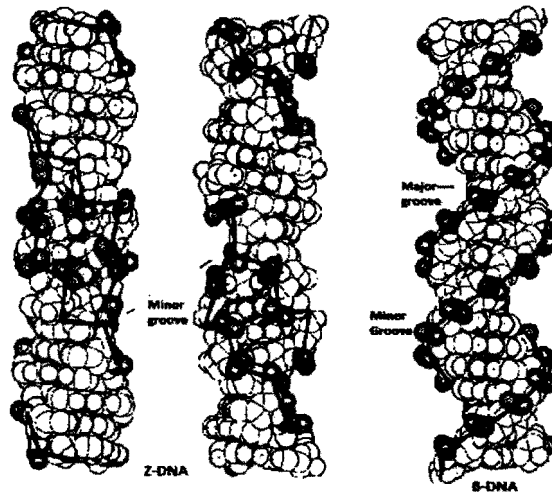
Geometry Attribute	A-form	B-form	Z-form
Helix sense	right-handed	right-handed	left-handed
Repeating unit	1 bp	1 bp	2 bp
Rotation/bp	33.6°	35.9°	60°/2
Mean bp/turn	11	10.5	12
Inclination of bp to axis	+19°	-1.2°	-9°
Rise/bp along axis	2.4 Å (0.24 nm)	3.4 Å (0.34 nm)	3.7 Å (0.37 nm)
Rise/turn of helix	24.6 Å (2.46 nm)	33.2 Å (3.32 nm)	45.6 Å (4.56 nm)
Mean propeller twist	+18°	+16°	0°
Glycosyl angle	anti	anti	pyrimidine: anti, purine: syn
Sugar pucker	C3'-endo	C2'-endo	C: C2'-endo, G: C2'-exo

Adapted from reference 109-110

Figure 2.14: B and Z Form DNA Double Helix Conformations

The major difference between B-DNA and Z-DNA is that B-DNA possesses a minor and major groove. Z- DNA only has minor grooves

B and Z Form DNA



Adapted from: <http://bioinf.mpi-inf.mpg.de>

Triplex DNA

Three stranded helical DNA structures have been observed and have been studied intensively by some researchers. The formation of the triplex DNA occurs when pyrimidine or purine bases occupy the major groove of the DNA double helix forming Hoogsteen pairs with purines of the Watson-Crick base pairs. The purine bases of DNA have hydrogen bonding donors and acceptors that are able to form two additional hydrogen bonds (Hoogsteen base pairs) in the major groove.¹¹¹

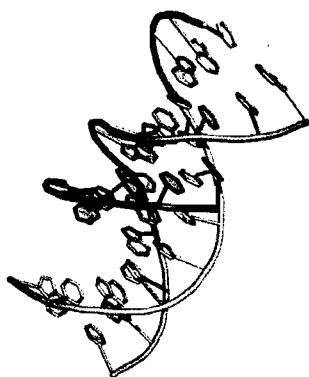
As a pre-requisite, the DNA duplexes must contain only purine bases in one strand and only pyrimidines in the complementary strand. These duplexes are capable of

forming a triplex with a third pyrimidine strand in a homopyrimidine/homopurine region of DNA. Thus, the triple-helical DNAs using Hoogsteen pairings consist of two homopyrimidines and one homopurine and the homopyrimidine third strand is parallel to the homopurine strand. Triple helices consisting of one pyrimidine (T, C) and two purine (A, G) strands were also proposed. For example: A*AT or G*GC.¹¹²⁻¹¹³

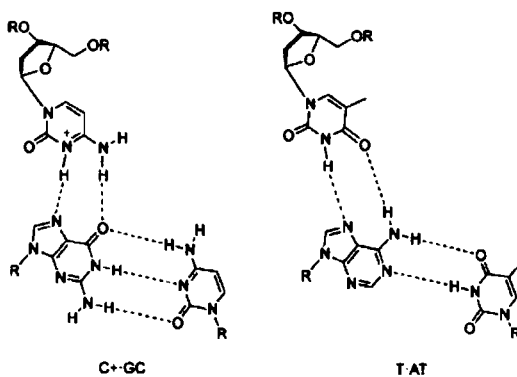
Figure 2.15: Triplex DNA

A third strand of DNA can fit in the major groove of duplex DNA to form triplex DNA. Duplex DNA (grey) interacts with the third DNA strand to form a triplex (blue).

a)



b) Example of the Chemical Structure of triplex DNA



Adapted from www.atdbio.com/content/13/oligonucleotides-as-drug

2.3 DNA, Telomeres and Telomerase

2.3.1 Mechanism of Gene Delivery System

Since the mid-1960s there has been interest in using gene therapy applied to the possible treatment of genetic disorders. In 1990, the first phase I gene therapy clinical trial was reported with promising results.¹¹⁴ Genes, the basic units of heredity, have specific sequences of bases that encode instructions for the production of proteins. When gene sequences are altered, the encoded proteins are not able to perform their normal functions, which create genetic disorders. Gene therapy is a technique which has the potential to correct the defective genes and treat the genetic disorder disease.

From the years 1989 to 1994, many gene-based therapy protocols were approved worldwide for treatment of the inherited genetic disorders.¹¹⁵ There are many different methods of gene delivery which have been developed for a variety of cell types and tissues, ranging from bacterial to mammalian.¹¹⁶⁻¹¹⁷ Gene carriers need to overcome many obstacles of both intra and extracellular barriers to reach the target site. The intra and extracellular barriers include crossing the plasma membranes, escape from endocytosis vesicles, migration to the nucleus, then release of the genetic information at the appropriate location.

Typically gene delivery methods can be divided into viral and non-viral systems. A virus is capable of transferring its genetic materials into host cells. Although viral vectors are highly efficient in gene delivery, there are still problems with safety and other limitations. The disadvantages have encouraged researchers to focus on alternative systems - non viral methods.¹¹⁸⁻¹¹⁹ Non-viral synthetic vectors are able to interact with

negatively charged DNA through electrostatic interactions and condense DNA particles; therefore allowing transfer of the genetic materials into target cells.¹²⁰⁻¹²¹

Figure 2.16 illustrates the formation of the polyplex and cellular uptake via an endocytic pathway in the following steps.

Step one: DNA is condensed with a mixture of polycations–ligand (for receptor-mediated uptake) to form a polyplex. Step two: Receptor-mediated uptake of the polyplex into the endosomal vesicles. Step three: Acid-triggered deshielding and exposure of the positive inner polyplex core.¹²²

Figure 2.16: Cellular Uptake via an Endocytic Pathway

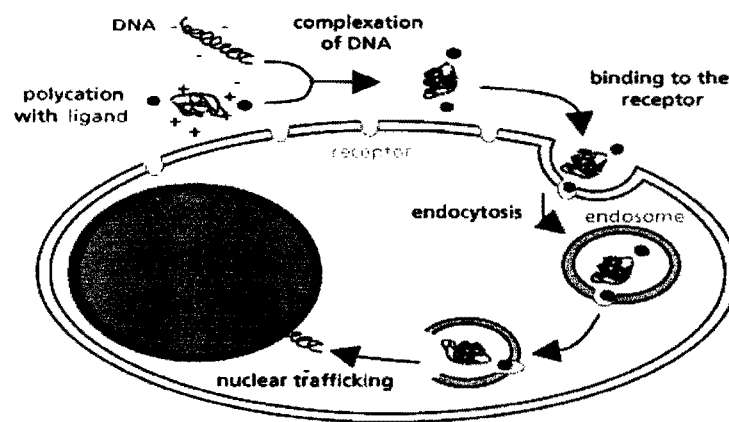


Image adapted from website: nano-lifescience.com

2.3.2 DNA Replication

In all living organisms, DNA replication is the basic process for passing down biological inheritance. Before cell division, a copy of DNA must be made for the daughter cells. This process is called DNA replication.

The replication begins with the "unzipping" of the parent molecule and uses the original double-stranded DNA molecule as a template for the reproduction of the complementary strand. Hence, following DNA replication, two identical double stranded DNA daughter molecules have been produced from each original double-stranded DNA molecule. Figure 2.17 gives the explicit structure of the DNA replication fork.

Figure 2.17: DNA Replication Fork

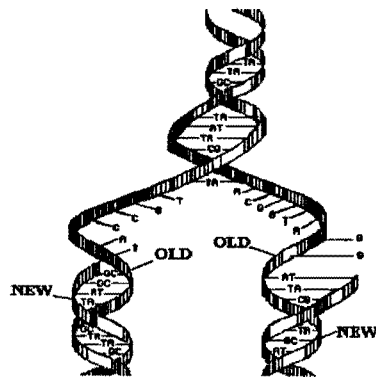


Image adapted from <http://notesforparkistan.blogspot.com>

When completing the replication processes; two DNA molecules are formed identical to each other and identical to the parent strand. DNA polymerase and other proteins work together to initiate the elongation of DNA.¹²³⁻¹²⁴ These two strands serve

as the templates in which one is called the leading strand and the other is called the lagging strand. The DNA polymerase can read the template and continuously adds complementary nucleotides to the template. The leading strand template is oriented in a 3' to 5' direction. The lagging strand is oriented 5' to 3' but will create DNA fragments in the 3' to 5' direction. DNA has a ladder-like structure with hydrogen bonds holding two DNA strands together. When the hydrogen bonds are broken, the resulting structure can form a fork shape which is made up from two single strands DNA. The replication fork is a structure that forms within the nucleus during DNA replication.¹²⁵

A problem that occurs during the replication process is that on one strand the replication process creates discontinuous fragments of daughter strand DNA. This is because, DNA synthesis can only occur in one direction (5' to 3'). The original DNA strand must be read from 3' to 5' to produce a 5' to 3' nascent strand. One of the daughter DNA molecules must synthesize in a discontinuous manner. The resulting polynucleotide segments (called Okazaki fragments) are then stitched together into the lagging strand by DNA ligase I.

Figure 2.18 illustrates the process of the DNA replication.¹²⁶⁻¹²⁷ Step 1 is the unwinding process. Step 2 is preparation for replication. Step 3 is elongation of the 5'-3' template and the 3'-5' template. Step 4 is a connection step (join DNA fragments). In the lagging strand the DNA polymerase I (exonuclease) reads the fragments and removes the RNA primers. The gaps are closed with the action of the DNA polymerase and DNA ligase.

Figure 2.18: The Steps of the DNA Replication

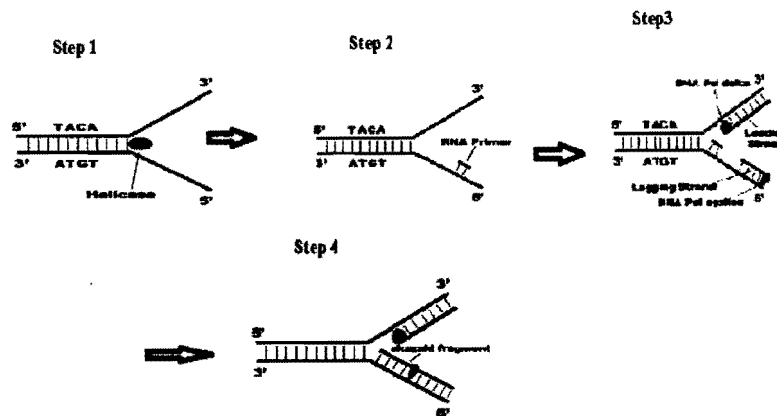


Image adapted from www.DNA.Replication.Info

2.3.3 Telomeres and Telomerase

In 1938 Hermann J. Müller, a remarkable scientist, was the first to discover and name the telomeres. Müller found that telomeres served as protective caps that could protect DNA from damage when the DNA replication cycle took place.¹²⁸ In the past few decades, telomeres have gained attention for many researchers because of many interesting topics relating to cellular aging and cancer. Telomeres have been shown to form a variety of G-quadruplex structures.¹²⁹ G-quadruplex structures are now being considered as targets for drug design.¹³⁰

Telomeres are structures located at the ends of the chromosomes which protect chromosomal DNA from degradation and recombination, and is part of the complex cascade of organism aging.¹³¹⁻¹³³ The chromosomes are a long strand of coiled DNA, located inside the nucleus. The structure of the telomere consists of simple tandem repeat DNA sequences. Human telomeres have the sequence $(TTAGGG)_n$.¹³⁴⁻¹³⁵ These

repeating sequences make up a portion of the double-strand telomeric DNA with a piece of single-strand tail overhanging the G-rich 3' end DNA which contributes to the secondary structure of the telomere. The human overhanging sequence consists of 100–200 telomeric repeating units which could form G-quadruplex structures.¹³⁶⁻¹³⁷

The chromosomes shorten at the ends in every cycle of cell division, eventually impacting needed genetic material. Telomeres play an important role in preventing the degradation of the chromosomes.¹³⁸⁻¹⁴⁰ The known biological function of telomeres is to protect the chromosome ends from fusion, degradation and to maintain the integrity of the genetic material in the chromosomes.¹⁴¹⁻¹⁴³

In 1940, Barbara McClintock discovered the behavior of the ruptured chromosomes which resulted in fusion and adhesion of the end of the chromosome. Barbara McClintock demonstrated that the telomere had the ability to repair the damage to the end of the chromosomes.¹⁴⁴⁻¹⁴⁵ In 1973 Alexey Olovnikov, a Soviet biologist, hypothesized that the telomere is critical in the understanding of aging and cancer.¹⁴⁶ It was not until 1978 that Elizabeth Blackburn and Joseph Gall discovered that a reverse transcriptase enzyme, telomerase, plays a key role in normal cell functions as well as in cell aging or cancers. Elizabeth Blackburn, Carol Greider and Jack Szostak were awarded the Nobel Prize in 2009 for resolving the end replication problem.¹⁴⁷ Telomerase has the ability to elongate the G- rich strand of telomeric DNA. Thus telomeres and telomerase may be proposed as attractive targets for the discovery of new anticancer drugs.¹⁴⁸

2.3.4 Telomerase and Aging

There is increasing evidence to indicate that telomerase plays an important role during the replication of mammalian telomeres.¹⁴⁹ During a life span, cells divide over and over to keep the body alive, but the telomeres grow shorter with each division. To address the consequences of incomplete replication, nearly all eukaryote cells have the ability to employ a telomere at the ends of chromosome. In the absence of a special telomere maintenance mechanism, telomeres will lose or damage some essential parts of DNA sequences during the cell replication cycles; which is due to the inability of DNA polymerase to fully replicate the chromosome ends. The length of the telomeres over time is connected to cell aging and lifespan.

In 1987, Blackburn and her coworkers made the astounding discovery that telomerase (a ribonucleoprotein reverse transcriptase) activity might be able to extend telomeric sequences.¹⁵⁰ Telomerase can synthesize telomeric repeats units and add them onto the ends of chromosomes. A variety of premature aging syndromes are associated with short telomeres.¹⁵¹ However, the premature aging can be reversed by telomerase enzyme that can prevent the shortening at the of chromosomes.¹⁵² In 2000, Geron Corporation revealed a study results that addressed the telomerase-based therapies could not only prevent but also reverse the aging process in humans.¹⁵³

2.3.5 Telomerase and Cancer

Telomerase enzymes were found active in most human tumor cells and the telomerase activity is found to be involved in about 85% to 90% of human cancers.¹⁵⁴⁻¹⁵⁶ Cancer is a condition in which certain cells in the body are growing and dividing uncontrollably. Most cancers are the result of "immortal" cells which have ways of

evading this programmed destruction.¹⁵⁷ Normally telomeres shorten significantly and will lead to cell death or sustain damage that can cause cancer.¹⁵⁸ Every living system should maintain a balance of the cells replicating and dying. If there are too many of the same types of cell gathering together this will lead to cell abnormality or cancer.¹⁵⁹⁻¹⁶² In about 90% of cancer cells telomerases have been found.¹⁶³⁻¹⁶⁶ For this reason, many researchers believe that part of forming an abnormal cell in cancer is the activation of telomerases. These cells use telomerase to overcome the incomplete end-replication problems. Telomerase will extend the leading strand of DNA to elongate the telomere. Telomerase inhibition has been identified as a new approach to cancer therapy.¹⁶⁷⁻¹⁷⁴

Dr. Michael Fossil has suggested that telomerase therapy may be used not only to combat cancer but also to have an anti-aging effect and extend the lifespan significantly in the human body.¹⁷⁵ This assumption has inspired a number of potential therapeutic strategies. The inhibition of telomerase has become an attractive strategy for anticancer therapy since the first demonstration of telomerase inhibition by a G-quadruplex interactive compound in 1997.¹⁷⁶ The formation of G- quadruplex complexes by telomeric DNA has become a new direction cancer therapeutics.¹⁷⁷⁻¹⁷⁸

2.3.6 Quadruplex DNA

G-quadruplex structures are a class of DNA structures that may be useful in targeting telomeres. Quadruplexes are four stranded higher order nucleic acid structures. That guanine-rich oligonucleotides can form a quartet structure was recognized more than forty years ago. Gellert *et al.* proposed that guanine base sequences could form a quartet structure through hydrogen bonding.¹⁷⁹ A G-quartet is formed by four guanine

bases in a square planar arrangement which provides a central cavity where each guanine acts as both donor and acceptor for hydrogen bonds. The oxygen lone pair of the carbonyl groups within the G-quartet can associate with the metal cation in the cavity site. G-quartets can arise between G-rich strands (intermolecular) or within G-rich nucleic acid sequences (intramolecular).

The level of interest in the G-rich structures have increased markedly in the past decade due to the fact that guanine-rich single-stranded overhang structures can be folded into quadruplex structures under certain physiological conditions.¹⁸⁰ These guanine-rich quadruplex structures were found in G-rich eukaryotic telomere ends as well as in non-telomere genomic regions including gene promoter regions,¹⁸¹ immunoglobulin switch region,¹⁸² and sequences associated with disease.¹⁸³ There are studies on some naturally occurring eukaryotic telomere repeat DNA sequences which all contain a 3' single strand overhang to form quadruplex structures such as d(TTAGGG)_n (found in vertebrate chromosome including *Homo sapiens*),¹⁸⁴ d(TTTTGGGG)_n (from *Stylonychia*), d(TTTAGGG)_n (from *Arabidopsis*), and d(TGGGGT)_n (from *Tetrahymena*)

G-quadruplex DNA displays an amazing structural polymorphism, and different typologies of G-quadruplex may be associated with different cellular processes. The polymorphism of the G-quadruplex structure may provide insight for achieving therapeutic selectivity for drug design.¹⁸⁵

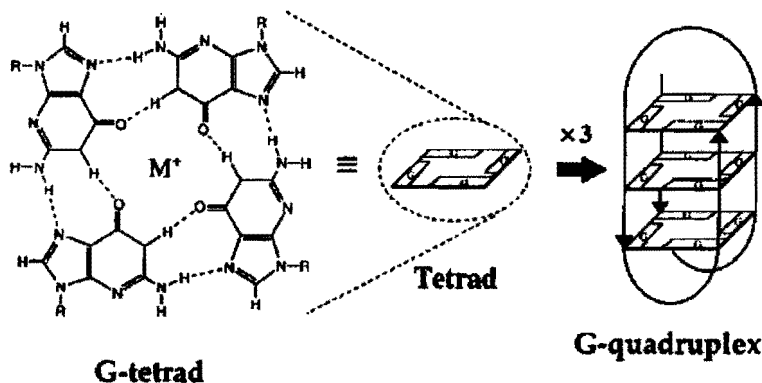
2.3.7 Quadruplex Structure

G-rich four-stranded structures can form in different ways, by folding and base-pairing of one, two, three, or four DNA strands. In particular, the number of structures involving guanine tetrads has been an area of increasing interest in the past few decades.

It is well known that DNA oligomers containing repeating guanine bases can form specific motifs. The fundamental structural units of the quadruplex consist of a planar arrangement of four guanines connected by hydrogen bonds for each side (tetrad), with a central channel formed by stacking of guanine tetrads that can accommodate selectively certain cations.¹⁸⁶ These planar G-quartets will stack on each other to form a higher-order DNA structure, which is called a G-quadruplex.¹⁸⁷⁻¹⁸⁸ Figure 2.19 illustrates the forming of the G-tetrads and G-quadruplex structures.

Figure 2.19: G-tetrads and G-quadruplex Structure.

Structure of tetrad shows hydrogen bonds between four guanines and the a cation (M^+) located in the center.



Numerous studies have been shown that G-quadruplex structures are biologically important in both *in vivo* and *in vitro* systems.¹⁸⁹⁻¹⁹⁰ The structural polymorphism of G-quadruplex DNA has been proven to affect the cellular functions.¹⁹¹ The biological relevance of the G-quadruplex may be involved in many areas: regulation of telomerase activity, controlling biological phenomena, functional molecules, and nano-materials.

The polymorphic nature of the G-quadruplex structure might also explore the promising future for using as a building block of the novel nanomaterials.¹⁹²

2.3.8 G-Quadruplex Architectures

G-quadruplex structures have a rich structural diversity which can align through mismatch, triple, triad, tetrad and hexad alignments, resulting in unique DNA architectures, that differ in the number and orientation of strands and pairing alignments.¹⁹³ The organization of the chain direction gives rise to a large number of possible topologies. The possible structural folding topologies of the quadruplex have multiple conformations which can be described as parallel, antiparallel or mixtures of these two forms. The Viglasky group has reported how protruding nucleotides can destabilize the G-quadruplex structure, and the overhanging sequences can influence the folding of the quadruplex.¹³⁶

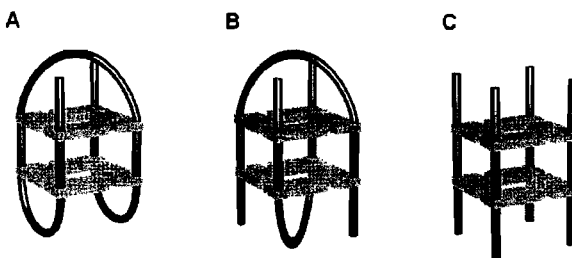
The topologies of different G-quadruplexes are affected by the orientation of the G-quartet core, the syn/anti conformation of guanine residues, the association of metal cations, and the types of linking loops.¹⁹⁴⁻²⁰⁰ The possible orientation of the G-quadruplex architectures may exist as unimolecular, bimolecular or tetramolecular structures which connect their backbones with a variety of loop types to build different conformations of the G-quadruplexes.²⁰¹ In recent review articles of G-quadruplex structures, 26 possible topologies have been reported.²⁰² However, only a few topologies have been proven to exist *in vitro*²⁰³, and there is even less knowledge of *in vivo* architectures.

The G- quadruplex structure appears to be stabilized by a hydrogen-bonding network which comprises a stack of two or more G-quartets linked by the phosphodiester backbone and stabilized by a specific monovalent ion. The structural diversity and stability of G-quadruplex structures depend on many factors: strand stoichiometry, connecting loops, strand polarity, glycosidic torsion angle, and coordinated cations.

Strand stoichiometry: Strand stoichiometry allows G-quadruplexes to be formed from one, two, three or four strands from unimolecular to quadrimolecular structures.²⁰⁴⁻²⁰⁶

Figure 2.20: Examples of Various Strand Stoichiometries of G-Quadruplex Structures

- (A) One-stranded: a unimolecular G-quadruplex.
- (B) Two strands: a bimolecular G-quadruplex.
- (C) Four separate strands: a quadrimolecular G-quadruplex.



Loop connectivity: A loop can connect guanines in a variety ways to form unimolecular or bimolecular G- quadruplexes.²⁰⁷ Figures 2.21 and 2.22 show examples of loop connectivity of guanine tetrads.

Figure 2.21: Unimolecular: Different way of Strand Loop Connectivity for Guanine Tetrad Structure (A, B, C)

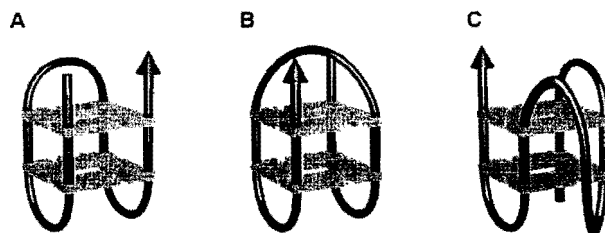
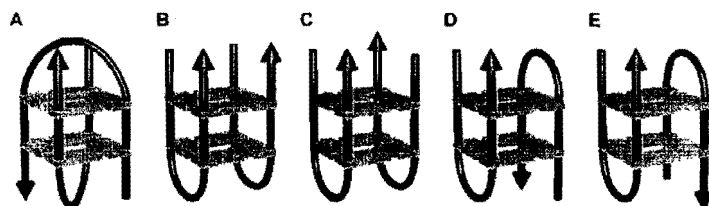
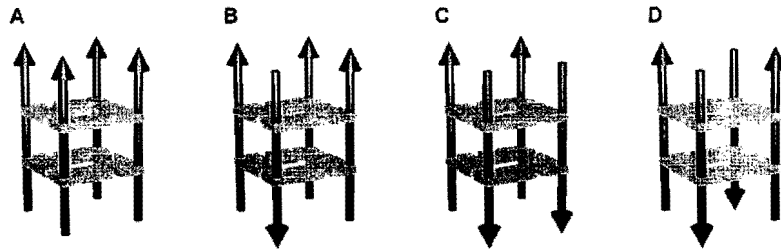


Figure 2.22: Bimolecular: Strand Loop Connectivity to form Various Guanines Tetrad Structures (A, B, C, D, E).



Strand Polarity: Strand polarity can induce the various sequences and different structures arrangement in G-quadruplex. For example: all parallel, mixed parallel and antiparallel, adjacent parallel or alternating antiparallel.²⁰⁸⁻²¹¹

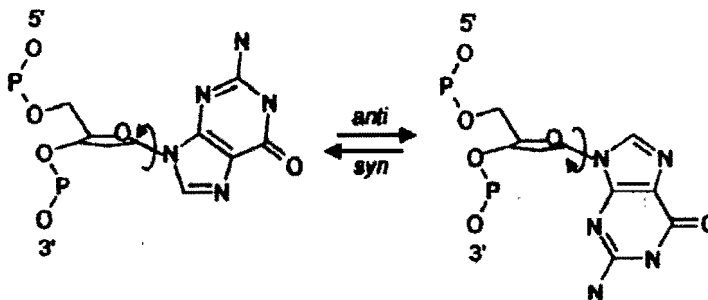
Figure 2.23: Strand Polarity Arrangements in G-Quadruplex Structures: (A) all parallel, (B) three parallel and one antiparallel, (C) adjacent parallel and (D) alternating antiparallel. Arrows indicate 5' to 3' polarity



Torsion Angle: The glycosidic torsion angle is the key factor to determine the G-quadruplex structure's orientation for parallel or anti-parallel strands. The glycosidic conformation changes the relative orientations of the bases in contiguous guanine tetrads and affects the stacking energy. Parallel strands have the same glycosidic torsion angle. Antiparallel strands have the opposite glycosidic torsion angle. Rotation around the glycosidic bond enables the guanine base to interconvert between the syn and anti conformations. The stacking of the guanine tetrads for parallel and antiparallel conformations will produce different spaces in the grooves. A parallel strand will create four medium sized grooves; an antiparallel strand will create three types of grooves: wide, medium and narrow grooves.²¹²⁻²¹⁵

Figure 2.24: Example of the syn/anti conformation structure by the rotation of the glycosidic bond

The bond rotation can convert syn into anti or reverse conformations.

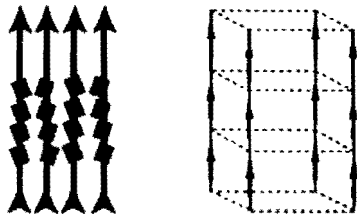


The presence of cations is an essential element for the formation of G- quartets. The nature of the cation can induce the conformational changes (parallel or anti-parallel) in G-quadruplex structure. For example, the potassium ion (K^+) will often induce a parallel structure.²¹⁶ Venczel and Sen reported that divalent cations (Mg^{2+} , Ba^{2+}) are also present in a parallel G-quadruplex structure. The sodium ion (Na^+) usually induces an anti-parallel conformation. The calcium ion (Ca^{2+}) can induce a structural transition of G-quadruplex from the antiparallel to parallel conformation.²¹⁷

Figure 2.25: Depiction of the G-Quadruplex DNA Structures: Example of the Parallel and Anti-Parallel

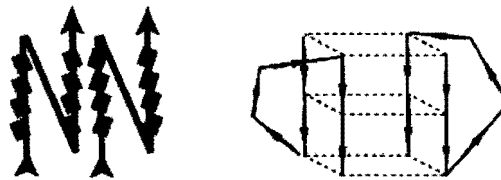
Parallel Structure

d(TGGGGT)



four stranded parallel structure

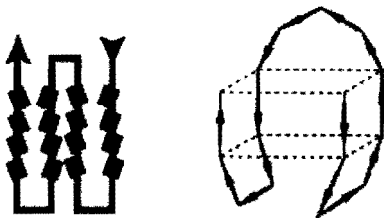
d(ATGGGUTAGGGT)



external loops, propeller type structure

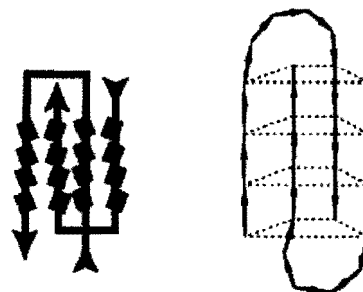
Anti-Parallel Structure

d(GGTTGGTGTGGTTGG)



lateral loops, chair type structure

d(GGGGTTTTGGGG)



diagonal loops, basket type structure

Adapted from Paramasiva, S. et al, *Method* 2007, 43(4), 324-331

Groove Effect: Groove dimension is controlled by the glycosidic torsion angles (*syn* /*anti*) and strand polarities. The space between the glycosidic torsion angles and strand polarity of the quadruplex can be classified as wide (w), medium (m) or narrow (n) size of the grooves.¹⁹⁹ Figure 2.26 and 2.27 show the examples of the groove effect.

Figure 2.26: Two pairs of adjacent Parallel Strands-create two Medium Grooves

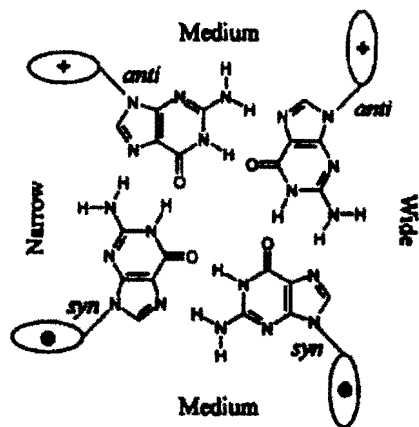
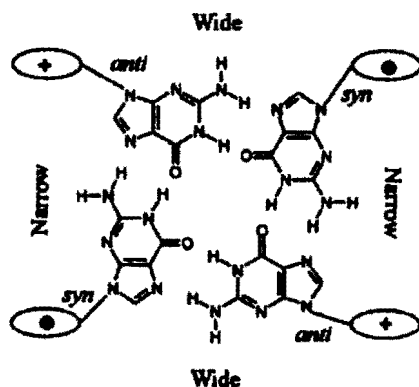


Figure 2.27: The alternating Anti-Parallel Strands: generate two Medium and two Narrow Grooves



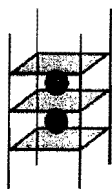
G-quadruplex DNA displays an amazing structural polymorphism; different topologies of G-quadruplex may be associated with different cellular functions.

Therefore, the polymorphism of the G-quadruplex can provide insight for achieving therapeutic selectivity for drug design. As shown in Figure 2.28 and 2.29, the overall topologies available to G-quadruplex structures depend on the combination of antiparallel/parallel orientation of guanine tracks and arrangement of the loop.

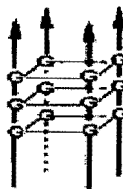
Figure 2.28: Structures of G-Quadruplexes. Schematic representation of G-quadruplex structure: (a) G-quadruplex with three stacked quartets, (b) A tetramolecular parallel G-quadruplex and antiparallel (c) intermolecular antiparallel G-quadruplexes (d) intramolecular fold over G-quadruplex.

- (a) G-quadruplex, linked by the DNA backbone (b) Parallel and Antiparallel quadruplex

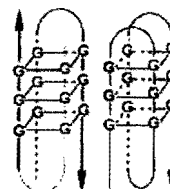
**Three stacked quartets
G-quadruplex**



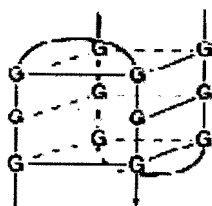
Parallel



Antiparallel



(c) Intermolecular antiparallel
G-quadruplex



(d) Intramolecular foldover
G-quadruplex

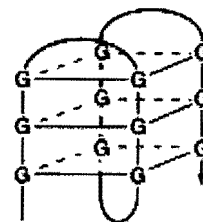
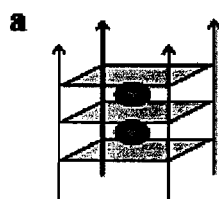


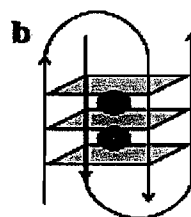
Figure 2.29: Examples of inter-and intramolecular quadruplex DNA conformation

(a) Tetramolecular parallel. (b) Bimolecular antiparallel. (c) Unimolecular antiparallel. (d) Unimolecular antiparallel. (e) Unimolecular parallel. Many sequences can also form mixed structures or are polymorphic

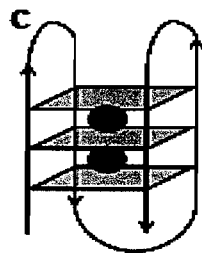
Tetramolecular parallel



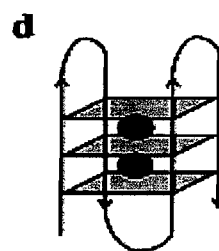
Bimolecular antiparallel



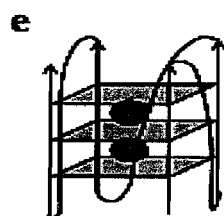
Unimolecular antiparallel



Unimolecular antiparallel



Unimolecular parallel



Adapted from Huppert, J.L., *Phil. Trans. R. Soc. A*, 2007, 365, 2969-2984

2.3.9 The Stability of Quadruplex Structures

The quadruplex DNA structures are considered as compact and resistant to DNAses, preventing the cleavage of phosphodiester linkages in the DNA backbone. The quadruplex structures are more stable than duplex DNA due to the presence of more hydrogen bonding between the guanine bases. Quadruplex DNA has higher melting temperatures than duplex DNA, which could also be due to the presence of the G-quartet stacks stacking.¹⁹⁹ There have been a large number of publications on structure and other properties of the quadruplex structures since the late 1980s.²⁰²⁻²⁰³ However, there is still insufficient understanding of their basic physical properties.

The stability of the quadruplex structures are determined by the following factors: the base stacking, hydrogen bonding, van der Waals forces, electrostatic interactions, the nucleotide sequence, ionic strength, cations and temperature. Hydrogen bonding is one of the important factors which can control the formation of both secondary and tertiary structures. The hydrogen bonds, van der Waals forces, ionic interactions, and hydrophobic interactions are intermolecular or intramolecular attractions which can influence the nature of the biological structure.

The structure and stability of intramolecular quadruplexes are profoundly influenced by the length and composition of the loops.²¹⁸ Increasing the loop length will increase the binding affinity of the quadruplex DNA. The loop length will influence the quadruplex conformation; short loops favor parallel conformations. With increasing loop length, quadruplex conformations prefer intra-molecular and anti-parallel conformation.²¹⁹

The ion-binding site is a cavity between two G-quartets that is lined with eight O-6 atoms from guanines participating in the coordination of cations. The negatively charged cavities located between the G-tetrads can be stabilized by the coordination of cations (monovalent or divalent) present in the center of the cavity. With the presence of the monovalent or divalent cations in the center, the size of the ion will affect the interaction with the G-quartet.²²⁰ In general, the ionic radius is a parameter that decides how well guanine tetrads are stabilized by various cations.

Kang and coworkers, using X-ray, studied the d(G₄T₄G₄) and reported that pocket stacking stabilized the quadruplex structure by forming the stacking in the adjacent G-quartet.²²¹ The switching between various conformations can be induced by the presence of different cations and difference in temperature. Miyoshi's group had found that, in low concentration, divalent cations can destabilize the antiparallel G-quartet of d(G₄T₄G₄) structure in the following order Zn²⁺>Co²⁺>Mn²⁺>Mg²⁺>Ca²⁺.²²² Particularly, higher concentrations of divalent cations can induce structural transition from antiparallel to parallel structure.²²³ Chen reported that divalent cation induced quadruplex structural change such as self-assembly (Mg⁺²) and formation of quadruplex (Sr⁺²).²²⁴⁻²²⁵ Monovalent as well as divalent cations are an integral part of G-quadruplex structure, and without these cations, G-quadruplexes are unstable.²²⁶

2.3.10 The Biological Role of the G-quadruplex DNA

Rising interest in G-quadruplex structures has been evident in the large number of publications, books and articles. The biological functions of quadruplex DNA were a relatively unexplored area for decades. In the last few years, the biological significance

of these G-quadruplex structures has been explored. Evidence has been found that quadruplex structures may be involved in many different biological phenomena.²²⁷ G-quadruplex DNA has been studied *in vitro* and *in vivo* for some biological species. The studies have indicated that G-quadruplex DNA might play important roles in cellular functions such as control of gene expression,²²⁸ regulation of gene transcription, and genomic stability.²²⁹⁻²³⁴

The unusual conformation of G- rich quadruplex-forming sequences have led to considerable interest by association with cancers, cell aging processes²³⁵⁻²³⁸ and also participation in gene regulation and telomere maintenance.²³⁹⁻²⁴⁵ The G- quadruplex structures were described as playing a role in the inhibition of telomerase activity by negatively regulating through the G-quadruplex, influencing multiple cellular processes (transcription, translation, and replication).²⁴⁶⁻²⁴⁷

G-quadruplexes have been considered as a potential therapeutic target for human cancer because they can inhibit telomerase activity, and some quadruplex-interacting drugs can induce senescence and apoptosis of cancer cells.²⁴⁸ Therefore, the use of specifically designed G- rich sequences has motivated scientists to develop new classes of anticancer therapeutics, therapeutic interventions and as potential targets for the design and development of novel anticancer drugs.²⁴⁹⁻²⁵³

2.3.11 Porphyrin Chemistry

5,10,15,20-tetra-(N-methyl-4-pyridyl)porphyrin (TMPyP4), a heterocyclic aromatic conjugated compound, is composed of four pyrrole subunits. These pyrrole rings with conjugated double bonds are connected so that electrons are delocalized over the

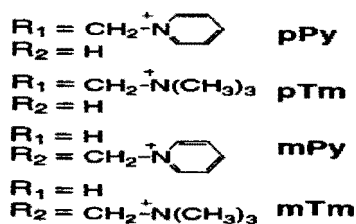
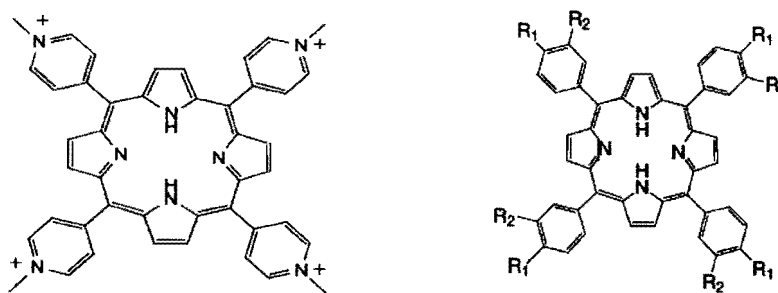
macrocycle, which induces intense absorption bands in the visible region. The stabilization of quadruplex DNA by TMPyP4 is in part due to π - π stacking interaction between the porphyrin ring and the guanine-tetrad. A porphyrin with no metal ion in the central cavity is called a free base. There has been considerable interest in the synthesis of porphyrins with various substitution patterns in their ability related to the biological functions.³⁷ Cationic porphyrins have been known to interact with DNA and form DNA-porphyrin complexes. The interactions between porphyrins and their derivatives with DNA have been widely studied for potential applications in biological and medicine sciences.²⁵⁴⁻²⁵⁹ It has been reported that the cationic porphyrins can interact with native DNA and nucleotides through various binding modes including intercalation,²⁶⁰⁻²⁶² external binding,²⁶³⁻²⁷¹ random binding,²⁷²⁻²⁷⁴ and self-stacking.²⁷⁵⁻²⁷⁹

It has been proposed that the mode of binding to the quadruplex DNA is “face on”, including the end stacking to G-tetrad or nearby diagonal loop. In the external stacking mode, the cationic side arms of the porphyrins probably stabilize the quadruplex structure by reducing the electrostatic repulsion between the anionic phosphates of the backbone of the lateral or loops. In the external groove binding mode, the antiparallel quadruplex DNA structure, it has been found that the porphyrin binding might be located in the narrow or wide groove by outside stacking.²⁸⁰ The cationic porphyrin and derivatives (TMPyP2, TMPyP3, and TMPyP4) have been reported to be G-quadruplex-interactive agents that demonstrated selective binding behavior with different G-quadruplex conformations.²⁸¹

The UV-Vis absorption spectra of TMPyP4 have shown to be responsive to the quadruplex stabilization.²⁸² However, it has been reported that this occurs through external stacking rather than intercalating with G-quadruplex structures.

TMPyP4 is a potent inhibitor of human telomerase. The interaction of the cationic porphyrin derivative with G-quadruplex DNA has the ability to inhibit telomerase due to stabilization of the telomere.²⁸³⁻²⁸⁴ In addition, porphyrins can be used as photo chemotherapy agents to treat cancer since they remain longer in cancer cells than in normal cells after injection.²⁸⁵⁻²⁸⁶ Porphyrins linked to oligonucleotides produce various types of photo-damage to the target site of DNA. Figure 2. 30 shows the chemical structure of the porphyrin and its derivatives.

Figure 2.30: The Chemical Structure Porphyrin and derivatives

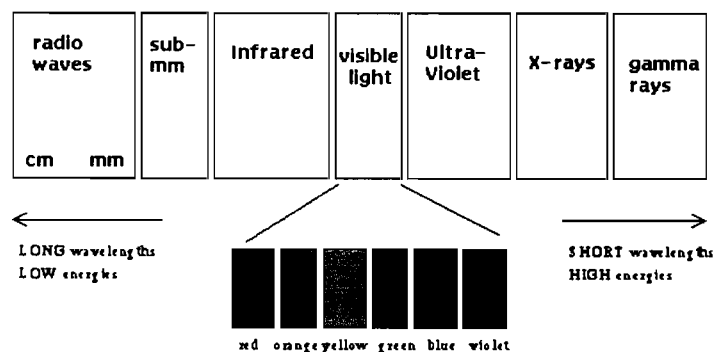


CHAPTER 3 INSTRUMENTATIONS

3.1 Spectroscopy

Spectroscopy is the study of the absorption and emission of light with matter. The interaction between the matter and radiated energy depends on the process and is a function of wavelength. Light has particle-like or wave-like characteristics which can serve as the reference of electromagnetic radiation. The given frequency or wavelength of light is associated with an energy (photon). Frequency (ν) and energy changes are proportional to one another, but wavelength (λ) as an inverse relationship to these quantities ($\nu = c/\lambda$). Different regions of the electromagnetic spectrum provide different kinds of information about the structure of the atoms or molecules. The electromagnetic spectrum ranges from very short wavelengths (including gamma and x-rays) to very long wavelengths (including microwaves and broadcast radio waves). The following chart displays the important regions of the electromagnetic spectrum.

Figure 3.1: The Electromagnetic Spectrum



Adapted from course.umass.edu

3.1.1 Quasi-Elastic Light Scattering / Dynamic Light Scattering

Dynamic Light Scattering (DLS), also known as Photon Correlation Spectroscopy or Quasi-Elastic Light Scattering (QELS), is widely used in determining the size distribution profile of small particles, diffusion coefficients, and molecular weights of polymers in solution.

The incident light on the particle scatters in all directions, and one is able to determine the distribution of the particles' movement by measuring dynamic fluctuations intensity of scattered light. The intensities of the scattered light are determined by size, shape and molecular interactions in the scattering particles. Light scattering is a valuable tool for measuring molecular weight, radius of gyration, translational diffusion constant and so on.²⁸⁷

When the laser light strikes the dispersed particles or macromolecules suspension in a medium, it is interacting with randomly moving particles. The intensity of the fluctuating scattered light at a different angle and time will depend upon the size of the particles. The small particles move faster than the big particles. These fluctuations occur due to Brownian motion; analysis of the fluctuation will yield the velocity. The velocity of Brownian motion is measured as the translational diffusion coefficient. This translational diffusion coefficient (D) can be related to particle size through the Stoke-Einstein equation. Therefore, it is possible to estimate the size of distribution, diffusion coefficient and the hydrodynamic radius of a molecule from DLS measurements.²⁸⁸⁻²⁹⁰

The molecular weight measurements are usually obtained by static light scattering; however, there are a few advantages for using dynamic light scattering techniques to determine the molecular weight. For example: (i) it can be used to analyze the broad

distributions of species of wide molecular masses; (ii) its high sensitivity allows detection of very low amounts ($< 0.01\%$) of higher mass species; (iii) there is no mass loss during the measurement (not like chromatography method, SEC); (iv) time saving due to a short experimental time; (v) automation; (vi) a modest development costs for using LS instrument.

The major parts of the light scattering instrument include a monochromatic coherent laser as a light source, photon detector and auto-correlator (Figure 3.2). When a laser light beam passes through the sample, that light is scattered by particles at all angles. The scattering light passes through the photon detector which detects the scattered light at a given angle. The purpose for using the same scatter angle is to produce the identical mean size particles. The fluctuations of scattered light are converted into electrical pulses and pass the digital correlator. The auto-correlator generates the autocorrelation function for data analysis.

Polydisperse samples (with a broad distribution of particle size) have shown a number of modes in DLS measurement, such as a main peak and aggregation information. Measuring the intensity of fluctuations at a given scattering angle can provide information about the scattering particles hydrodynamic radius. When particles in a suspension diffuse through the suspending medium, the effective radius of an irregularly shaped particle is called the hydrodynamic radius of a particle.

Figure 3.2: Schematic diagram of a conventional, 90° dynamic light scattering Instruments

A conventional dynamic light scattering instrument is including:
A monochromatic coherent laser (light source) with a fixed wavelength of 633nm; a focusing lens, one detector only detects the scattered light at one angle (usually 90°), a digital correlator.

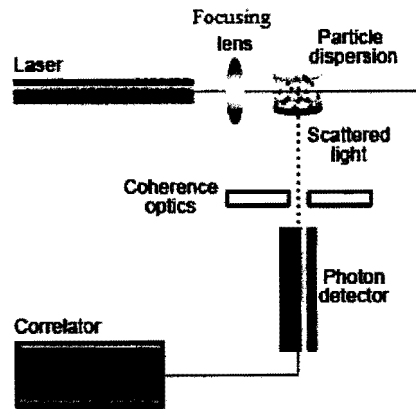


Image from Malvern.com

3.1.2 Theory

As spherical monodisperse non-interacting particles are placed in a dust-free fluid; the scattering light will mutually interfere in different directions. In reality, all the scatter particles are undergoing Brownian motions and leads to fluctuations of the scattered intensity $I(t)$. Dynamic light scattering is measuring the intensity of fluctuations which is recorded in the time domain via a time autocorrelation function. The scattered light intensity in time t is described as $I(t)$; in a very short time, the intensity of the scattered light is described as $I(t+\tau)$. As time goes on, the measured intensities will no longer correlate to the beginning state due to there is no similarity between the starting state and the current state. The light-scattering spectrum can be obtained from the autocorrelation

function of the scattering light intensity. A characteristic autocorrelation function (Eq.1) of the scattered light is shown below where intensity (I) can be determined experimentally.

As the particle moves through the beam the intensity reaches a maximum and then decays. The decay time of the correlation function is inversely proportional to the line width of the spectrum. The decay of the autocorrelation is described by an exponential decay function $G(t)$ which relates the autocorrelation to the diffusion coefficient (D) and the measurement vector K. Therefore, the diffusion coefficient and either particle size or viscosity can be found by fitting the measured correlation function to a single exponential function. The decay of the autocorrelation is described by an exponential decay function in equation 2.

Equation 1: Autocorrelation Function

$$\Gamma_t = \frac{\sum_{i=1}^{N-k} (Y_i - \bar{Y})(Y_{i+k} - \bar{Y})}{\sum_{i=1}^N (Y_i - \bar{Y})}$$

Equation 2 : Decay of Autocorrelation

$$G(T) \propto e^{-2DTK^2}$$

Equation 3 : Monodisperse Particles- Correlation Function

$$G(\tau) = A \exp(-2\Gamma \tau) + B$$

$G(\tau)$: the sum of all exponential decays contained in the correlation function

A : baseline of the correlation function

B : intercept of the correlation function

Γ : decay constant proportional to the diffusion coefficient (D)

Equation 4: Polydisperse Particles: Correlation Function

$$G(\tau) = A[1 + Bg_1(\tau)^2]$$

g_1 : Sum of all exponential decays contained in the Correlation Function

Equation 5: Decay Constant

$$\Gamma = Dq^2$$

D: Translational Diffusion Coefficient

q: $(4\pi n/\lambda_0) \sin(\theta/2)$

n : Refractive index of solution

λ_0 : Wavelength of Laser

θ : Scattering angle

Diffusion coefficient:

By fitting the points of the autocorrelation to the function $G(t)$, the diffusion coefficient can be measured and related to the equivalent sphere of diameter d using the Stokes - Einstein equation (Equation 8). The diffusion coefficient (D) of the particles can be calculated in the following equation.

Equation 6: Diffusion Coefficient (D)

$$D = \frac{T K_B}{3\pi\eta d}$$

T : Absolute temperature

K_B : Boltzmann constant

η : Viscosity

Equation 7: Frequency of the Scattering Light

$$K = \frac{2n\pi}{\lambda} \sin \left[\frac{\theta}{2} \right]$$

K is a constant related to the frequency of the scattering light (λ)

n : Refractive index of the medium

λ : Laser wavelength

θ : Scattering angle

With the assumption that the particles are spherical and non-interacting, the hydrodynamic radius can be calculated from the Stokes-Einstein equation. The hydrodynamic radius is calculated based on an equivalent sphere with the same diffusion coefficient.

Equation 8: Stokes-Einstein equation

$$r = \frac{k T}{6\pi\eta d}$$

r = hydrodynamic radius (m)

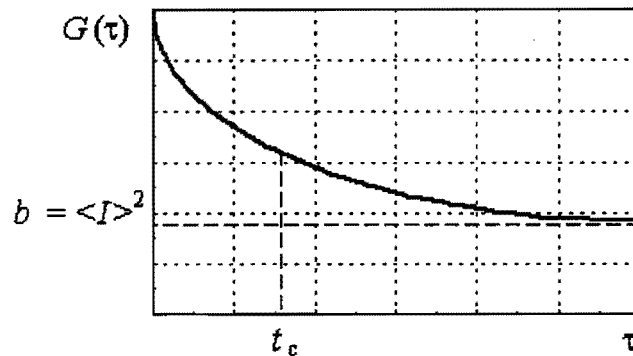
k = Boltzmann constant ($J/K = kg \cdot m^2/s^2 \cdot K$)

T = temperature (K)

η = solvent viscosity ($kg/m \cdot s$)

d = diffusion coefficient (m^2/s)

Figure 3.3: Example of Autocorrelation Function of the scattered light



The dynamic scattering technique can be used to distinguish protein secondary structures. The advantage of using dynamic scattering is the possibility to analyze samples containing broad distributions of species of widely differing molecular masses (e.g. a native protein and various sizes of aggregates), and to detect very small amounts of the higher mass species. Commercially, dynamic light scattering is a rapid, reliable, accurate and cost saving powerful tool for determining the size of particles and related information. Also, sample concentration is not a critical issue for obtaining the needed information.²⁹¹⁻²⁹³ Actually, the main benefit is that the measurement doesn't require solution or multiple concentrations like MALLS. Data can be obtained at a single concentration.

In the present study, we apply the light scattering technique to measuring the particle size of the cross-linked polymer nanoparticles and also studied the interaction and aggregation between the polymer (PEI) and cross-linker.

3.2 Nuclear magnetic resonance (NMR)

Nuclear magnetic resonance spectroscopy (NMR) is a prominent technique that addresses many questions of structure and dynamics using the interaction of radio frequency electromagnetic radiation with matter. NMR spectroscopy is widely used by chemists and biochemists to investigate the properties of organic compounds and determine structure at the molecular level. Some isotopes are of particular interest to organic chemists e.g., ^1H , ^{13}C , ^{19}F and ^{31}P , which have spin of $\frac{1}{2}$ ($I = \frac{1}{2}$). The versatility of NMR makes it pervasive in scientific research. NMR has the capability to perform multi-dimensional and multinuclear experiments. One-dimensional NMR spectroscopy is commonly used to elucidate simple chemical structure. Some advanced applications of NMR techniques can be used to assist scientists to investigate further details in the determination of molecular structure, such as multidimensional NMR, solid state NMR, and gradient enhanced spectroscopy.

3.2.1 ^{31}P NMR and ^1H NMR

We will not attempt to discuss the basic theory of the ^1H or ^{31}P NMR. ^1H NMR and ^{31}P NMR are important analytical tools for structure elucidation in chemistry, biology and medical science. The ^{31}P NMR spectroscopy has proven to be a useful technique in probing the secondary structure of DNA and RNA in solution. The ^{31}P nuclei, with 100% natural abundance and spin $\frac{1}{2}$, are sensitive to the environment (such as O-P-O bond angle and P-O torsional angle).²⁹⁴⁻²⁹⁵ We have used ^{31}P NMR to investigate the binding interaction between quadruplex DNA and polymers.

3.2.2 Diffusion NMR

Many methods for structure elucidation of small molecules and proteins have been well established for many years. The study of the solution behavior of molecules, proteins and nucleic acids for aggregation or interaction properties in solution are interesting fields for biochemical science. The intermolecular interactions, molecular recognition processes, and binding behaviors at the molecular level provide essential and important information for understanding the biological activities of molecules. Nuclear magnetic resonance spectroscopy is the method of choice for studying molecular dynamics in chemical and biological systems.²⁹⁶⁻²⁹⁸

In the past years, diffusion NMR methods have become useful for measuring diffusion in solution. In principle, translational diffusion is one of the most basic forms of transport in chemical and biological systems. When diffusion occurs in a homogeneous medium it will be a free and isotropic diffusion. The diffusion coefficient will reflect the shape and size of a molecular species; which provides information on the molecular aggregation as well as size and structure of labile systems. Diffusion NMR measurements are now widely used to explore and understand the interactions and shapes of the diffusion molecules.³⁰⁴⁻³⁰⁸

Diffusion NMR spectroscopy is commonly used to examine closely separated mixtures, or to screen ligands for binding interactions. It can give unique insight as a reliable guide for measuring the apparent molecular weight, secondary and tertiary structures.³⁰⁴⁻³⁰⁸ Some scientists accredit it as a special chromatographic method for physical component separation.

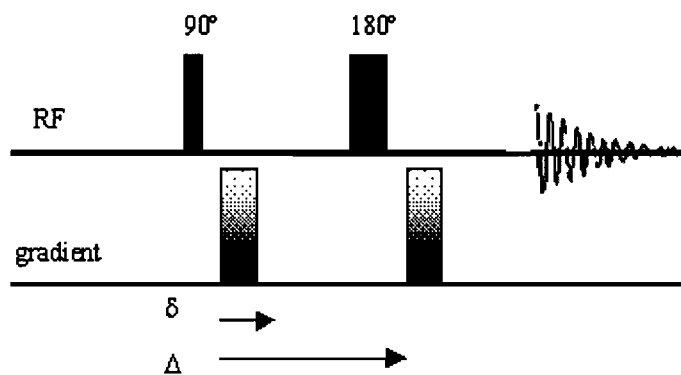
The diffusion ordered spectroscopy, or DOSY, experiments provide a way to separate the different compounds in a mixture based on the differing translation diffusion coefficients. Diffusion is analyzed in the DOSY experiment by observing the exponential decay of the NMR signal due to the diffusion taking place between a coding and a decoding gradient. The pulse field gradients methods are used as a direct or indirect way to probe molecular dynamics in solutions. The diffusion measurement usually carries out by observing the attenuation of the NMR signals during a pulsed field gradient experiment. During the experiment, a series of NMR diffusion spectra are acquired as a function of the gradient strength. The degree of attenuation is a function of the magnetic gradient pulse amplitude (G) and is proportional to the diffusion coefficient (D) of the molecule. The vertical axis shows the corresponding diffusion constants (D) of the molecules; the horizontal axis is encoded the chemical shift of the nucleus observed (such as ^1H). The molecular structural properties and size relationships can be obtained from the diffusion coefficient constant.³⁰⁹

3.2.3 ^1H NMR: Diffusion Experiment

In proton diffusion experiments, there are two gradient pulses applied: one before the refocusing 180° pulse and the other is after the 180° pulse. These two gradient pulses are identical in amplitude (G) and width (d). They are separated by a time (δ) and are placed symmetrically about the 180° pulse. The first gradient pulse is to dephase magnetization according to its position in the NMR tube. During the subsequent δ period, the spins are left to evolve and diffuse. Their chemical shift is refocused by applying the usual 180° pulse. At the end of the δ period, the spins that have diffused to a new

location in the NMR tube will not be refocused by the second gradient and will therefore attenuate the signal. These gradient pulses have no effect on stationary spins. During the experimental process, the echo time is left constant while the gradient strength G is varied (usually along the z-axis). The loss of magnetization can be plotted against the gradient strength to extract the diffusion coefficient D .

Figure 3.4: Example of the ^1H NMR: Diffusion Experiment



The self-diffusion coefficient for Brownian spheres is given by the Stokes-Einstein equation. The Stokes-Einstein Equation (equation 8) relates the diffusion coefficient (D) of a particle to its molecular shape via a friction coefficient (f) and temperature.

Equation 9: Diffusion Coefficient (D)

$$D = \frac{kT}{f}$$

- T : Temperature (Kelvin)
- K : Boltzmann constant
- f : Friction coefficient

If the solute is considered as a spherical particle with the effective hydrodynamic radius (R_D) in a solution of the viscosity (η); the friction coefficient (f) is given as the following equation. It should be noted that different theoretical descriptions are needed to describe the hydrodynamic frictional coefficient (f) for molecular species of different geometries.³¹⁰⁻³¹²

Equation 10: Friction Coefficient (f)

$$f=6\pi \eta R_D$$

f: Friction coefficient
 R_D : hydrodynamic radius
 η : solution viscosity

Indeed, the diffusion coefficient factors are affected by molecular shape, size, solvent viscosity, and the solution properties such as salt concentration, pH, and temperature, etc. It is well known that molecular self-diffusion coefficients (D) are measured by a pulsed field gradient spin-echo NMR experiment. Three most practical gradient field methods are pulsed gradient spin echo (PGSE), pulsed field gradient stimulated spin echo (PFG-SSE) and bipolar pulse longitudinal eddy current delay (BPP-LED). This technique is based on the application of the gradient field, which encodes and decodes the translational diffusion motion of the components in samples. To obtain the diffusion coefficient distribution from these experiments, the signal attenuation is detected and it depends on the gradient strength, the delay time between the pulse gradients and the diffusion coefficient of the molecules. Using the pulsed field gradient method, motion can be measured by evaluating the attenuation of the spin-echo signal.³¹³ The attenuated signal (A) can be calculated by the following equation.

Equation 11: Attenuated Signal (A)

$$\frac{A}{A_0} = \exp \left[-G^2 g^2 d^2 \left(T - \frac{d}{3} \right) \right] D$$

- A : Measured peak intensity
- A₀: Maximum peak intensity
- D : Translational diffusion coefficient (in cm²/s)
- g : Gyromagnetic ratio (2.675197x10⁴ G⁻¹s⁻¹ for ¹H)
- d : Duration of gradient
- T : Diffusion time (time between gradients)
- G : Gradient strength (G/cm)

Data are plotted according to the following equation and D is calculated as the slope.

Equation 12:

$$-\ln (A/A_0) = G^2 g^2 d^2 (T-d/3) D$$

The self-diffusion constant is measured in m² s⁻¹. Smaller molecules have larger D values (diffuse faster); the larger molecules move more slowly with small D values.

The Stokes-Einstein equation assumes spherical molecules that are much larger than the solvent molecules.

3.2.4. Nuclear Overhauser Effect Spectroscopy (NOESY)

The Nuclear Overhauser Effect (NOE) is the transfer of nuclear spin polarization from one nuclear spin population to another via cross-relaxation. The nuclear spins undergoing cross-relaxation are those which are close to one another in space, and the

effect decays at a rate of r^{-6} (r is the distance between the two nuclei). Thus, only atoms within a close distance (smaller than 5Å) can give a nuclear Overhauser effect. The spin-spin coupling can be observed by short-range dipolar couplings through close proximity in three-dimensional space.

NOESY, two-dimensional nuclear magnetic resonance spectroscopy (2D NMR), is one of the widely used techniques to study the conformation of molecules. NOE's are observed as the cross-peaks between two coupled nuclei. NOESY cross peaks of a spectrum indicate which protons are close in space. Thus, NOESY will allow for an estimation of the inter-nuclear distances and can provide precise molecular conformation.³¹⁴⁻³¹⁵ The NOESY spectrum can provide all possible correlations information such as the nuclear Overhauser effect, chemical exchange and conformational exchange to provide insight into molecular conformation and dynamics.³¹⁵

3.3 Ultraviolet-Visible Spectroscopy (UV/Vis)

UV/Vis absorption spectroscopy (sometimes called electronic spectroscopy) covers the ultraviolet-visible region ranging from the near-UV to the near-IR. The absorption measures electronic transitions from the ground to the excited state as a function of frequency or wavelength due to its interaction with a sample. UV/Vis spectroscopy is commonly used in the quantitative determination of solutions of transition metal ions and highly conjugated compounds. The UV and visible wavelength ranges are from 190 to 800 nm. Figure 3.5 displays the visible spectrum ranges from 400 nm to 800 nm.

Absorption of ultraviolet and visible (UV-Vis) radiation in both atoms and molecules is associated with excitation of electrons from low energy to higher energy

levels. The electron transition can either emit or absorb the energy. Most of the absorption in the UV-Vis spectroscopy occurs due to π -electron transitions or n-electron transitions within the molecules. Bonding to antibonding ($\pi \rightarrow \pi^*$) and non-bonding to antibonding ($n \rightarrow \pi^*$) transition usually occur in UV/VIS spectroscopy. The energy of light absorbed energetically is from the highest energy bonding π -orbital (HOMO) to the lowest energy antibonding π -orbital (LUMO). Figure 3.6 shows the diagram of the electron transition between the bonding, non-bonding and anti-bonding orbitals.

Figure 3.5: Diagram of visible spectrum wavelength (400nm -800nm)

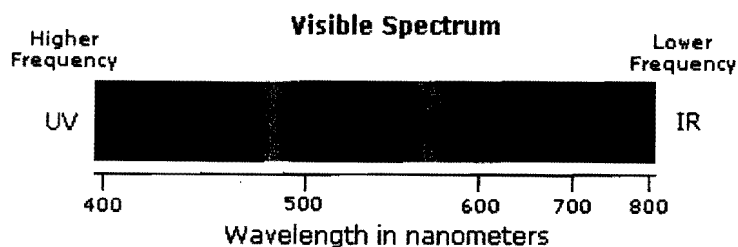


Image adapted from www.oocities.org

Figure 3.6: Diagram of the electron transition between the bonding, non-bonding and anti-bonding

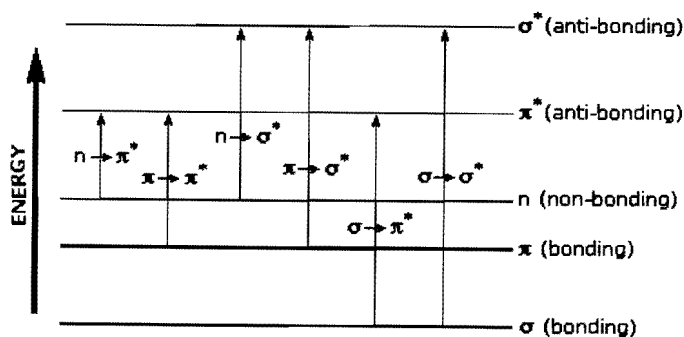


Image adapted from pharmaxchange.info

UV/Vis can be used in a wide range of analytical applications to measure the absorptive behavior of substances. The most routine measurement for UV-Vis is used as qualitative or quantitative analysis of the sample species. The qualitative measurement is served as identification for determining the molecular species, in which a given molecular species absorbs light in specific regions of the spectrum. For example, UV/Vis can be used in HPLC detector to identify the unknown analyte species. The quantitative analysis is measured the beam of radiation through a sample and detects the intensity of radiation that passes through the sample. The Beer-Lambert law is often used as a quantitative method to determine concentrations of absorbing species in solution. The absorbance (A) is directly proportional to the concentration of the absorbing species in the solution and the path length. Thus, UV/Vis spectroscopy can be used to determine the concentration and molar absorptivity of the compound in dilute solution.³¹⁶ The molar absorption, known as molar extinction coefficient (ϵ), is measured the molecule absorbs light at a particular wavelength.

Equation 13: Beer –Lambert Law

$$A = \epsilon bc$$

A: absorbance (no units, since $A = \log_{10} (I_0 / I)$)
 ϵ : molar absorptivity with units of $L \text{ mol}^{-1} \text{ cm}^{-1}$
b: the path length of the cuvette (cm).
c: concentration of the compound in solution, (mol L^{-1})
I : Intensity

Figure 3.7: A Diagram of a Double Beam Spectrometer

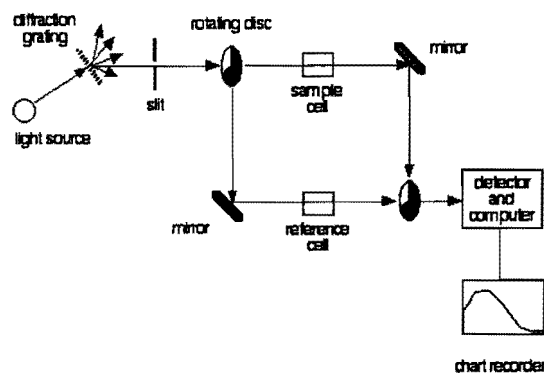


Diagram adapted from www.chemguide.co.uk/analysis/uv-visible/spectrometer

3.4 Circular Dichroism (CD)

3.4.1 Basic Theory

Circular dichroism (CD) is a chiroptical method which can be used to measure the differential absorption of rotational plane-polarized light of optically active compounds. The interaction between the chromophores in the chiral field introduces the perturbations leading to optical activity. CD measures the difference of the absorption of right- and left-handed circularly polarized light from chiral molecules. CD spectroscopy is used extensively to study higher order structures of chiral (asymmetric) macromolecules of all types and sizes, particularly in proteins and DNA. The wavelength range of CD is included far UV, ultraviolet light as well as infrared light. The UV light range from 180–300 nm is most commonly used in CD for DNA measurement because the DNA bases absorb light in this range.

The majority of biological molecules are chiral compounds. CD is sensitive to the conformational changes, structure and stability of the secondary or tertiary structure of proteins and DNA. CD spectroscopy can provide the representative structural information about the molecules, such as kinetic and thermodynamic information on macromolecules. Therefore, circular dichroism makes it an attractive and powerful tool in the biomolecule field.³¹⁷

The CD instrument measures the difference in left (L) and right (R)-handed absorbance of the circularly polarized light, ($\Delta A = A_L - A_R$) A more convenient characterization of CD is the difference in the molar extinction coefficients, $\Delta \epsilon$ (Delta Epsilon) is a function of wavelength which typically corresponds to an ellipticity (Θ) and is expressed in millidegrees.³¹⁸

Circular dichroism (CD):	$\Delta A(\lambda) = A_L(\lambda) - A_R(\lambda)$, where λ is the wavelength.
Molar circular dichroism ($\Delta \epsilon$):	$\Delta \epsilon = \epsilon_L - \epsilon_R$ (ϵ_L and ϵ_R is molar circular dichroism of left and right circularly polarized light)
Molar extinction coefficients:	ϵ_L : left circular polarized light (LCP) ϵ_R : right circular polarized light (RCP)
Molar concentration:	C (g/L), C is concentration
Path length:	l (centimeters)

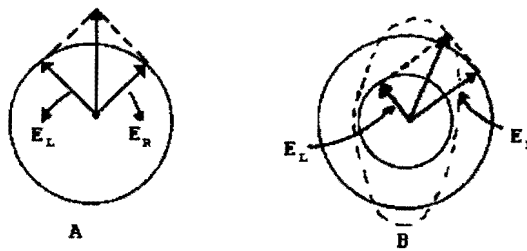
$$\Delta A = (\epsilon_L - \epsilon_R) Cl, \text{ measured as degrees of ellipticity}$$

If a right (R) and a left (L) circularly polarized wave of equal amplitude, are superimposed, the result is plane-polarized light. Figure 3.8 shows how the E vector of each will sum up in part A. Similarly, plane-polarized light can be decomposed into R and L components. If the amplitudes of the two circularly polarized waves are not the

same, the resultant E vector will follow an elliptical path and such light is said to be elliptically polarized. Elliptical polarized light is composed of unequal contribution of E_R and E_L circular polarized light. The degree of ellipticity (θ) is defined as the tangent of the ratio of the minor to major elliptical axis. Linear polarized light has 0 degrees of ellipticity. Figure 3.9 shows the examples of the left-handed and right-handed ellipticity.

$$\text{Degree of ellipticity } [\theta] = \tan^{-1} \left(\frac{E_L}{E_R} \right)$$

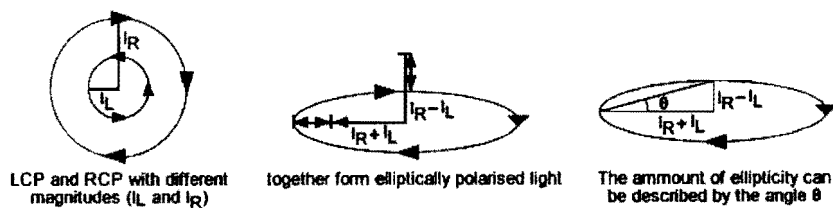
Figure 3.8: Elliptical Polarization



<http://www.zeably.com>

E_R : magnitude of the electric field vector of right-circularly polarized light
 E_L : magnitude of the electric field vector of left-circularly polarized light

Figure 3.9: Example of the left-handed and right-handed ellipticity (θ)



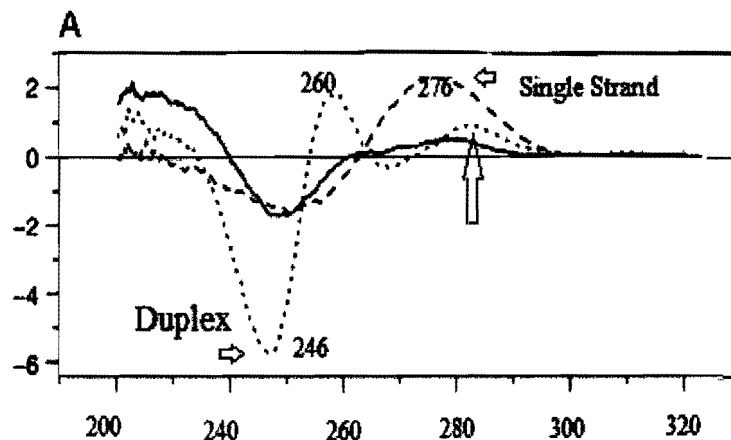
Adapted from www.analyticalchemistrygsu.com

A circular dichroism signal is defined as positive or negative, depending on whether L-CPL(circular polarized light) is absorbed to a greater extent than R-CPL (a positive CD signal) or to a lesser extent (a negative CD signal). The CD instrument is quite sensitive and is capable of measuring with millidegree precision.

CD is a particularly powerful technique for examining the conformational changes of proteins and nucleic acids. CD is usually used in monitoring the structural changes due to changes in environmental condition, such as temperature, ionic strength, denaturants and pH.³¹⁹ The advantages of using CD spectroscopy are as follows: (1) very little amount of sample is required in biological buffers (200 μ l of 0.5 mg/ml solution in standard cells), (2) CD will not destroy or decompose the compound and (3) CD can be monitored very accurately. One drawback of CD measurement is interference by solvent absorption in the UV region. For better performance in CD measurement, the sample is required to be in dilute solution with non-absorbing buffer for measurements below 200 nm. Figures 3.10 and 3.11 give examples of CD spectra to provide useful references for a variety of nucleic acid structures, ranging from single-stranded to quadruplex forms. Single strand has one positive peak at 276 nm and one negative peak at 250 nm. Duplex DNA has one negative at 246 nm and two positive peaks at 260 nm

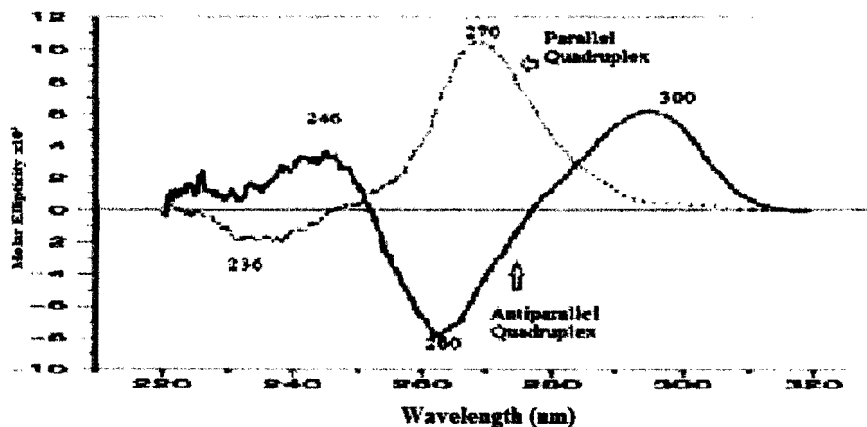
and 285 nm . Parallel quadruplex DNA has one negative peak at 236 nm and one positive peak at 270 nm. The antiparallel quadruplex DNA show two positive peaks at 246 nm , 300 nm and one negative peak at 260 nm.

Figure 3.10: Example of typical reference spectra of single strand and duplex DNA



Adapted from Bishop, G. R. et al, *Current Protocols in Nucleic Acid Chemistry*,2003.

Figure 3.11: Typical reference spectra of parallel and anti-parallel quadruplex DNA



Adapted from Bishop, G. R. et al, *Current Protocols in Nucleic Acid Chemistry* 2003.

CHAPTER 4 MATERIALS AND METHODS

4.1 Materials

Polyethylenimine, high molecular weight, water-free polymer (M_w 25000 D, unit molecular weight 45 D) was purchased from Aldrich (St. Louis, MO, USA). The cross-linking agent, isophthalaldehyde, 97% and D₂O deuterium oxide 99.9 atom % D were also purchased from Aldrich. The phosphate buffer solution was prepared with 5 mM KH₂PO₄, 5 mM K₂HPO₄, 1 mM EDTA at pH 7.0. All the solid buffer chemical compounds were purchased from Sigma Chemicals. EDTA disodium salt was purchased from Fisher. Tris buffer solution was prepared and the pH adjusted with concentrated KOH to pH 7.1. TRIZMA BASE was purchased from Sigma-Aldrich. Tris HCl was purchased from J.T Baker. Potassium chloride was purchased from Fisher Scientific.

Dichloromethane was purchased from PHARMCO-AAPER, HPLC grade. The 0.2 μ m filters were purchased from Millipore Corporation. The DNA primer TTTTGGGG was purchased from Invitrogen or Sigma Aldrich (St. Louis, MO) (custom primers, 5' to 3' TTTTGGGG). 5,10,15,20-tetrakis (1-methyl-4-pyridyl)21H,23H-porphine,tetra-p-tosylate salt -Porphyrin (H₂TMP_yP) was purchased from Aldrich. Polyvinylpyridine, polyallylamine, poly (L-lysine), polyethylene oxide (PEO), poly(4-vinylpyridinium bromide), poly(4-vinylpyridine N-oxide), poly(N-vinylpyrrolidone); poly(ethylene glycol), Poly(L-ornithine)HCl, poly(2-vinylpyridine), Poly(4-vinylpyridine) were purchased from Polysciences. Metafectene Pro and Metafectene Easy are a gift of Biontex, poly (2-ethyl-2-oxazoline) with the MW200,000 and 50,000 were purchased from Alfa Aesar Company. The polymers were used without further purification.

4.1.1 Buffer Solutions

Potassium phosphate buffer solution (KPBS): 10X KPBS was prepared and utilized as a stock solution to prepare subsequent working buffer solutions for samples. Table 2 shows the KPBS 10X stock solution preparation. The reagents were weighted and transferred into the volumetric flask (1L) and Q.S with the milli Q distilled deionized water. The buffer solutions were mixed well and filtered through a 0.45 μm filter (stored at 4⁰C).

Table 2: Potassium Phosphate Buffer (KPBS) 10 X Stock Solution

Reagent	Molecular Weight	Grams(g)	Moles
Monobasic KH_2PO_4	136.09	5.716	0.042
Dibasic K_2HPO_4	174.18	10.102	0.058
$\text{K}_2\text{EDTA}\cdot 2\text{H}_2\text{O}$	404.5	0.405	0.001

Working solutions were prepared by transferring 100 mL of the KPBS stock solution (10X) into 1 L volumetric flask and QS to the volume. The buffer solution was then adjusted to pH 7.0 by adding KOH (1M) solution.

Tris buffers were prepared by adding 2.9 g of Tris-HCl, 0.072 g of TRIZMA BASE and 10.8 g of potassium chloride into one liter of distilled water. The buffer solutions were mixed well and adjusted with KOH to pH 7.1, then stored under 4⁰C condition.

4.2 Methods

4.2.1 DNA Preparation

4.2.1.1 Dialysis Procedure

The purpose of the dialysis treatment of the DNA oligomers is to ensure the purification of the oligomers. Dialysis tubing from Spectro-Pro industries with a 1000 molecular weight cutoff (MWCO) pore size was used for DNA dialysis. Pre-treatment of the dialysis tubing to remove the preservative before use is required. The dialysis tubing was placed in DI water and heated to boiling, and sodium carbonate was added, along with EDTA and boiling continued to one hour. After the solution was cooled, the solution was removed and replaced with a large amount of distilled water. The magnetic stirring bar was placed in the bottom of the beaker to keep the water agitated. This procedure needed to be repeated several times to ensure that all the preservatives were removed. After the pre-treatment, the dialysis tubing is stored at 4°C in the refrigerator for future use.

If the DNA oligomers are not HPLC grade, the DNA must be purified by dialysis before use. The DNA samples were placed into dialysis tubing with a large amount of DI water with continuing stirred during the procedures. The water was changed every 4 hours and this was continued for 48 hours. These procedures were repeated several times to ensure the complete removal of any unwanted salt from the oligomers.

4.2.1.2 Quadruplex DNA Preparation

DNA stock solutions were prepared just prior to use by reconstitution of the oligomer in purified distilled water. The dry oligomers were reconstituted into a given volume of DI water depending on the DNA concentration needed. The oligomers were reconstituted into DI water, and then each sample solution was lyophilized at room temperature to remove the water. Unused portions of the stock samples were stored frozen at -20 °C. The DNA concentration was determined by UV-Vis (CARY 100 Bio UV-Vis Spectrophotometer, Varian Company). The concentrated stock solution of DNA was diluted before the measurement. The concentration of the T₄G₄ was calculated spectrophotometrically using the Beer's Law ($A = \epsilon bc$) equation.

The milli-Q purified deionized water was used to prepare the buffer solutions. Appropriate amounts of the DNA stock solutions were aliquot for analysis, lyophilized, and reconstituted into buffer. In this experiment, the dry oligomers were reconstituted into 1 mL of potassium phosphate buffer (5 mM KH₂PO₄, 5 mM K₂HPO₄, 150mM KCl, pH 7.0) prior to quadruplex formation. The sample solution was treated in water bath at 95°C in a Fisher Scientific, model 9100 water bath for 2 minutes and slowly cooled down to room temperature. This process was done by heating the samples in a dry water bath, then turning the power off after 2 minutes, and letting the samples cool to room temperature slowly within the heating block. Slow cooling is to ensure a slow annealing of the DNA and subsequent formation of stable quadruplex DNA. The samples were equilibrated for 48 hours at 4 °C prior to analysis. The formation of quadruplex DNA structure was verified by circular dichroism measurement. The gel electrophoresis (SDS PAGE) also confirmed the formation of the quadruplex T₄G₄ structure.

4.2.2 Polyethylenimine Intra-Molecular Cross-Linking

4.2.2.1 Intra-molecular cross-linking (in solution)

The stock solution of saturated isophthalaldehyde was prepared by adding the appropriate amount of the compound in water. This saturated solution was filtered through filter paper to remove any undissolved material. The PEI solutions were prepared with different concentrations. The PEI solution was added to a saturated isophthalaldehyde in a drop-by-drop manner. The resulting solution was stirred for two hours. After two hours reaction time, the solution was precipitated by adding 2-propanol. The precipitated solid was air dried and re-dissolved into D₂O for NMR experiments.

4.2.3 Cross-Linking Examined by NMR Experiment

The VARIAN INOVA 500 MHz MNR Spectrometer System was used in ¹H *in situ* study. This NMR spectrometer is interfaced to a workstation that controls the NMR via the Varian software.

4.2.4 In Situ Study

The ¹H NMR *in situ* samples were prepared by adding a sufficient amount of isophthalaldehyde into D₂O solution. Due to the low solubility of the isophthalaldehyde, the excess amount of the isophthalaldehyde was filtered through the filter paper. The clear solution was used to run ¹H NMR as isophthalaldehyde standard spectra. The polyethylenimine ¹H NMR sample was prepared by transferring the sufficient amount of compounds into 5 mL of D₂O. In order to identify the optimum PEI/isophthalaldehyde ratio in this study, the concentration of the corresponding polymer solution was adjusted to produce different ratios. The PEI/isophthalaldehyde ratio was prepared at 5, 15, 25, 67

and examined by *in situ* ^1H NMR. The NMR spectra were recorded on GE 300 MHz spectrometer at different time points.

4.2.5 Identify the Intra- Molecular Cross-Linking by Organic Solvent Extraction and Examined by UV-Vis

4.2.5.1 UV-Vis Experiment

A Cary 300E Bio or Cary 100E spectrophotometer (Varian, Inc.), interfaced to a Windows based computer with Cary/Varian Win UV Bio version 2.0 software, was used for studies. Both spectrophotometers are equipped with a Peltier thermoelectric heating/cooling system which include a multi-cell device and a sample compartment. The spectrophotometers have the capabilities of using either external probe to measure the temperature inside of sample cuvette or the ability to use the cell block to measure the temperature of the sample compartment.

To effect the intramolecular cross-linking formation, the stock solution of PEI was prepared at 0.0184 M. The isophthalaldehyde stock solution was prepared at 0.0012 M. The volume ratio of the PEI and isophthalaldehyde was prepared at 1:1, 3:1, 5:1 and 16:1. The equivalent mole ratio of the PEI (by monomer mass)/ isophthalaldehyde was 15, 45, 75 and 240.

The extraction samples were prepared by adding the dichloromethane into the cross-linked sample with 1 to 1 ratios. The mixtures were shaken for 10 min and allowed to stand for 20 minutes to separate the top and bottom layers. The pure isophthalaldehyde extraction sample was used as a control sample. The PEI/isophthalaldehyde mole ratio at 75 and 240 were prepared in the same manner with the same volume of the

dichloromethane. All the samples were prepared with potassium phosphate buffer at pH 7.0. The samples were analyzed using an Olis HP 8452 A Diode Array Spectrophotometer.

4.2.5.2 Intermolecular Cross-Linked PEI: bulk preparation

The bulk samples were prepared by transferring 1 g of water free 25 kD polyethylenimine into a beaker and adding 0.1 g of the isophthalaldehyde. The mixture was placed into a water bath and stirred for 15 minutes under 100°C temperature control. This process was to remove any remaining water from PEI. The products of the PEI and isophthalaldehyde mixture turned into a yellow solid color. In order to test the solubility in water, a sufficient amount of water was added into the final products and stirred for 30 minutes. The PEI and isophthalaldehyde cross-linked bulk samples remained solid yellow color materials. The bulk samples continued to stir overnight and the remaining compound was still insoluble in water. This observation provided the indications that the bulk PEI/isophthalaldehyde reaction formed intermolecular cross-linked PEI.

4.2.6 Characterization of Particle Size by Light Scattering (QELS)

Light scattering spectroscopy was performed in a Wyatt Dawn EOS light scattering spectrometer (Wyatt Technology Corporation). The Wyatt spectrometry has provided the multi-angle light scattering (MALS) detector and the quasi-elastic light scattering detector (QELS) selection. The MALS-QELS system can be used to measure radius of gyration (r_g) and radius of hydrodynamic (r_h) at the same time; the radius of gyration is determined from the angular dependence of scattered light intensity. The radius of

hydrodynamic is measured the fluctuation of the light scattering of the diffusion molecules. MALLS utilized 18 detectors at various angles, ranging from 15° to 180°; each detector was normalized to the 90-degree detector using an isotropic scatterer standard.

The molecular aggregation behavior was studied by dynamic light scattering. The measurements were performed at 4°C with an incident laser light beam of 685 nm at a scattering angle of 90°. Polyethylenimine solutions were prepared at concentrations of 0.1 M and 1.8 M in phosphate buffer at pH 7.0. Water was pre-filtered through 0.02 µm Whatman nanotop filters before being used to prepare the solution. The sample solutions were filtered through 0.2 µm filters prior to use and stored at 4°C. The isophthalaldehyde solutions were prepared at 0.004M in a phosphate buffer solution. The solutions were filtered through 0.2 µm filters and stored under 4°C condition. The isophthalaldehyde was titrated into the PEI solutions. The mixing solution was stirred for 10 minutes followed by 2 minutes of sonication. The molecular cross-linking reaction was performed by dynamic light scattering to investigate whether the formation of inter-molecular cross-links (aggregation) or intra-molecular cross-links.

4.2.7 PEI / Quadruplex DNA Circular Dichroism Study

Circular dichroism measurement was carried out using a 62 A DS AVIV CD spectropolarimeter (Aviv Associates, Lakewood, NJ) equipped with a multi-cell holder. The temperature of the Peltier heating/cooling device was assisted by an Isotemp water bath model 9100 (Fisher Scientific). A cold water supply circulates around the Xenon lamp to prevent overheating. The spectrophotometer was interfaced to a DOS-based

computer. The AVIV version 3.14 software was used for data collection and processing. A nitrogen purge was used to eliminate any moisture on the optics. Cuvettes were scanned versus water prior to experiments to ensure that no CD active impurities remained in the cuvettes. CD measures the interaction of circularly polarized light with molecules. All CD spectra were read from 210-320 nm at 1.0 nm increments with a bandwidth of 1nm and a time constant of 1.0 sec at 25°C.

Samples were prepared by reconstituting lyophilized DNA oligomer into 100 mM phosphate (K^+) buffer solution (pH 7.0). The experiment was performed by titration with pre-mixed DNA/10x PEI solution. This procedure is designed to keep the DNA concentration constant. The DNA-PEI titration was conducted by adding the stock solution of DNA/10x PEI stepwise (aliquot of stock) directly to 250 μ L of starting volume of DNA in solution. CD spectra were measured subsequently after the spectra were stabilized. The stock concentration of the quadruplex DNA was 47 μ M. 50 μ L of DNA stock solution was transferred into 450 μ L buffer solution which was made up the final quadruplex DNA concentration at 4.7 μ M. The stock solution of PEI was 470 μ M. The DNA/10x PEI pre-mixed solution was prepared at 500 μ L for the titration purpose. The DNA pre-mixed solution was transferred 1 μ l and 20 μ l of the each aliquot into cuvette of 250 μ l of DNA (4.7 μ M) solution. This fixed quadruplex DNA concentration is used to more readily monitor changes in the structure.

4.2.8 Polymers Screen Using UV-Vis Spectroscopy Studies

To investigate the interaction between polymers and quadruplex DNA, optical studies were carried out using the tetra (N-methylpyridyl) porphyrin as a probe. The polymers used in this study are the following: poly(2-vinylpyridine-N-oxide), polyallylamine, poly (L-lysine), poly(4-vinylpyridinium bromide), poly(4-vinylpyridine N-oxide), poly(N-vinylpyrrolidone); poly(ethylene glycol), poly(L-ornithine)HCl, poly(2-vinylpyridine), poly(4-vinylpyridine), and the lipid agents Metafectence Pro, Metafectence Easy. All experiments, except where specifically indicated, were performed at 25°C in potassium phosphate buffer at pH 7.0. The concentration of the polymer solutions was varied according to their solubility in phosphate buffer. A stock solution of the porphyrin was prepared at a concentration of 5 μ M and stored in phosphate buffer. The porphyrin solution must be protected from light to prevent degradation. The order of the experiment is as follows:

- 1.) UV-Vis of porphyrin solution used as a control spectrum.
- 2.) Addition of quadruplex DNA into porphyrin solution, measurement of the UV spectrum.
- 3.) Addition of polymer into the DNA / porphyrin mixed solution, measurement of the UV spectrum.

The porphyrin UV maximum peak (Soret band) is at 422 nm when it is a free porphyrin. The UV spectrum of the maximum peak of the quadruplex DNA/porphyrin complex was observed at 433 nm. When polymer is added to the DNA /porphyrin complex, the Soret band may stay at 433 nm (DNA-porphyrin complex intact) or shift back to 422 nm (DNA-porphyrin complex disrupted).

4.2.9 ^{31}P NMR Study: Binding Interaction of Quadruplex DNA / Polymer

All ^{31}P NMR experiments were carried out on a Bruker DPX400 NMR spectrometer equipped with a BBFO broad-band probe. The spectra were taken at ^{31}P frequency of 161.975 MHz, with a spectral width of 40 ppm, a 90° pulse of 9.2 μs . The spectra were referenced to an external 85% phosphoric acid sample (0 ppm). All spectra were processed using Bruker TopSpin 1.3 software. The quadruplex (T_4G_4) DNA was incubated in a saline solution at 150mM KCl at pH 7.0 (not in potassium phosphate buffer) to avoid signal from the buffer. The deionized water containing KCl would lower the buffer solution pH which will require the researcher to adjust the pH back to pH7.0 with 1M KOH. All polymers (polyethylenimine, poly (4-vinylpyridine N-oxide) and poly (N-vinylpyrrolidone) were prepared with 98% D_2O .

4.2.10 Diffusion NMR Experiment

4.2.10.1 Sample preparation

DNA quadruplex (T_4G_4) concentrations were adjusted to range from 0.5-1.0 mM in phosphate buffer (pH 7.0). Deuterium oxide (D_2O) was added to DNA samples prior to loading into NMR tube. NMR samples were prepared about 500 μL for the experiment. Polymers preparation: The maximum concentration of the polymer depends on the solubility of the polymer. Poly (N-vinylpyrrolidone) was prepared at 4 mM. Poly (4-vinylpyridine N-oxide) was prepared at 1 mM. PEI was prepared from 2 mM to 10 mM.

4.2.10.2 Experiment conditions

All samples were prepared in 90% H_2O /10% D_2O in order to observe the exchangeable imino proton of the G nucleotides. The 1D and 2D ^1H NMR spectra were obtained on a Bruker Avance 600 MHz spectrometer equipped with a triple-resonance TCI cryoprobe, operating at 600.11 MHz for the proton frequency and using the following parameters: 90° ; pulse, 7.60–8.50 μs ; 4–8 scans; recycle time 3–8 s; spectral width 6000 Hz and 16–32 k data points.

The DOSY experiment spectra were recorded on Bruker Avance 700 MHz for proton equipped with a pulsed gradient unit. The experiments used a stimulated echo and bipolar gradient pulses for diffusion.³²¹ The duration of the magnetic field pulse gradients (δ) was optimized for each diffusion time (Δ) in order to obtain 1–5% residual signal with the maximum gradient strength. The gradient strength was varied linearly from 2% to 95% in 16 steps. The temperature was set and controlled to 300 K with an air flow of 670 L per hour in order to avoid any temperature fluctuations due to sample heating during the magnetic field pulse gradients. After Fourier transformation and baseline correction the diffusion dimension were processed and analyzed using Bruker Topspin 2.1 software.

2D DOSY experiments with a ^1H detection for quadruplex (T_4G_4) DNA and Poly (N-vinylpyrrolidone) mixture sample were performed on a Bruker Avance 700 MHz using stimulated echo and bipolar gradient pulses for diffusion.

2D DOSY experiments with ^{31}P detection for quadruplex (T_4G_4) DNA and Poly (4-vinylpyridine N-oxide) samples were performed on a Bruker DPX 400 MHz NMR spectrometer using the same pulse sequence as above.

4.2.11 PEI and Quadruplex DNA Complex Structural Transition Study by CD

PEI samples were prepared at the concentration of 3.76 mM and quadruplexes (T₄ G₄) DNA was prepared at the concentration of 0.7536 mM. The DNA concentration was determined on the basis of UV absorption at 260 nm of the sample measured in phosphate buffer (pH 7) at 95°C. The molar extinction coefficient ($71400 \text{ cm}^{-1}\text{M}^{-1}$) was using the previous experiment data which was determined by Beer Lambert law. The samples were prepared using 1 to 1 and 1 to 5 molar ratio of the quadruplex DNA and PEI. The experiments were performed on Aviv Associates CD Spectropolarimeter Model 62-ADS. The data were collected every 1 nm, with averaging time of 3 sec and bandwidth of 1 in a 0.1 cm path length cuvette.

The time interval profile was carried out at initial, two and half and four hour for quadruplex DNA/PEI complexes. The evaluations of the temperature influence on the structures were also included in the study. The incubation temperature at 4°C and 9°C were used to investigate the structural transition. All the experiment conditions are described as above.

CHAPTER 5 RESULTS AND DISCUSSION

5.1 Molecular Cross-Linking Studies

5.1.1 ^1H NMR investigates PEI cross-linking

Polyethylenimine is a well-known macromolecule for binding DNA.³²²⁻³²³ Several recent studies have been reported where the structure of PEI was altered to change the nature of the macromolecule and its binding properties.³²⁴ It was our intention to develop a cross-linker for PEI, which would alter the DNA binding and allow for molecular imprinting on specific DNA structures.

Accordingly, we examined the reaction of isophthalaldehyde (1,3-benzene dialdehyde) with PEI. Aldehydes and primary amines react to form imines. Purely aliphatic imines are unstable in the presence of water. When either the aldehyde or amine is aromatic, such imines are relatively stable to hydrolysis. The cross-linking of PEI by isophthalaldehyde occurs when the two aldehydes react with two of the primary amine ($-\text{NH}_2$) groups found in highly branched PEI. Cross-linking could be intra-molecular (both $-\text{NH}_2$ groups on the same PEI molecule) or inter-molecular ($-\text{NH}_2$ groups on different PEI molecules). The cross-linking reactions were studied by a variety of techniques including NMR, UV-Vis, and QELS.

First, cross-linking reactions were conducted in deuterium oxide and monitored by ^1H NMR. The proton NMR spectra revealed that the cross-linker (isophthalaldehyde) reacted with PEI very rapidly. We have found that the ratio of the PEI/isophthalaldehyde is a critical factor for the formation of the intra-molecular cross-linking. When the ratio of the PEI/isophthalaldehyde is low (high concentration of isophthalaldehyde), the mixing solution immediately formed chunks of white precipitate. These white solids were

insoluble in D₂O. When the PEI/isophthalaldehyde ratio is too high (low concentration of isophthalaldehyde), few cross-links are formed during the reaction. Table 3 showed the observation results of bulk quantity reactions of PEI and isophthalaldehyde in different ratio. The resulting white precipitate compounds were re-dissolved in D₂O and examined by proton NMR. The ¹H NMR spectra of isophthalaldehyde and polyethylenimine are shown in figure 5.1 and figure 5.2, respectively. Figure 5.3 shows the ¹H NMR spectrum of an initial time point of the PEI cross-linking reaction. The CHO proton resonance can be observed at about 9.9 ppm. However, two hours after initiation of the PEI cross-linking reaction, the CHO proton resonance can no longer be observed in the ¹H NMR spectrum (figure 5.4). Comparing figures 5.3 and 5.4, we have observed that the ¹H NMR peak for the isophthalaldehyde CHO proton disappeared after reacting with PEI for two hours. This indicates that the isophthalaldehyde has cross-linked the PEI molecules, while the broadening of the aromatic isophthalaldehyde peaks also supports cross-linking.

Table 3: Summary of the PEI/ Isophthalaldehyde Cross-linking Reaction

	Molar Ratio	Comment
PEI/Isophthalaldehyde	1/8	Large white precipitate , cross-linking reaction occurred immediately
PEI/Isophthalaldehyde	25	Cross-Linking Reaction occurred
PEI/Isophthalaldehyde	67	Cross-Linking Reaction occurred
PEI/Isophthalaldehyde	75	Cross-Linking Reaction occurred

Note: The molar ratio in the experiment is mole PEI monomer/mole isophthalaldehyde not moles PEI polymer/moles isophthalaldehyde.

Figure 5.1: ^1H NMR of Isophthalaldehyde

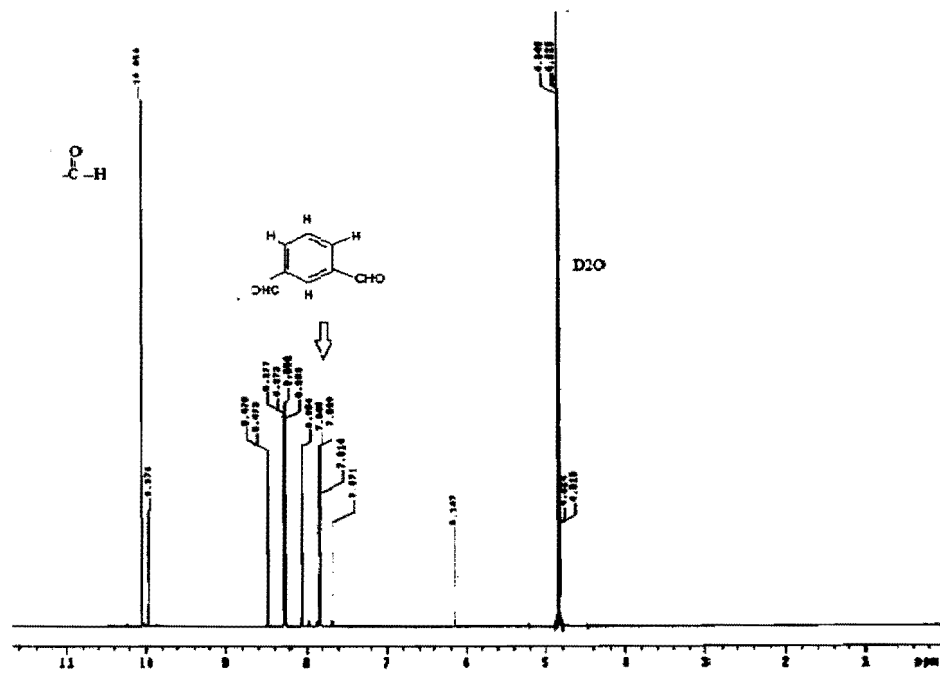
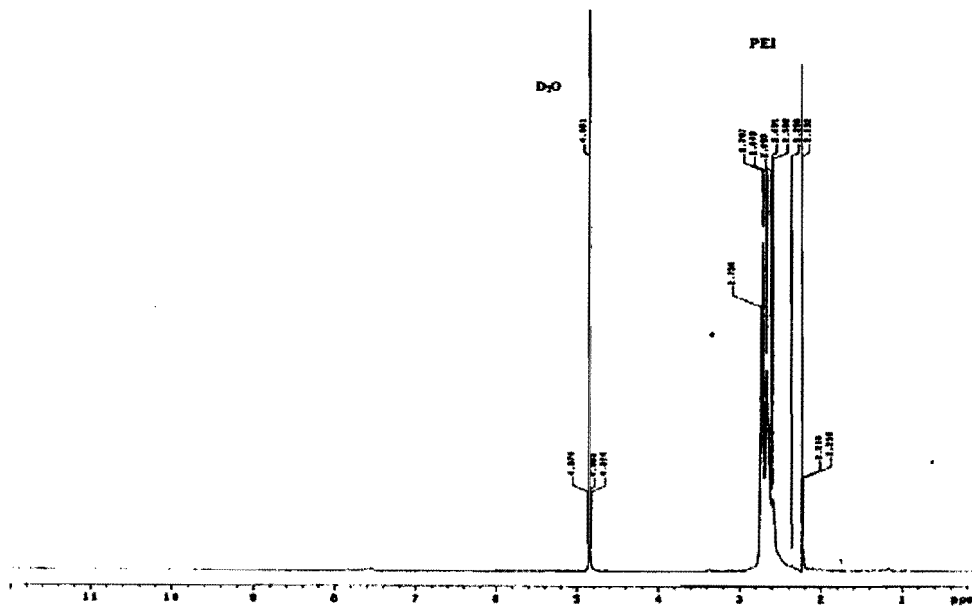


Figure 5.2: ^1H NMR of Polyethylenimine



5.1.2 UV-Vis/Extraction Experiments to Identify the Cross-linking Reaction

To show that isophthalaldehyde is being chemically incorporated into the PEI as a cross-linker, the extraction studies were performed. The concept of the extraction experiment was to examine whether the isophthalaldehyde could be removed by extraction with dichloromethane. If isophthalaldehyde can be removed, the isophthalaldehyde is not cross-linking covalently. If isophthalaldehyde cannot be removed, this will support the cross-linking by covalent bonding. The UV-Vis spectra of isophthalaldehyde and PEI were recorded as reference standard spectra.

PEI and isophthalaldehyde were prepared in stock solutions and aliquots were mixed in different ratios. In figure 5.5 (A) shows the isophthalaldehyde and PEI reference spectra of UV-Vis absorption spectra. In figure 5.5(B) shows the UV-Vis absorption spectra of different ratios of isophthalaldehyde and PEI before extraction (PEI/ Isophthalaldehyde from 1:1, 3:1, 5:1 and 16:1). From the spectra, we observed that increasing the volume ratio of the PEI / isophthalaldehyde resulted in decreasing the intensity of the PEI/Isophthalaldehyde (as expected with less isophthalaldehyde).

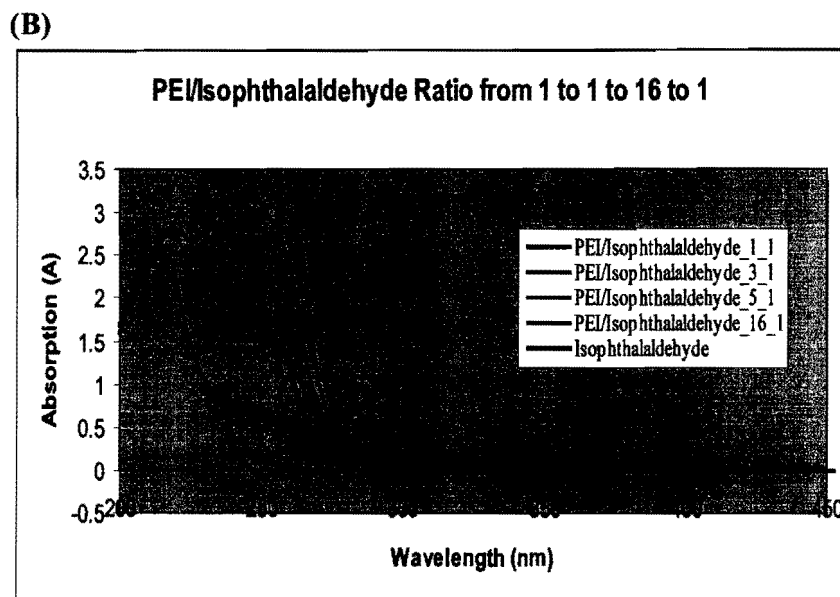
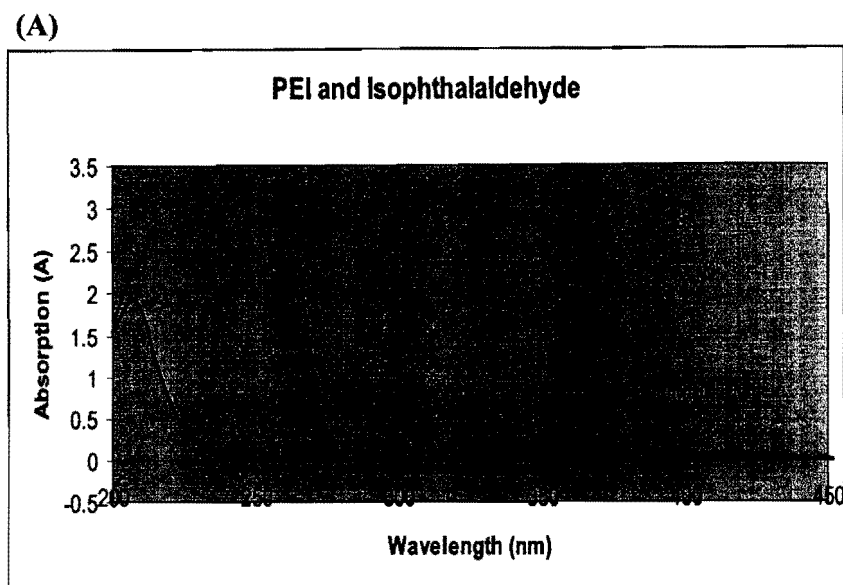
Table 4 summarizes the pre-extraction (before added dichloromethane) of the PEI/ isophthalaldehyde data in different ratios which were made by mixing stock solutions of the PEI and isophthalaldehyde in the volume ratios. If absorptivity stays constant (no change due to cross-linking) then we should find the predicted results same as observed results. The volume ratio of the PEI and isophthalaldehyde was prepared from 1:1, 3:1, 5:1 and 16: 1; we observed the decrease in % of relative amount of the isophthalaldehyde at wavelength λ_{\max} (294 nm) from 42% to 6.3% (Table 4). When no PEI added, the λ_{\max} absorption was observed 0.8868 absorption unit which is equivalent to the 100% of the

relative amount of isophthalaldehyde. In 1 to 1 ratio of PEI and isophthalaldehyde the results shows a 0.3737 absorption unit at λ_{\max} , which is corresponded to 42.1 % of relative amount of isophthalaldehyde (the expected value is 50%). In 16 to 1 ratio of PEI/Isophthalaldehyde, the λ_{\max} is decreasing to 0.0565 absorption unit which is corresponded to 6.3% of isophthalaldehyde remaining in the solution mixtures (expected value is 5.9%). The predicted value and observed value of isophthalaldehyde (at λ_{\max}) are shown in table 4 as expected.

Table 4: Summary the pre-extraction of PEI / Isophthalaldehyde from 1:1 to 16:1 (Isophthalaldehyde λ_{\max} = 294nm)

PEI/Isophthalaldehyde	A=λ_{\max}294nm	Predicted % relative amount of Isophthalaldehyde	Observed % relative amount of Isophthalaldehyde
0:1	0.8868	100.0	100.0
1:1	0.3737	50.0	42.1
3:1	0.1781	25.0	20.1
5:1	0.1572	16.7	17.7
16:1	0.0565	5.9	6.3

Figure 5.5: PEI/ Isophthalaldehyde in Variety Ratio Study by UV-Vis

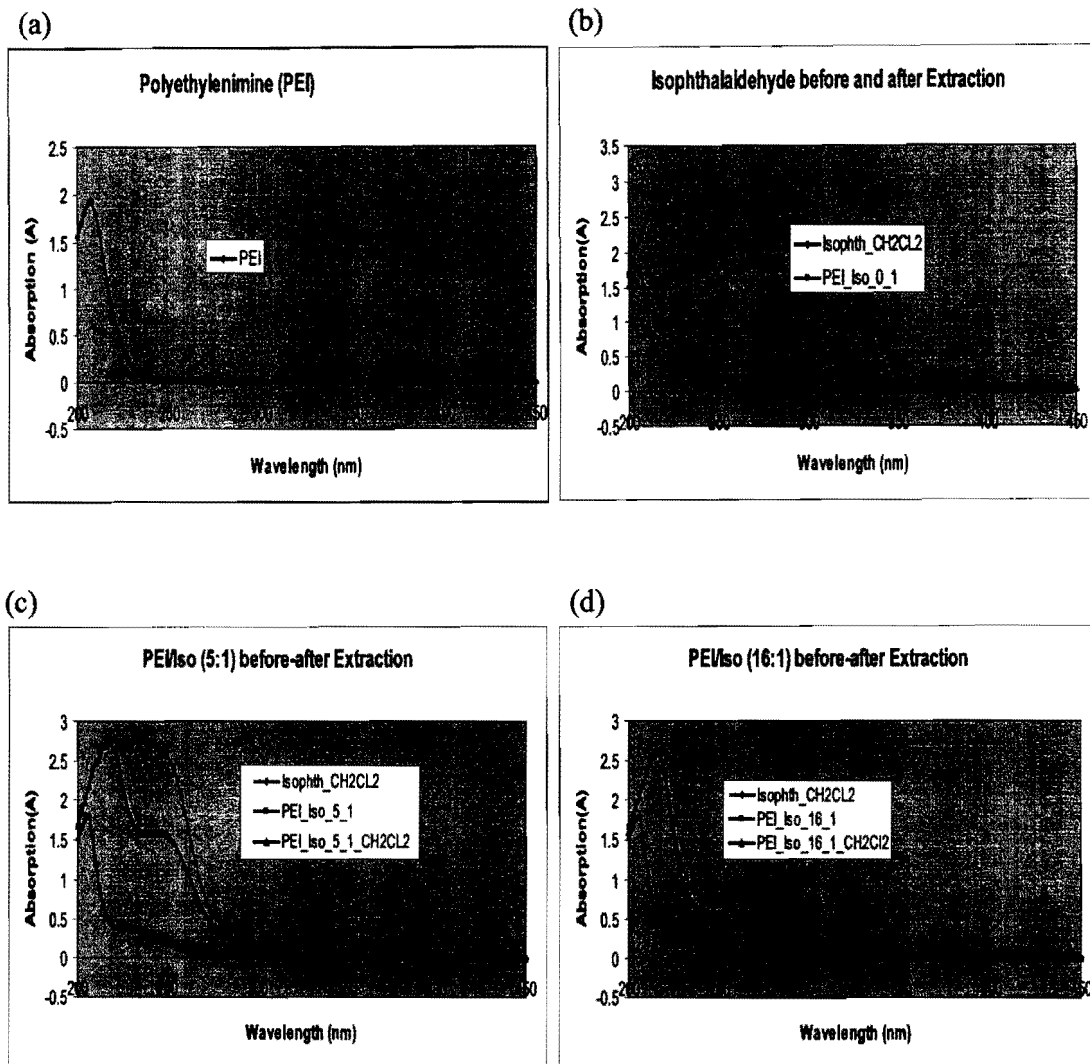


(A) UV-Vis Spectra of polyethylenimine and isophthalaldehyde. (B) UV-Vis Spectra of polyethylenimine and isophthalaldehyde in a different ratio from 1 to 1 up to 16 to 1

Figure 5.6 shows the UV-Vis spectra of the PEI/ isophthalaldehyde mixtures before and after extraction by dichloromethane (CH_2Cl_2). The UV-Vis spectra of PEI/ isophthalaldehyde mixtures were recorded before and after extraction with dichloromethane (DCM). The figure 5.6 spectra data shows that the isophthalaldehyde alone is extracted into dichloromethane with 98.1% efficiency. If isophthalaldehyde is chemically incorporated into PEI, it cannot be extracted into dichloromethane. We compared the UV-Vis spectra of the PEI/Isophthalaldehyde at ratio of 5: 1 and 16:1 before and after the dichloromethane extraction. From the DCM extraction data, we have observed the mixtures of PEI/ isophthalaldehyde at a ratio of 5 to 1; the isophthalaldehyde has 63.6% of remaining in the mixtures. The PEI/isophthalaldehyde at a ratio of 16 to 1 has 77.8% of isophthalaldehyde remaining in the mixtures (Table 5).

From these results, it can be concluded that the PEI/isophthalaldehyde volume ratio of 16:1 has smallest percentage of isophthalaldehyde removed from the mixture. The higher ratio of PEI to isophthalaldehyde allows a greater proportion of the aldehyde to form cross-links.

Figure 5.6: Polyethylenimine and isophthalaldehyde extracted by dichloromethane



(a) UV spectrum of PEI (b) UV spectra of isophthalaldehyde before and after extraction by CH_2Cl_2 (c) UV spectra of PEI and isophthalaldehyde mixture at ratio of 5 to 1 before and after extraction by CH_2Cl_2 (d) UV spectra of PEI and isophthalaldehyde mixture at ratio of 16 to 1 before and after extraction by CH_2Cl_2 .

Table 5: Summary UV-Vis absorption data: the isophthalaldehyde extracted by dichloromethane in different ratios of PEI / isophthalaldehyde.

PEI/Isophthalaldehyde	A= λ_{\max} 294nm
PEI (no isophthalaldehyde)	0
Isophthalaldehyde	0.8868
Iso-Dichloromethane (extraction)	0.0173
PEI/Iso=5:1	0.2824
PEI/Iso=5:1 (extraction)	0.1797
PEI/Iso=16:1	0.0967
PEI/Iso=16 :1(extraction)	0.0753

Iso : an abbreviation of isophthalaldehyde

$$\% \text{ Remaining} = \frac{\text{Abs (after extraction)}}{\text{Abs (before extraction)}} \times 100\%$$

Abs : abbreviation of absorbance

Table 6: Percentage Remaining of Isophthalaldehyde: the mixture of PEI and isophthalaldehyde after extraction by dichloromethane.

PEI/ Isophthalaldehyde	% of Isophthalaldehyde Remaining
Isophthalaldehyde (no PEI)	1.9
PEI/Iso = 5:1	63.6
PEI/Iso = 16:1	77.8

Table 6 shows the percentage of isophthalaldehyde remaining from 1.9% to 77.8 % with respect to the ratio of PEI/Isophthalaldehyde from 0 to 16. In ratio 16 to 1 of PEI/Isophthalaldehyde, the 77.8% of isophthalaldehyde remaining indicates that after removing any unbound or physically bound isophthalaldehyde, there is still 77.8% with covalent chemical bonding to form the cross-linking within the PEI molecules. These results are strongly supportive that PEI cross-linking reaction is a covalent, chemical cross-linking reaction.

5.2 Light Scattering Analysis of Aggregation Behavior

Polyethylenimine particle size was performed by using QELS light scattering techniques. The PEI molecular hydrodynamic radius as a function of concentration was determined by QELS light scattering analysis. Table 7 shows how with increasing concentration of PEI, we observed a decrease of the macromolecules' hydrodynamic radii. This indicated that the molecular repulsion force plays a role with shortening intermolecular distance as the cationic polymers are forced to be closer together; they shrink slightly from these ionic repulsions.

Table 7: Polyethylenimine (in water) Hydrodynamic Radius as a function of the concentration

Polyethylenimine(M)	Hydrodynamic Radius (nm)
0.1	4.88
0.4	4.76
0.6	4.76
1.0	4.68
1.2	4.66
1.4	4.54
1.8	4.51

Figure 5.7: Polyethylenimine (in water) Radius in different Concentration

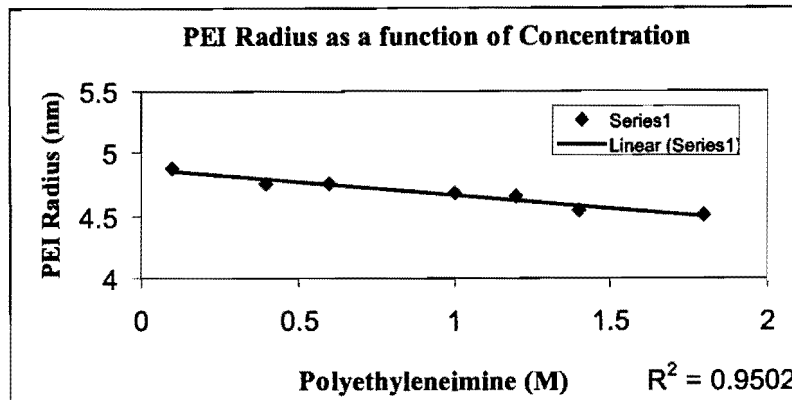


Figure 5.7 shows the PEI radius (Y axis) as function of the concentration of the polyethylenimine (X axis). The results showed a slightly decrease in the polyethylenimine radius with increasing PEI concentration. PEI molecules, as polycationic polymers, are far apart from each other in very dilute solution. The PEI molecules are not repelled much by other molecules due to the long range distance. As the PEI concentration goes up, the molecules are closer to each other. The molecular charges repel, and as this force increase the radius of the molecules decreases.

5.2.1 Cross-Linking Hydrodynamic Radius Measurement by QELS

The molecular radius (r) of cross-linked PEI hydrodynamic radius was also investigated by light scattering analysis. The experiment was designed by studying the cross-linking reaction with two PEI concentrations (0.1 M and 1.8 M) titrated into a fixed concentration of the isophthalaldehyde (0.004 M).

From Table 8, we have observed the molecular radius of the cross-linked PEI decreasing from 5.82 nm to 3.89 nm as isophthalaldehyde solution (up to 1.8 mL) was added into the low concentration of PEI (0.1 M). This observation indicates that the cross-linking reaction was intra-molecular in low PEI concentration. At low concentration, once the isophthalaldehyde has reacted with one PEI molecule, it is much more likely to react again with a free NH_2 from that same molecule. Collisions between the widely dispersed polymer chains are infrequent, so reaction of the second aldehyde with a different PEI molecule to form an intermolecular cross-link is unlikely.

The aliquot volumes of the isophthalaldehyde (0.004 M) solutions were added into higher concentration of PEI (1.8 M) solution. Table 9 shows a similar reduced radius pattern (as seen in table 8) with addition of isophthalaldehyde, but the slope is much shallow in 1.8 M PEI. When adding an increasing amount of isophthalaldehyde into the PEI solution, the PEI molecular particle size decreased only slightly. This observation indicated that the PEI and isophthalaldehyde cross-linking reaction is still an intra-molecular reaction (compact in size). The reduced slope occurs since the number of cross-links in each PEI molecule is smaller. No increase in radius - as would occur from intermolecular cross-linking - was observed.

Our ^1H NMR, UV-Vis extraction, and light scattering studies results are strongly support that isophthalaldehyde acts as a cross-linker for PEI. The cross-linking reaction is primarily an intra-molecular cross-linking with PEI concentration up to 1.8M.

In conclusion, whether inter or intra molecular cross-linking reaction occurred depends on the concentration of PEI. At very high concentrations of PEI (reactions in bulk or pure PEI), we have observed the aggregation and insolubilization behavior which

indicated the inter-molecular cross-linking between the PEI molecules. However, in a low concentration of PEI, the cross-linking reaction is intra-molecules cross-links. The cross-linking experiments have suggest that the idea of using PEI as an imprinting medium for DNA seems viable- PEI is known to bind DNA and can be cross-linked with isophthalaldehyde.

Table 8: Low concentration of PEI (0.1 M) Titrated with Isophthalaldehyde (0.004M) in Phosphate Buffer pH7.0

Isophthalaldehyde added(mL)	Radius (nm)	Normalized Radius
0.0	5.82	1.00
0.1	5.62	0.97
0.3	5.40	0.93
0.5	5.13	0.88
0.8	5.03	0.86
1.0	4.71	0.81
1.5	4.45	0.76
1.8	3.89	0.66

Figure 5.8: Isophthalaldehyde (0.004 M) Titrated into Low Concentration of Polyethylenimine (0.1 M)

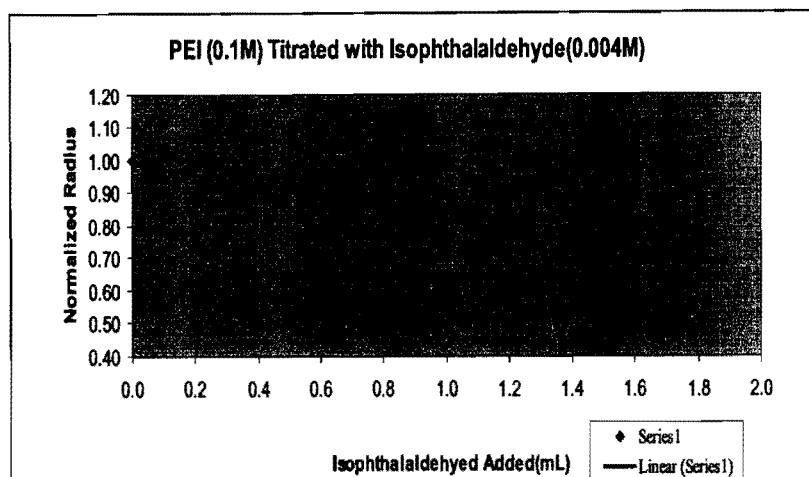
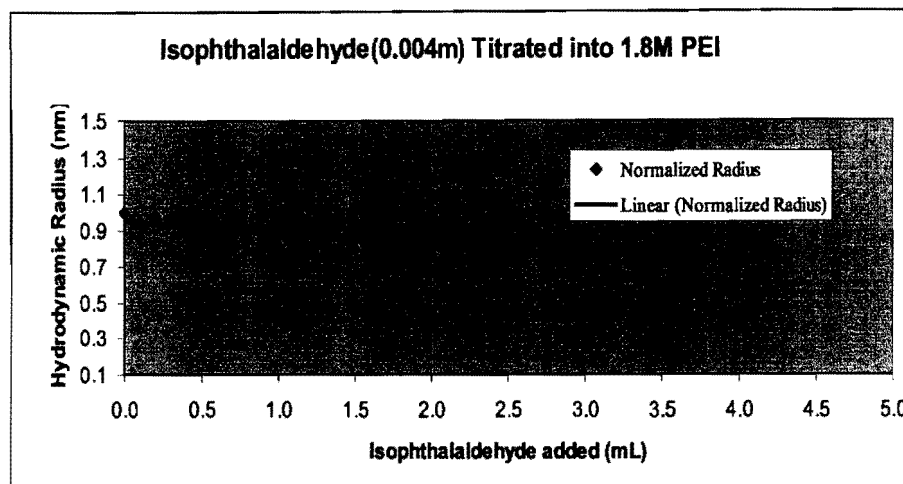


Table 9: High Concentration of PEI (1.8 M) Titrated with Isophthalaldehyde (0.004 M) (in phosphate buffer, pH 7.0)

Isophthalaldehyde (mL)	Hydrodynamic Radius (nm)	Normalized Radius
0.0	5.64	1.00
0.2	5.53	0.98
0.6	5.37	0.95
0.8	4.86	0.86
1.0	4.62	0.82
1.5	4.53	0.80
2.0	4.33	0.77
3.0	4.16	0.74
4.0	4.06	0.72

Figure 5.9: Isophthalaldehyde (0.004 M) Titrated into 1.8 M PEI (both prepared in Phosphate Buffer Solution at pH 7.0)



5.3 Binding Study of Polyethylenimine / Quadruplex DNA

Figure 5.10 shows the CD spectrum of G-quadruplex (T_4G_4) DNA. This CD spectrum displayed a positive maximum peak at near 265 nm and a negative minimum peak at 240 nm. These are the characteristic features of the parallel G-quadruplex DNA structure.²⁰⁶ The quadruplex (T_4G_4) DNA has been reported to have a parallel G-quadruplex structure.

Figure 5.10: CD Spectrum of Quadruplex T₄G₄ DNA (Parallel)

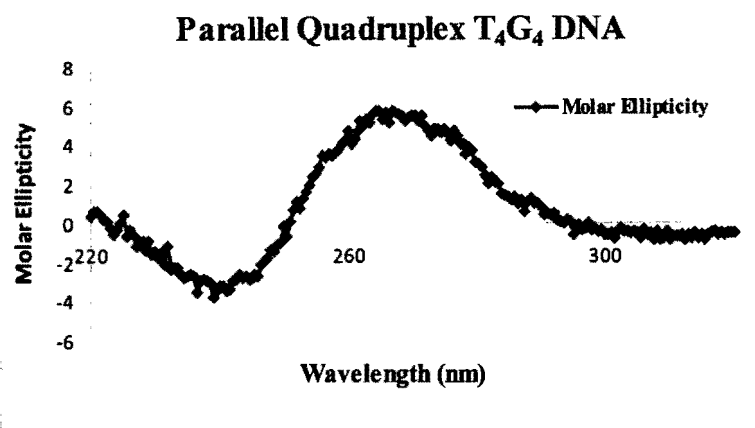
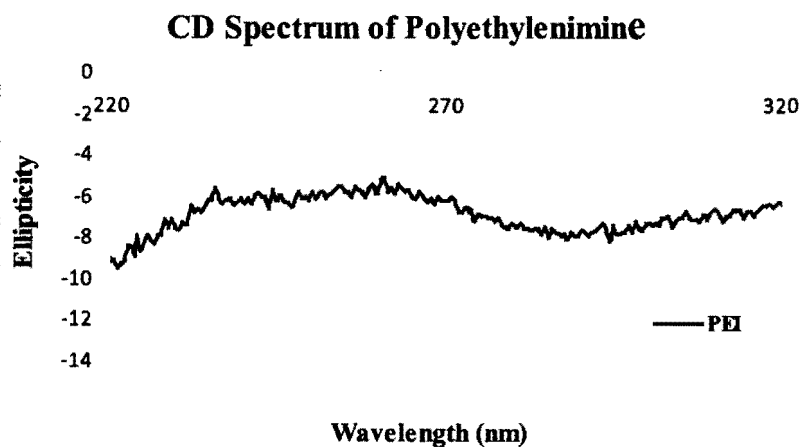


Figure 5.11 shows the CD spectrum of the polyethylenimine. CD is characteristic of the molecular and environmental asymmetrical effects. Because PEIs has no significant CD signal within the UV region, we are not able to see any absorptivity in spectra. The CD spectrum of the PEI is simply showing the noise level.

Figure 5.11: CD Spectrum of the Polyethylenimine



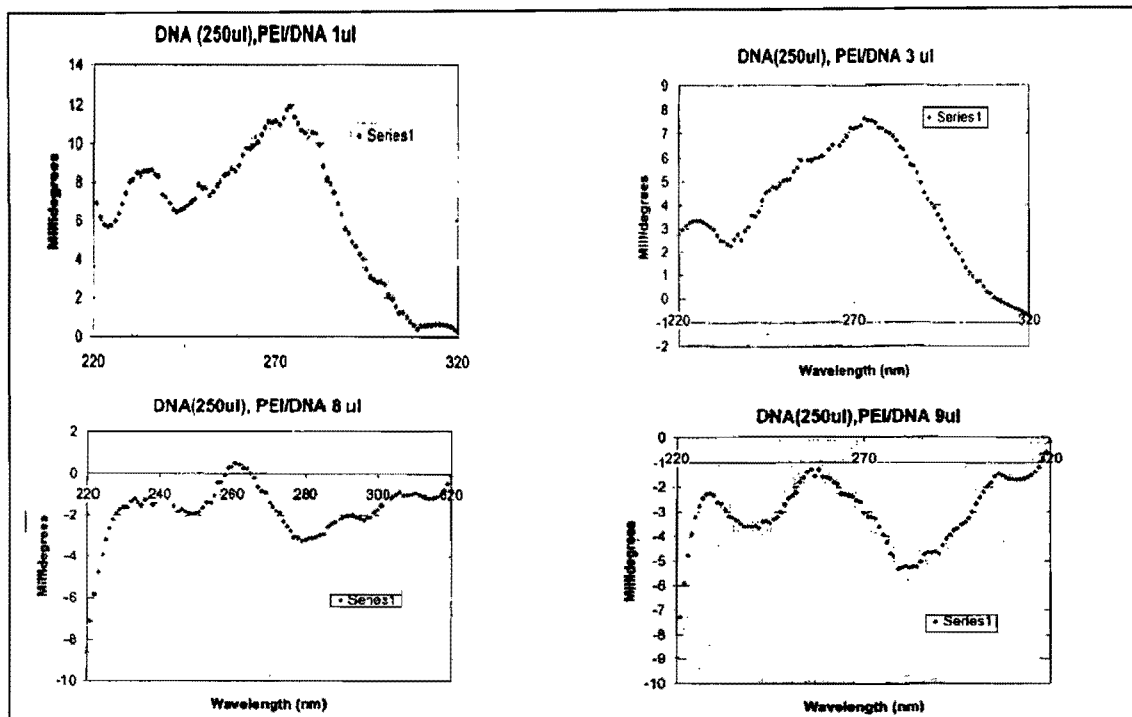
5.3.1 Circular Dichroism (CD) Titration Experiments

In this work, we have used CD spectroscopy to monitor the quadruplex T₄G₄ DNA conformational changes in PEI/T₄G₄ quadruplex DNA complex solutions. A pre-mixed quadruplex DNA with PEI at a tenfold excess solution were prepared for use in our first titration study. DNA is included in the titrating solution to maintain a constant DNA concentration (and therefore a constant CD signal). PEI has no CD signal within the UV region. Hence, the observed signals recorded only from the quadruplex DNA molecules.

Figure 5.12 shows the titration experiment, where the pre-mixed solution of 10X PEI/ quadruplex DNA was titrated into G-quadruplex DNA (250 μ l) solution. The titration began from the pre-mixed sample (PEI/quadruplex DNA) by additionally added 1 μ L into G-quadruplex T₄G₄ solution. As we observed from the CD spectra, quadruplex DNA conformation was changed by adding more PEI (a pre-mixed 10X PEI/DNA solution) into DNA solution. We observed a change in the positive maximum peak near 265 nm, gradually changing to a negative peak near 285 nm. The CD spectra show that quadruplex DNA maximum positive peak in the vicinity of 265-270 nm (parallel), then gradually decreased in intensity when more pre-mixed solution was added to the quadruplex DNA solution.

From the observed changes in the CD spectra, there are a few possible interpretations: PEI might disrupt the quadruplexes (T₄G₄) DNA conformations completely to single strand DNA or could change the conformation from a parallel orientation to different conformation – antiparallel, mixed, or some other transitional structure.

Figure 5.12: 10X PEI/Quadruplex DNA pre-mixed Solution with 1 μ L each addition titrated into Quadruplex T₄G₄ DNA Solution (250 μ L)



In order to gain further insight into the conformational changes, we have conducted additional titration profiles. Figure 5.13 shows the profile of the pre-mixed DNA/10X PEI titrated into 250 μ L G-quadruplex DNA. The CD spectra show that quadruplex DNA maximum positive peak in the vicinity of 265-270 nm (parallel), then gradually decreased in intensity when more pre-mixed solution was added to the quadruplex DNA solution.

Table 10 summarizes the overall data from the quadruplex DNA and PEI titration. When the (T₄G₄)₄/PEI ratio is at 25, the positive peak \sim 265-270 nm showed a slightly change in conformation, compared with the quadruplex DNA alone. It was noted that the quadruplex DNA maximum peak decreased and gradually turned negative when higher

amounts of the pre-mixed DNA/PEI solution were added to the quadruplex DNA solution. These results indicated that the cationic polymer PEI might disrupt the quadruplex (T_4G_4) structure or change it in a complex manner. However, fully understanding of the (T_4G_4)₄ DNA and PEI interaction remained a challenge.

Figure 5.13: Pre-mixed (T_4G_4)₄/PEI Titrated into Quadruplex DNA (250 μ L)

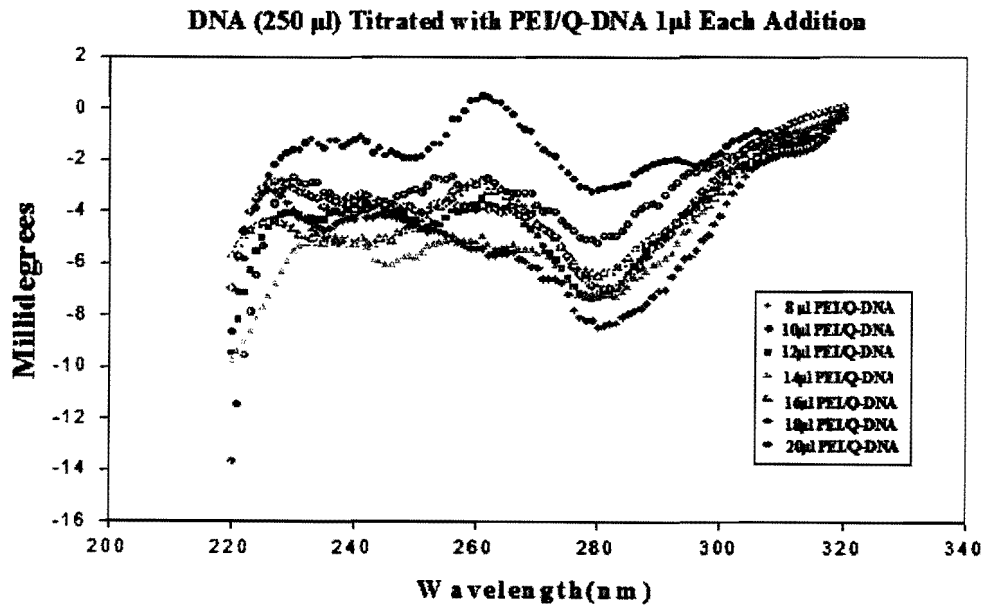
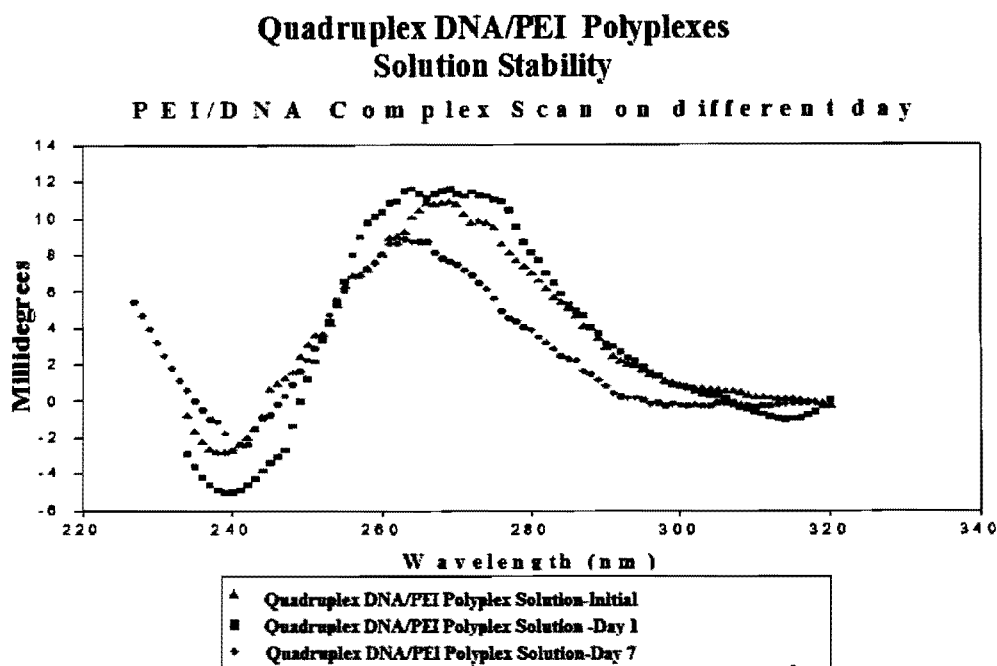


Table 10: Parallel Quadruplex DNA (T₄G₄) (250μL) Titrated with Pre-Mixed (PEI/10x DNA), A Positive Maximum Peak in the Vicinity of 265-270 nm

Added Pre-Mix PEI/10x DNA solution (μL)	Overall ratio DNA/PEI	Comment
1	25/1	Positive peak ~265 nm ,12 mdeg, showed little change in confirmation
3	~8/1	Positive peak ~265 nm, now only 7 mdeg
8	~3/1	Positive peak ~265 nm is lost, -1 mdeg
10	5/2	Negative peak ~265 nm ,-2 mdeg
20	~1/1	Negative peak ~265 nm, -4mdeg

Figure 5.14 shows stability of the (T₄G₄) quadruplex DNA/ PEI complex solution. Quadruplex DNA solutions with added PEI solution were scanned by CD at initial, day 1 and day 7. The CD spectra of quadruplex DNA / PEI polyplex solutions showed only small changes from day 0 to day 7. This result suggested that the quadruplex (T₄G₄) DNA/PEI conformation is relatively stable at 4 °C condition for up to 7 days.

Figure 5.14: Quadruplex (T_4G_4) DNA/PEI Solution Stability



It had been our original intention to imprint PEI with the quadruplex DNA by cross-linking with isophthalaldehyde. The CD data shown above however, throws the viability of this approach into question. When mixed with PEI; the quadruplex DNA might change or disrupt the conformation and no longer be a parallel quadruplex structure (from the CD data). These results brought an uncertainty to our initial goal. We decided to study other polymers to find if a better candidate existed for our model of the imprinting with T_4G_4 quadruplex DNA.

5.4 Porphyrin/ Quadruplex T₄G₄ DNA / Polymers Interaction Study by UV-Vis

Porphyrins have a “ring of rings” structure of four pyrrole units, and are aromatic with an 18 π -electron scaffold which allow for the ability to absorb visible light. Porphyrins are also known to be able to associate or intercalate with the anionic phosphate backbone of DNA.^{280,325}

We investigated the interaction of polycationic and neutral polymers with a quadruplex (T₄G₄) DNA/ porphyrin complex; this acted as a screen for other polymers that will bind DNA. In screening the polymers, we have observed that the porphyrin Soret band shifts from 422 nm to 433 nm when quadruplex DNA is added into the porphyrin. On addition of polymer, the Soret band might shift back to 422 nm, as a result of dissociation of the porphyrin from the DNA; or the Soret band might remain at 433 nm indicating an intact porphyrin-DNA complex.

Figure 5.15 shows the UV spectra of polyethylenimine in the presence of the porphyrin-quadruplex DNA complex. When quadruplex DNA was added into porphyrin, the porphyrin maximum peak shifted to 433 nm, evidence of the formation of the DNA/porphyrin complex. After adding the polyethylenimine to the porphyrin-DNA complex, the porphyrin maximum peak shifted back to 422 nm. Figure 5.16 shows the interaction of the cross-linked PEI with the porphyrin/ DNA complex, where the cross-linked PEI demonstrated the same binding behavior as the non-cross-linked PEI.

Poly (4-vinyl-1-methylpyridinium bromide), an ionic polymer, also showed the same binding profile as PEI when porphyrin/ quadruplex DNA complex was added (figure 5.17). Polyethylene glycol (PEG) is a nonionic neutral polymer which is often used as protein stabilizing agent. Figure 5.18 shows the polyethylene glycol (PEG) with

the porphyrin/ T₄G₄ quadruplex DNA complex. The UV-Vis spectra have shown the porphyrin peak remains at 433 nm after addition of the PEG. This result might support hypothesis of the binding behavior as: (1) non-binding of the PEG and quadruplex DNA or (2) binding without the disruption of the quadruplex DNA with PEG.

When poly (N-vinylpyrrolidone) was added to the porphyrin / quadruplex DNA complex, the absorption maximum remained at 433 nm which might indicate an intact of porphyrin-DNA complex (figure 5.19). Figure 5.20 shows poly (4-vinylpyridine N-oxide) with porphyrin-quadruplex DNA complex. When poly (4-vinylpyridine N-oxide) interacted with porphyrin/ quadruplex DNA complex, the maximum peak remained at 433nm after polymers (PVNO) were added.

Figure 5.15: Polyethylenimine interaction with porphyrin-quadruplex T₄G₄ DNA complex

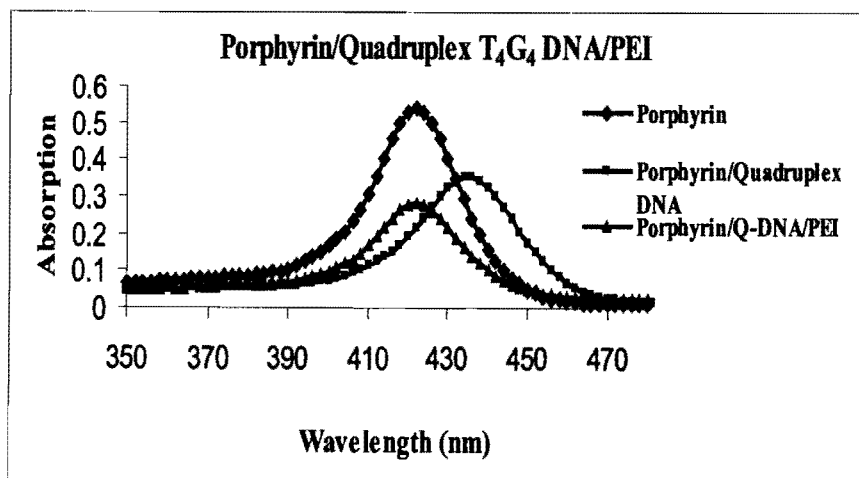
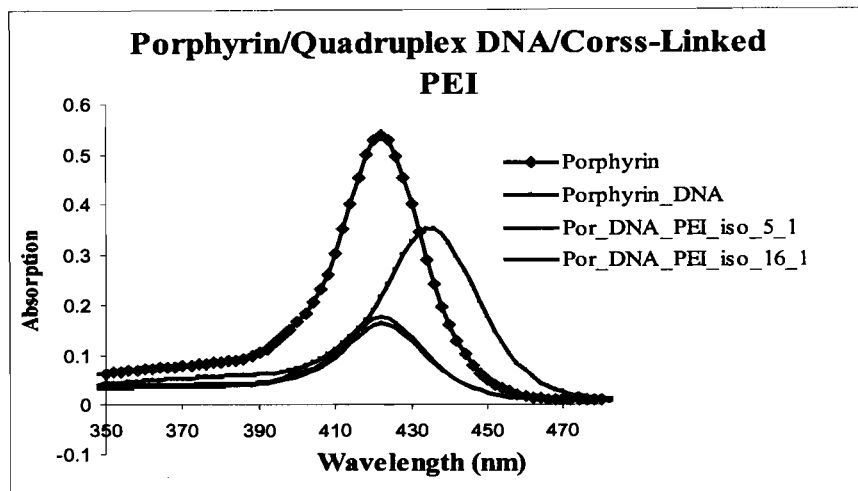
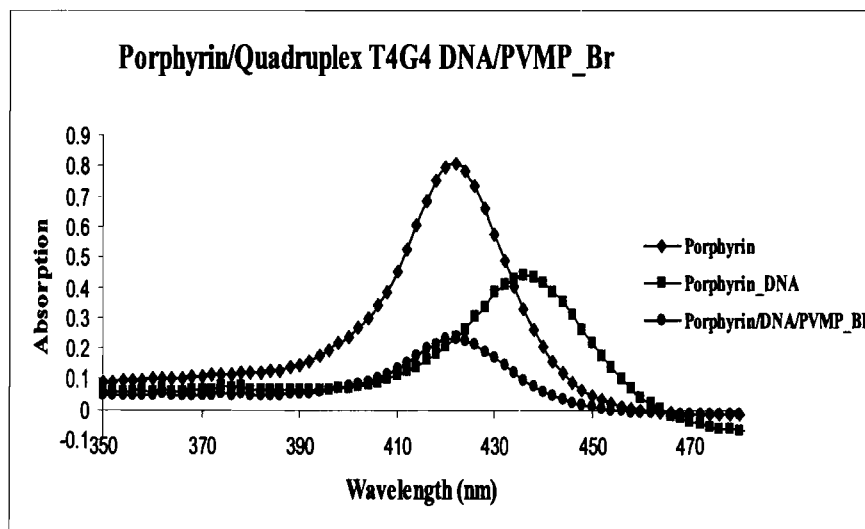


Figure 5.16: Cross-linked polyethylenimine interaction with porphyrin-quadruplex T₄G₄ DNA complex



Note: Por is the abbreviation of the porphyrin.
 Iso is the abbreviation of the isophthalaldehyde
 DNA is the abbreviation of quadruplex T₄G₄ DNA

Figure 5.17: Poly (4-vinyl-1-Methylpyridinium Bromide) interaction with Porphyrin/Quadruplex T₄G₄ DNA Complex



Note: PVMP_Br is the abbreviation of the Poly(4-vinyl-1-methylpyridinium bromide)

Figure 5.18: Polyethylene glycol (PEG) interaction with Porphyrin/Quadruplex T₄G₄ DNA Complex

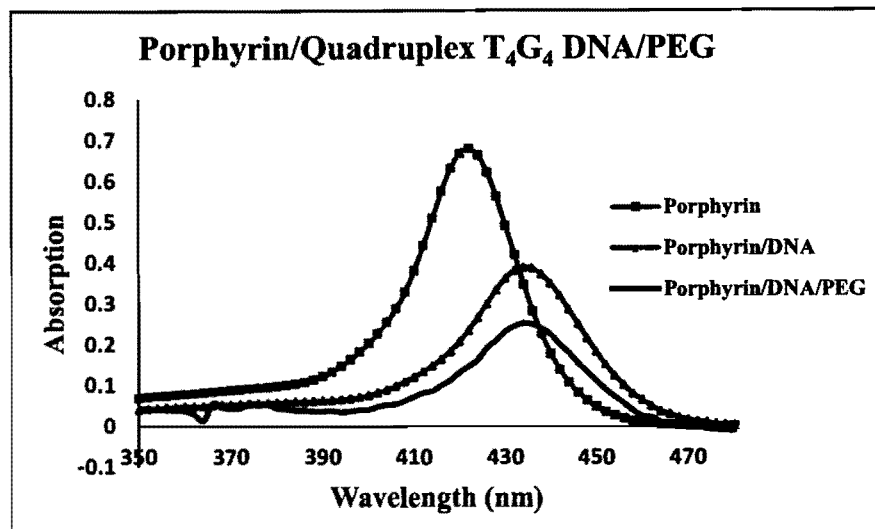
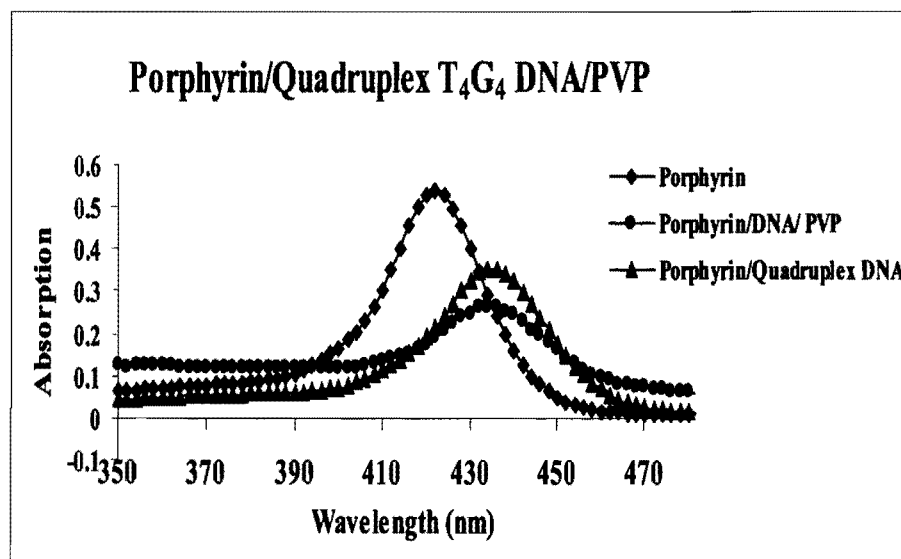
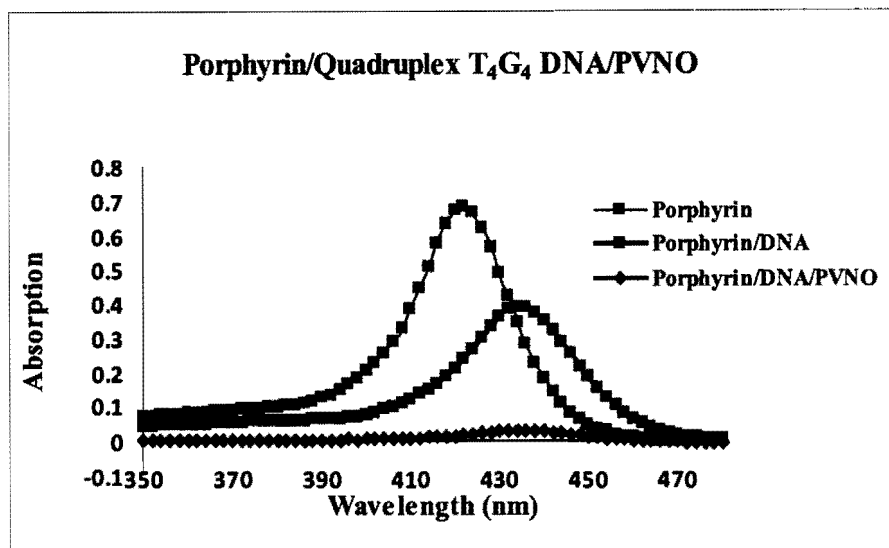


Figure 5.19: Poly (N-vinylpyrrolidone) interaction with porphyrin-quadruplex T₄G₄ DNA complex



Note: PVP is the abbreviation of the Poly (N-Vinylpyrrolidone)

Figure 5.20: Poly (4-vinylpyridine N-oxide) interaction with porphyrin-quadruplex DNA Complex



Note: PVNO is the abbreviation of the Poly (4-Vinylpyridine -N-oxide)

Table 11 summarizes the screening of neutral and cationic polymers. The UV-Vis spectra showed that the maximum peak of the porphyrin will shift back to 422 nm after adding cationic polymers into the porphyrin and quadruplex DNA complex. When neutral polymers were added to the porphyrin and DNA complex, the porphyrin maximum peak remained at 433 nm.

Table 11: Porphyrin Probe Screening of Candidate Polymers

Polymer C= Cationic N=Neutral	Porphyrin (nm) λ_{max}	Porphyrin λ_{max} after Added DNA (nm)	Porphyrin λ_{max} after Added DNA and polymer (nm)
Poly(2-vinyl pyridine) (C)	422	433	422
PEI (C)	422	433	422
Poly(allylamine) 20%wt (C)	422	433	422
Poly(L-lysine) (C)	422	433	422
Metafectene Easy (C)	422	433	422
Metafectene Pro (C)	422	433	422
Poly(4-vinyl-1- methylpyridinium bromide) (C)	422	433	422
Poly(L-ornithine) HCL (C)	422	433	422
Poly(N- vinylpyrrolidon) (N)	422	433	433
Ploy(4-vinylpyridine N-oxide) (N)	422	433	433
PEG (N)	422	433	433

These screening results show that neutral polymers might be considerable candidates to further study for the binding of the quadruplex DNA with minimal disruption. We have assumed that neural polymer might bind to quadruplex DNA without disrupting the quadruplex structure based on the UV-Vis data. But, the porphyrin λ_{max} peak remaining at 433nm might also lead to a different answer: that there is no interaction of these neutral polymers with quadruplex DNA (no binding). To determine if the neutral polymers are binding to DNA, we have further investigated the polymer and DNA interaction by 2D NMR techniques.

5.5 ³¹P NMR Polymer - Quadruplex DNA Binding Study

³¹P NMR is a powerful tool that has been applied to a wide variety of studies. ³¹P is a spin ½ nuclei and has 100% natural abundance. All phosphorus species within a compound can potentially be detected by NMR spectroscopy. Due to the overlap and interference of the proton chemical shifts of DNA and poly(4-vinylpyridine-N-oxide) in the aromatic region, we cannot use ¹H NMR diffusion experiments to study the mixture of the (T₄G₄) quadruplex DNA with poly(4-vinylpyridine-N-oxide). The ³¹P NMR diffusion experiment is therefore a preferred method to examine the interaction of the quadruplex DNA and PVNO polymer.

In figure 5.21, ³¹P NMR spectra show the binding interaction of the quadruplex DNA with the following polymers: poly(N-vinylpyrrolidone), poly(4-vinylpyridine N-oxide) and polyethylenimine. The spectrum of polyethylenimine was observed to shift to the left (down field) compared with the free (T₄G₄) quadruplex DNA. It is apparent that PEI has bound to quadruplex DNA from the change in the chemical shift. In figure 5.21, comparing with the free T₄G₄ quadruplex DNA pattern, we also observed no shift in peak maximum for the poly(N-vinylpyrrolidone) and poly(4-vinylpyridine N-oxide). This might indicate that there is a no binding relationship between the polymers and quadruplex DNA. However, other researchers' findings reported that poly(N-vinylpyrrolidone) is known to interact with the quadruplex DNA.³²⁶ It might therefore be more appropriate to suggested that the PEI has a stronger binding interaction than PVP and PVNO, one that is centered on association of the negative phosphates of DNA and positive ammonium ions of PEI. Another possibility is that PVP and PVNO do not interact with DNA phosphate backbone, but the interacting sites may close to the base.

This would have a maximum effect on the electron density and shielding at the P nuclei, resulting in a change in chemical shift. In comparing with the free (T₄G₄) quadruplex DNA, the PVNO and PNVP have shown the minor changes in contour line of spectra; however, there is still not sufficient evident for assessing whether these neutral polymer are binding with (T₄G₄) quadruplex DNA or not.

In order to assess whether the poly(N-vinylpyrrolidone) would bind to quadruplex DNA or not, we examined the interaction by increasing the polymer concentration in the NMR. In figure 5.22, we have observed that the peak maximum of the poly(N-vinylpyrrolidone) shifted downfield (to the left side) relative to the previous experiment (figure 5.21). This result confirmed that the poly(N-vinylpyrrolidone) is bound to (T₄G₄) quadruplex DNA; in addition, this result also suggested that the poly(N-vinylpyrrolidone) has a stronger binding interaction with quadruplex DNA than poly (4-vinylpyridine N-oxide).

Figure 5.21: ^{31}P NMR Spectra of $(\text{TTTTGGGG})_4$, free and in the presence of Poly(4-vinylpyridine N-oxide), Polyethylenimine and Poly(N-vinylpyrrolidone)

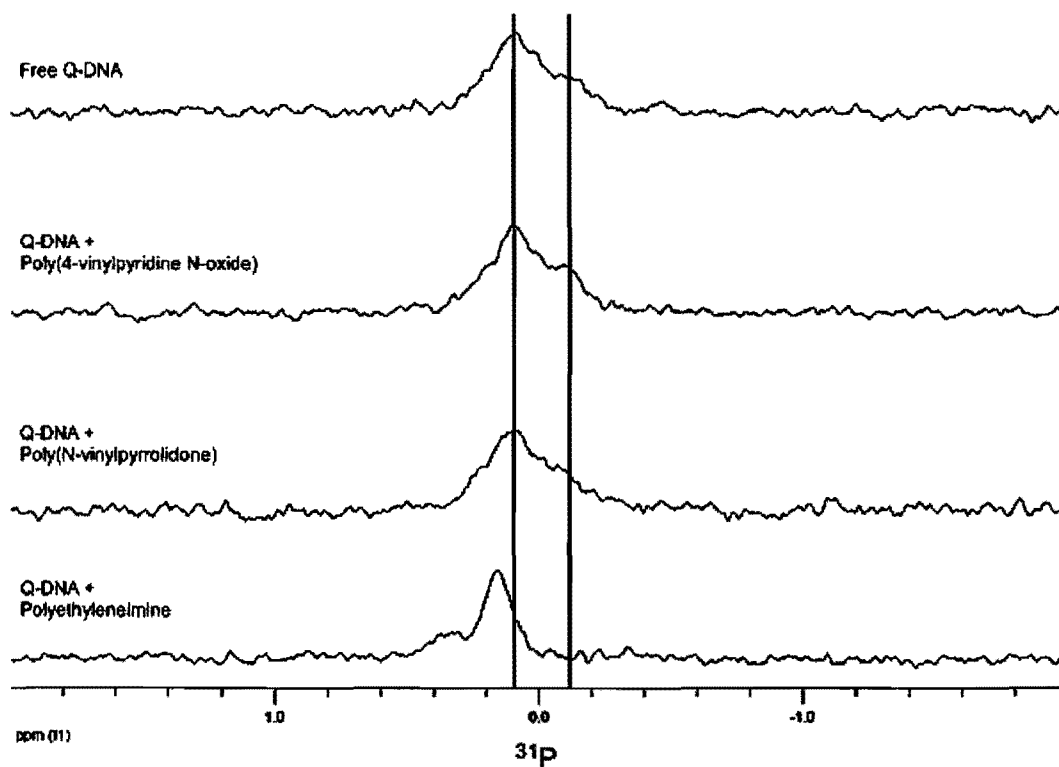
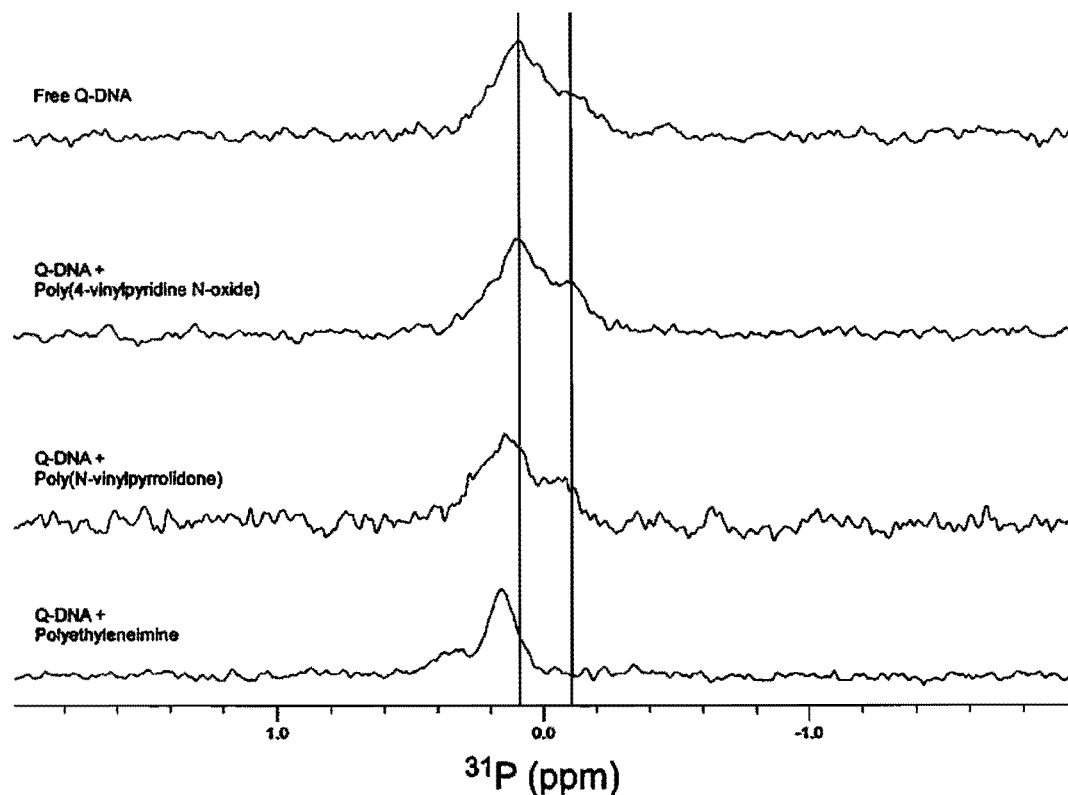


Figure 5.22: ^{31}P NMR Spectra of $(\text{TTTTGGGG})_4$, and with Poly(4-vinylpyridine N-Oxide), Polyethyleneimine and Poly(N-vinylpyrrolidone) with increased concentration of Poly(N-vinylpyrrolidone) and Poly(4-vinylpyridine-N-Oxide)



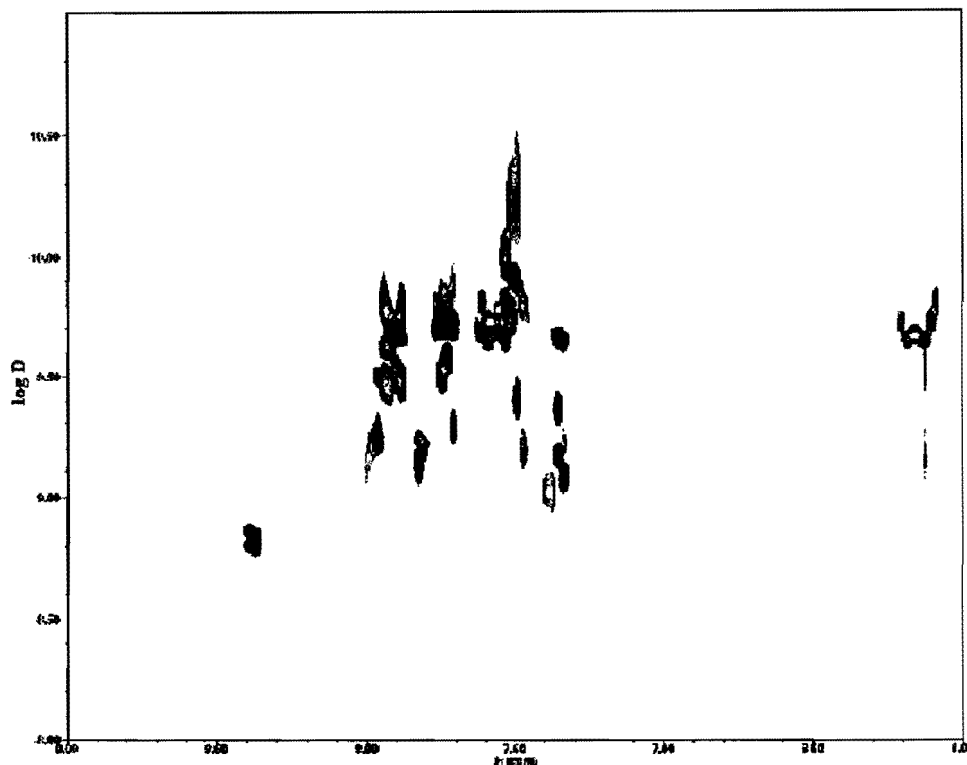
5.6 DOSY: Diffusion NMR Experiments

Diffusion-Ordered (DOSY) NMR spectroscopy provides a way to separate the spectra of different compounds in a mixture based on the different diffusion coefficients. DOSY applies the diffusion analysis through the pulse-field gradient NMR methods. In DOSY, the spectra are displayed in a 2D plot with chemical shift on one axis and the diffusion coefficient (often in a logarithmic scale) on the other.³²⁶ Compounds with the same diffusion coefficient will then appear correlated on the diffusion axis. Two

molecular species with different diffusion coefficients when measured alone show the different diffusion coefficients. If, when mixed together, they appear at the same diffusion coefficient, then it is reasonable to assume that the two molecules are bound into a single complex with a single diffusion coefficient.

In this pseudo two dimensional NMR technique, one dimension (X axis) represents typical chemical shift information (^1H or ^{31}P (ppm)) and the second dimension (Y-axis) distinguishes species by diffusion coefficient represent by the logarithm of diffusion constant (Log D). The size of the polymer is often much larger than (T_4G_4) quadruplex DNA (~10 kD) because the molecular weight of the polymer is much higher than (T_4G_4) quadruplex DNA. As a result, polymer displays a smaller diffusion coefficient and much broader peaks than T_4G_4 DNA does. In order to obtain stronger and more sensitive signal from diffusion NMR, we will need to monitor the DNA peaks rather than the polymer peaks. When DNA binds to polymer; the polymer diffusion will not change much - the diffusion rate will be dominated by the large polymer component. The DNA, on the other hand, will experience larger changes when it binds to polymer – and diffuses the same as the polymer. In these diffusion experiments, we will examine the aromatic peaks from the quadruplex DNA portions. Figure 5.23 shows the DOSY diffusion experiment for (T_4G_4) quadruplex DNA and poly (N-vinylpyrrolidone) (PVP) at the ratio of 1 to 1, 1 to 5 and 1 to 10, respectively.

Figure 5.23: DOSY NMR Experiment Study Binding Relationship of Quadruplex (T₄G₄) DNA alone (black) and with Poly(N-vinylpyrrolidone) (PVP) at the ratio of 1:1 (blue), 1:5 (red) and 1:10 (green)



In figure 5.23, the Y-axis represents of the logarithm of diffusion coefficient (Log D ($\text{m}^2 \text{s}^{-1}$)). So spectra which occur nearer the top have slower diffusion. The X-axis represents ^1H chemical shift (ppm). The different colors represent different ratios of the polymer with (T₄G₄) quadruplex DNA. The black color indicates (T₄G₄) quadruplex DNA only. The blue color, red, and green color represent the quadruplex (T₄G₄)/ PVP at ratio of 1 to 1, 1 to 5 and 1 to 10, respectively. We have observed that the DNA alone (black) and DNA:PVP 1 :1 (blue)spectra are almost superimposed, which indicated the mixture of the quadruplex (T₄G₄) and PVP (1:1) and DNA alone might have nearly identical diffusion coefficients. This can be explained by the fact that polymer and

quadruplex DNA at 1 to 1 ratio did not have much effect on the diffusion (weak binding). On the other hand quadruplex (T_4G_4) and PVP at 1 to 10 ratio gave multiple diffusion rates for small fragment species – faster diffusing than the intact quadruplex. These faster diffusing species might indicate that the Poly(N-vinylpyrrolidone) (PVP) begins to disrupt the quadruplex (T_4G_4) DNA into single strands or fragments at this high concentration. As we can see in the diffusion pattern, the quadruplex (T_4G_4) and PVP at 1 to 5 ratio (red color) showed a slowing down of the diffusion, which indicates the polymer (PVP) was bound to (T_4G_4) quadruplex DNA. The diffusion analysis shows that interaction of PVP and DNA is somewhat complex, with variability based on concentration.

Figure 5.24: ^{31}P Diffusion DOSY Experiment of Quadruplex T_4G_4 alone (black) and with Poly (vinylpyridine N-Oxide) (PVNO) (red)

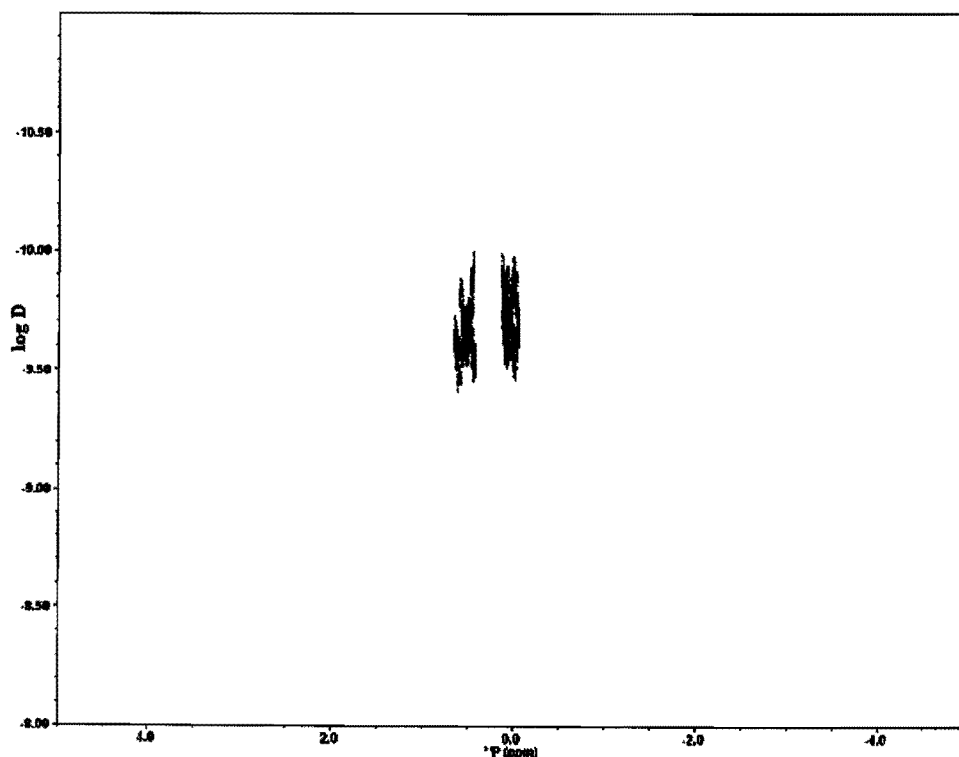
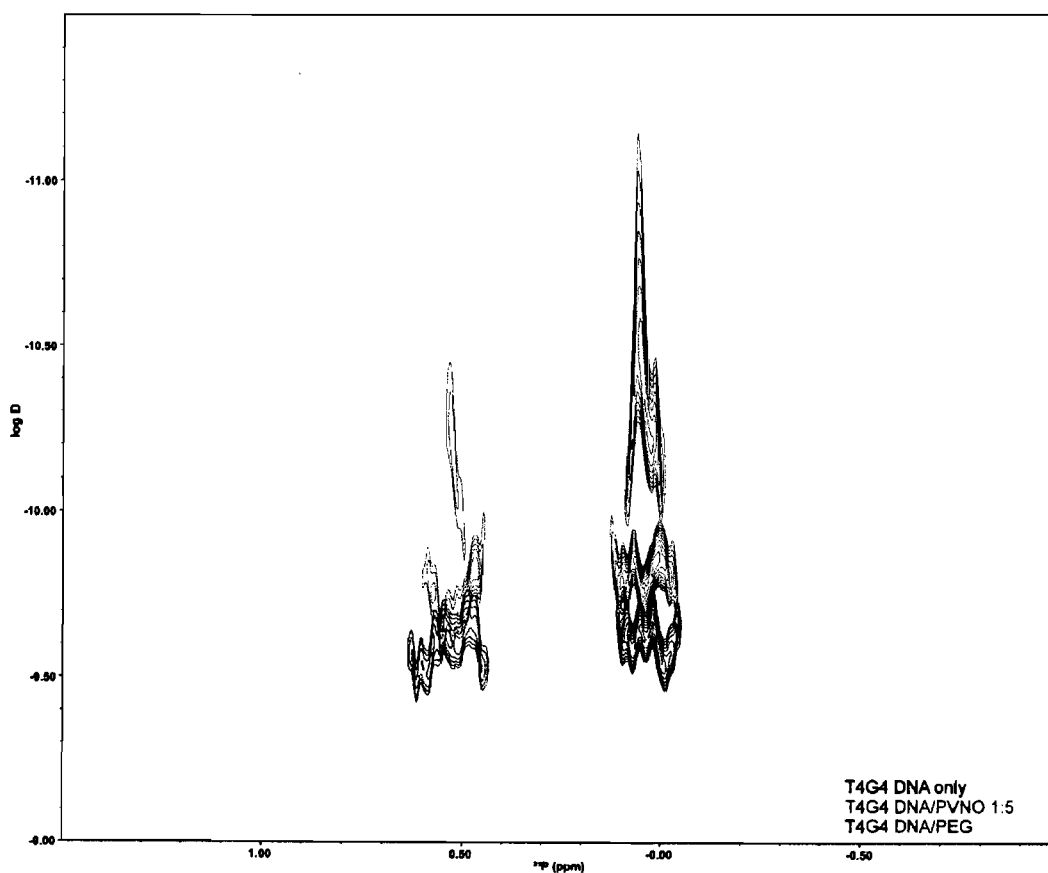


Figure 5.24 shows the diffusion pattern of the ^{31}P DOSY NMR showing the binding interaction of the quadruplex (T_4G_4) DNA and poly(4-vinylpyridine N-oxide) (PVNO). In the simple chemical shift experiment, we did not see any significant change with PVNO as compared to the free quadruplex DNA. We had some doubts about the interaction of PVNO with quadruplex DNA. Then we carried out a DOSY experiment for the further investigation. The overlap of the DNA and PVNO ^1H spectra required the use of ^{31}P NMR. The Y-axis represent logarithm of diffusion coefficient (Log D) and X-axis represents ^{31}P chemical shifts (ppm). The color codes again represent combination of the polymer PVNO and quadruplex DNA. The black color represents the quadruplex (T_4G_4) alone. The red color represents quadruplex (T_4G_4) DNA and PVNO at a ratio of 1 to 5. Quadruplex DNA log D is about -9.5, corresponding to a diffusion coefficient of 3.2×10^{-10} . For DNA with PVNO at a 1 to 5 ratio, the log D is about -9.8 which correspond to a diffusion coefficient of 1.6×10^{-10} , a factor of 2 slower. We have observed the similar diffusion pattern for PVNO and quadruplex DNA as PVP and quadruplex (T_4G_4). However, the diffusion coefficient ($D = (kT)/f$) is related to friction coefficient ($f = 6 \pi \eta R_H$). The effect of the viscosity (η) in solution will affect the diffusion constant. When polymer binds to DNA, the slight decrease in D might be due to the viscosity change in solution rather than the real binding interaction of the polymer and quadruplex DNA. We conducted another experiment to investigate the polymer viscosity effect in PVNO polymer.

In this experiment, we took the viscosity condition into account and examined the binding relationship by ^{31}P -DOSY techniques. A PEG concentration was prepared which had the same viscosity as the PVNO solution. The sample preparation was described in

the methods section. Figure 5.25 shows ^{31}P DOSY spectra of quadruplex DNA, mixture of the quadruplex (T_4G_4) DNA and PVNO and mixture of (T_4G_4) $_4$ and PEG. The concentration ratios of the polyethylene glycol (PEG) / quadruplex (T_4G_4) DNA, and the PVNO / (T_4G_4) $_4$ DNA are both 5 to 1. The red and blue color code are symbolized the (PEG) / quadruplex (T_4G_4) and PVNO / (T_4G_4) $_4$, respectively. The black color represents the quadruplex (T_4G_4) DNA alone.

Figure 5.25: ^{31}P DOSY Experiment for Quadruplex DNA, (T_4G_4) $_4$ / PVNO at 1:5 ratio and quadruplex (T_4G_4) / PEG at 1 to 5 ratio

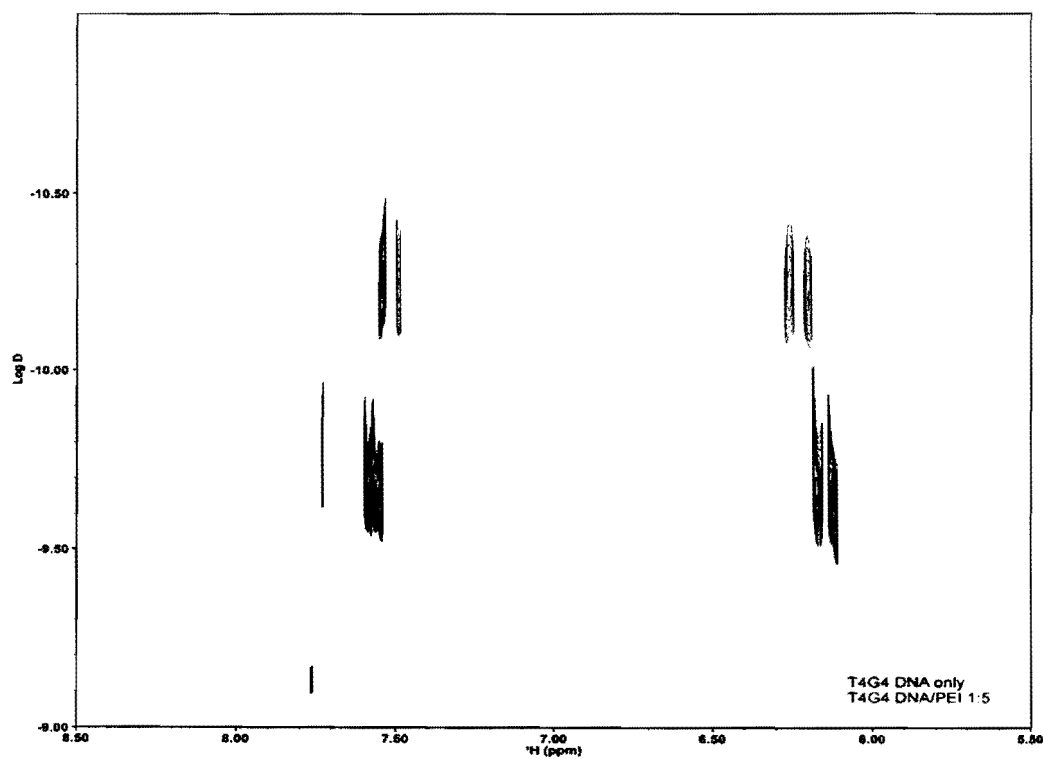


As observed in the spectra, the quadruplex (T₄G₄) alone displayed the log D about -9.6 which is corresponding to the diffusion coefficient of 3.98×10^{-9} . The mixture of the PVNO and quadruplex DNA had log D about -9.8. The corresponding diffusion coefficient for PVNO/ (T₄G₄)₄ complexes is 1.6×10^{-10} . The PEG / quadruplex DNA solution has a diffusion coefficient of 5.0×10^{-11} (logD is -10.3). The spectra of the PEG/ (T₄G₄)₄ displayed a broadened diffusion profile which illustrated the distribution of environments for DNA mobility when increased viscosity is the main contributing factor. The PEG is a neutral polymer which has been found to have no binding affinity with the quadruplex DNA but has the molecular crowding effect for the stabilization of the DNA.³⁴⁴ We have observed that the mixture of the PVNO/ (T₄G₄)₄ spectra have a sharp, narrow diffusion profile, but the reduction in diffusion coefficient is slight. We note that the diffusion coefficient of PVNO/ quadruplex DNA is only about 1.6 times higher than the quadruplex DNA alone, whereas a larger change would be expected for strong binding with the PVNO. The difference in diffusion profile with the viscosity agent PEG suggests a different mode of interaction than PEG. The nature of the association of DNA with PVNO remains ambiguous.

Figure 5.26 shows the mixture of the PEI and (T₄G₄) quadruplex DNA in ¹H DOSY Experiment. The (T₄G₄) quadruplex DNA in the experiment is used as the reference for the comparison for the PEI. The Y-axis represent logarithm of diffusion coefficient (Log D). The X-axis represents ¹H chemical shifts (ppm). The blue color code represented the combination of the polymer PEI and quadruplex DNA at a ratio of 5 to1. The black color represents the (T₄G₄) quadruplex DNA alone. The quadruplex (T₄G₄) displayed the log D about -9.7 which is corresponding to diffusion constant at 5.01×10^{-9} .

As observed in the spectra, the PEI and DNA at 5 to 1 ratio, the log D is about -10.3. The corresponding diffusion coefficient for PEI/ (T₄G₄)₄ complexes is 1.99×10^{-10} . PEI with quadruplex DNA showed a lower diffusion coefficient and a shifted in the spectra. This data suggested that the polymer (PEI) bound to quadruplex DNA.

Figure 5.26: ¹H DOSY Experiment for Quadruplex DNA (T₄G₄) alone (black) and DNA/PEI at Ratio of 1:5 (blue)



5.7 PEI Induced Conformational Changes in Quadruplex DNA (T_4G_4)₄: 2D NOESY NMR and CD Experiments

Figure 5.27 shows the 2D NOESY spectrum of the parallel G-quadruplex T_4G_4 . The G-quadruplex T_4G_4 NOESY spectrum has several clear regions. The resonances from 10.5-12 ppm are denoted as the imino proton resonances (H1 of the guanines). There are also amino protons from 8.0 – 10.5 ppm, aromatic protons from 6.8 -8.0 ppm, sugar protons from 4.0 – 6.5 ppm, and thymine methyl protons from 1.4-2.0 ppm. The imino protons (10-12 ppm) are characteristic of guanine imino-H8 cross-peaks for G-tetrads. The cross-peaks between the imino protons, between the imino and amino protons, and between the aromatic and sugar protons are characteristic of the G-quadruplex structures.

Figure 5.27: A 2D NOESY spectrum of G-quadruplex T₄G₄ Parallel Structure

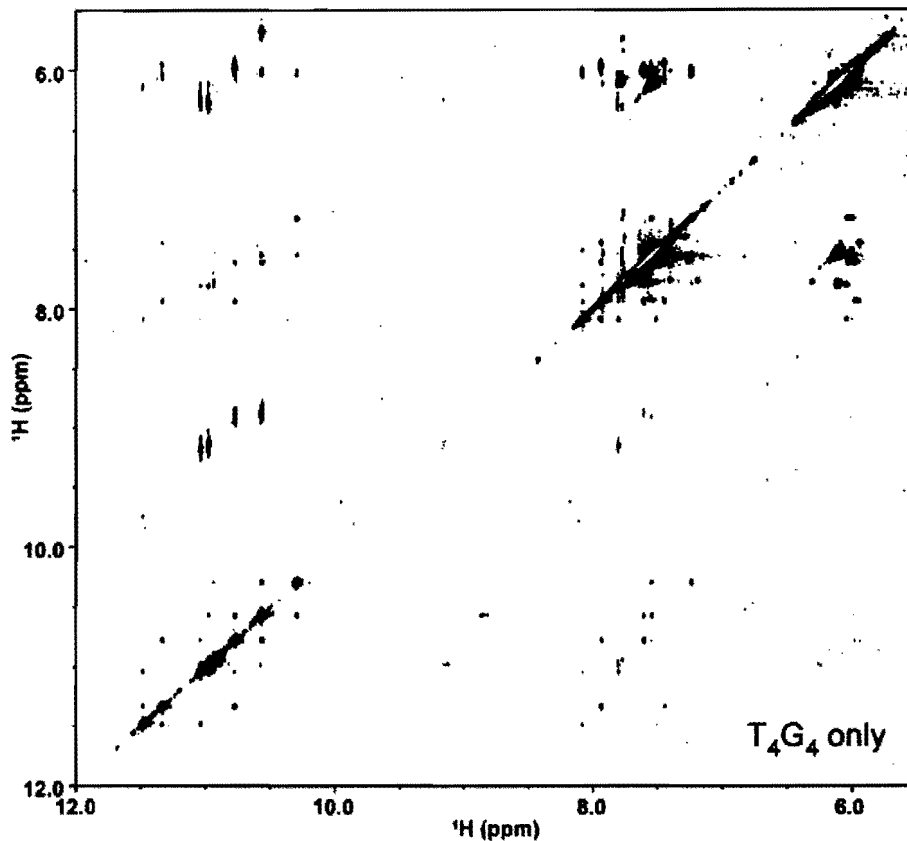


Figure 5.28 shows G-quadruplex (T₄G₄) DNA mixed with PEI at a 1 to1 molar ratio. In this experiment, the spectra recorded did not show the proton resonances peaks in the region of the 10 to 12 ppm, which typically indicated the imino proton resonances. The amino peaks from 8.5 – 10 ppm are also absent. These unresolved peaks may appear as broadened signals as a result of the NMR time scale detection limit and therefore invisible in this NMR spectrum. The signals may be broadened due to the conformational exchange between structures. These results indicated that the protons might undergo an intermediate exchange. However, the cross-peaks and diagonal peaks

could clearly be seen from 5.5 to 8.5 ppm, the aromatic and amino proton chemical shift region. These cross-peaks are not necessarily determinative of any quadruplex structure. This result suggest that the G-quadruplex (T_4G_4) DNA and PEI at 1 to1 ratio might have weak binding or be in equilibrium between multiple structures.

Figure 5.28: 2D NOESY spectrum of G-quadruplex (T_4G_4) DNA and PEI at 1 to1 Molar Ratio

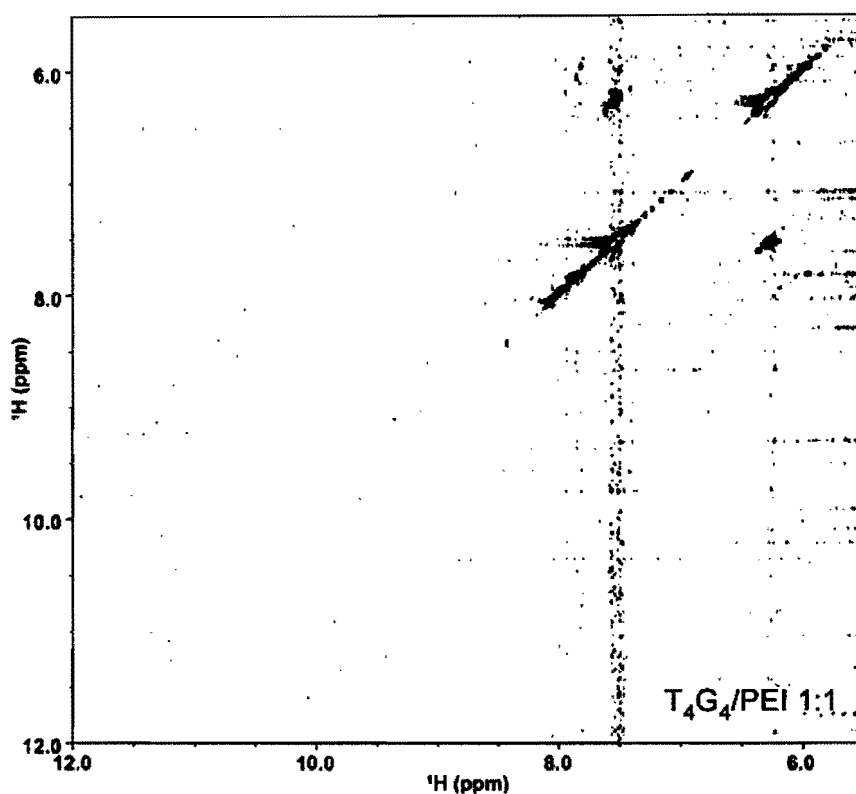


Figure 5.29 shows the 2D NOESY results for T_4G_4 quadruplex DNA and PEI mixed at a 1 to 5 molar ratio. Here two peaks can be observed in the diagonal region near 11.0 ppm, where the guanine imino proton resonances occur (10.8-11.6 ppm). While no amino peaks appear on the diagonal, imino-amino cross peaks are observed, which

suggests that the G-quadruplex structure is intact. The NOESY spectrum shows other changes which are suggestive of a structural transition, further evidenced by the CD data provided below.

Figure 5.29: 2D NOESY Spectrum of G-quadruplex T₄G₄ DNA and PEI at 1 to 5 Molar Ratio

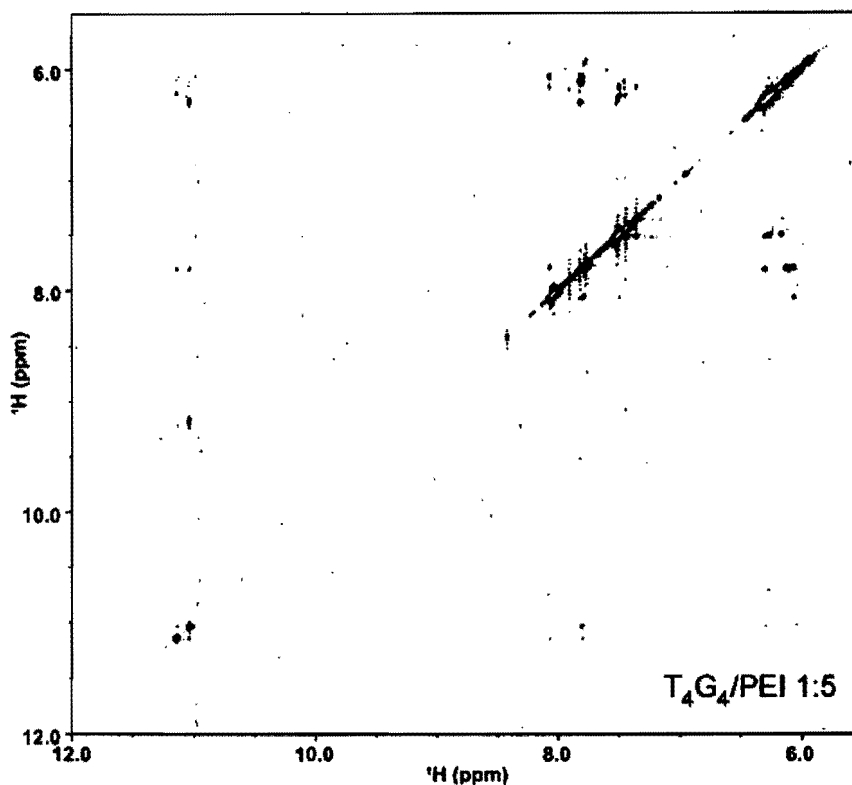


Figure 5.30 shows the imino-imino and imino-amino regions of the NOESY spectra for parallel T₄G₄ quadruplex DNA (A) and T₄G₄ DNA with PEI 1:5 (B). Comparison of the imino regions of the native, parallel T₄G₄ quadruplex and the T₄G₄ quadruplex mixed with PEI 1:5 shows a reduction in the number of peaks in the presence of PEI. The parallel T₄G₄ shows at least 8 imino peaks, and possible as many as 12, with

multiple cross peaks. The presence of more than 4 imino peaks shows that there are some differences within the individual tetrads of the parallel quadruplex. In the presence of PEI, only 2 imino peaks are seen, with one cross peak between them. There are several possible explanations for the reduced number of peaks: some of the peaks may be broadened and undetectable, or a change in conformation may have reduced the number of environments. The simplest changes in conformation would be the reversal of one or two strands to produce a mixed (3:1) or antiparallel quadruplex. However, even the most symmetric antiparallel quadruplex from T₄G₄ would have at least 4 different imino environments. For true assignments, isotopically labeled guanines are typically used – these were outside the scope of our experiments.

Figure 5.30: Imino-imino and Imino-amino regions of the NOESY spectra for parallel T₄G₄ quadruplex DNA (A) and T₄G₄ quadruplex DNA with PEI 1:5 (B)

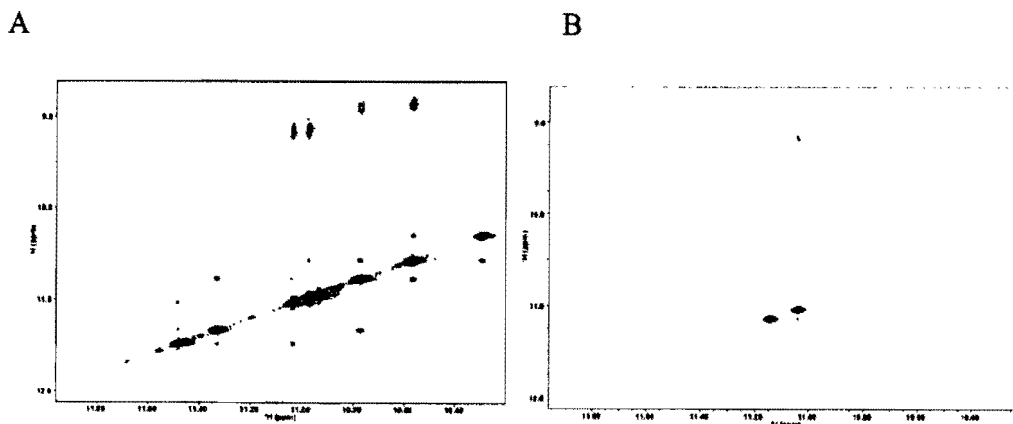


Figure 5.31 shows NOESY spectra of aromatic H6/H8 to sugar H1' region for parallel T₄G₄ quadruplex DNA (A) and T₄G₄ quadruplex DNA with PEI at 1:5 ration (B). One of the key areas of the NOESY spectrum for conformational analysis is that the aromatic (H6/H8) to sugar (H1') cross-peaks regions are showed between 7.0 – 8.0 and 5.4 – 6.6 ppm which enabled us to assign all aromatic and anomeric protons. The resonance of a thymine methyl group was assigned through strong intra-residual cross-peak with intra-residual H6 proton in 2D NOESY spectra. The conformation of the base with relation to the backbone can be syn or anti. Moving from 5' to 3', there are four possible arrangements with different cross-peak results. Anti to anti gives 3 strong cross peaks, syn to anti gives 3 strong and one weak cross peaks, anti to syn gives two strong cross peaks, and syn to syn gives two strong and one weak cross peak. In general, the presence of syn bases reduces the number of cross peaks. The number of cross peaks is in fact greatly reduced in the presence of PEI. A few are unchanged – for example between the aromatic peak at 7.8 and the sugar at 6.1 ppm. There are a few new ones – for example 7.5 to 6.25 ppm. But many have disappeared. This could be a result of increased syn conformations: the parallel T₄G₄ is expected to be all anti, while a change to the 3:1 or antiparallel structures would require some syn conformations. However, without the precise assignments from isotopic labeling, we cannot make an exact structural determination.

Figure 5.31: Aromatic H6/H8 to sugar H1' region of the NOESY spectra for parallel T₄G₄ quadruplex DNA (A) and T₄G₄ quadruplex DNA with PEI 1:5 (B)

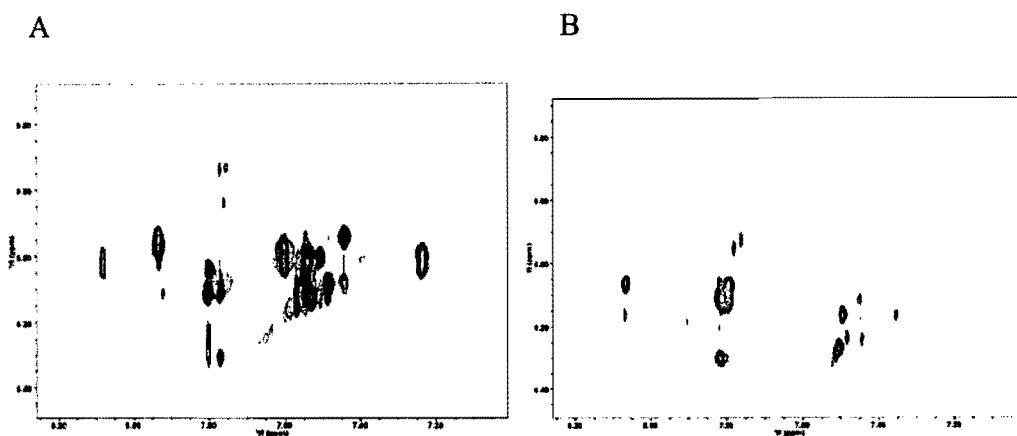
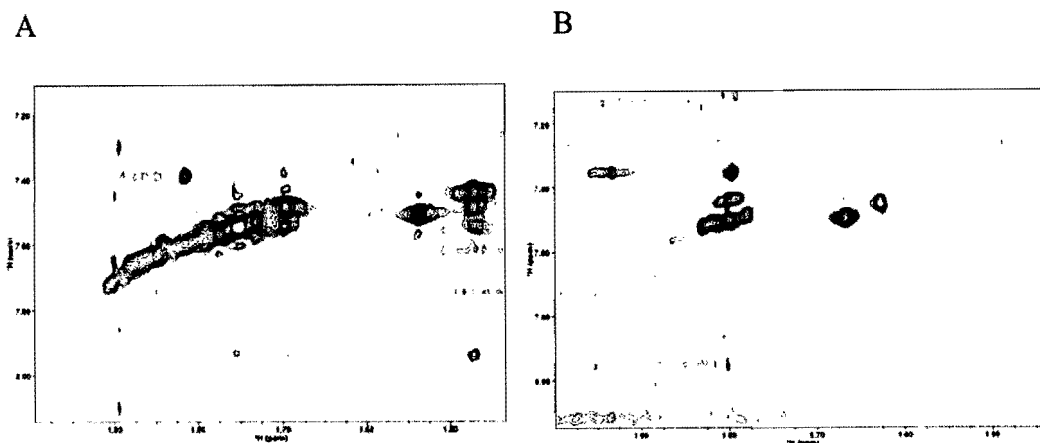


Figure 5.32 shows aromatic H6/H8 to thymine methyl region of the NOESY spectra for parallel T₄G₄ quadruplex DNA. Parallel T₄G₄ quadruplex DNA alone showed in part A. The T₄G₄ DNA with PEI in 1 to 5 ratios showed in part B. We have observed the Finally, the methyl groups of the T tails can be used. In the parallel structure, all of the tails are together, and more cross-peaks are expected as compared to an antiparallel arrangement. In fact, when in the presence of PEI, the number of cross peaks between the thymine methyl region (1.4 – 2.0 ppm) and the aromatic region (6.6 – 8.0 ppm) is reduced. Once again, this reduction could be due to broadening of resonances or to a structural transition. In summary, the NOESY spectra support a structural change induced by PEI but are not definitive.

Figure 5.32: Aromatic H6/H8 to thymine methyl region of the NOESY spectra for parallel T₄G₄ quadruplex DNA (A) and T₄G₄ DNA with PEI 1:5 (B)



5.8 Circular Dichroism Experiment of the PEI and quadruplex (T₄G₄)DNA: Structural Transition Investigation.

The NOE results caused us to re-examine our CD data, and acquire some new data as well. Samples were made up identical to those used for NMR study – quadruplex T₄G₄ DNA, quadruplex T₄G₄ with PEI 1:1, and quadruplex T₄G₄ with PEI 1:5. Figure 5.33 shows the CD spectra of the quadruplex (T₄G₄) DNA alone and with PEI at 1 to 1 and 1 to 5 molar ratio. The CD measurements were taken immediately after mixing, without allowing any equilibration time. In typical G-quadruplex parallel structure, guanines all have the same anti glycosidic conformation which exhibits a positive peak at 260 nm and small negative peak at 240 nm. The CD spectra of the PEI/quadruplex DNA at 1 to 1 and 5 to 1 molar ratio are showed a positive peak near 260nm and a negative

peak near 240 nm in all three sample, which are consistent with the typical parallel stranded G-quadruplex conformation. The CD spectra all appear similar; which indicated no conformational changes at the initial time point.

Figure 5.33: CD Spectra of the Quadruplex DNA alone and with PEI at 1 to 1 and 1 to 5 Molar Ratios at the initial Time Point

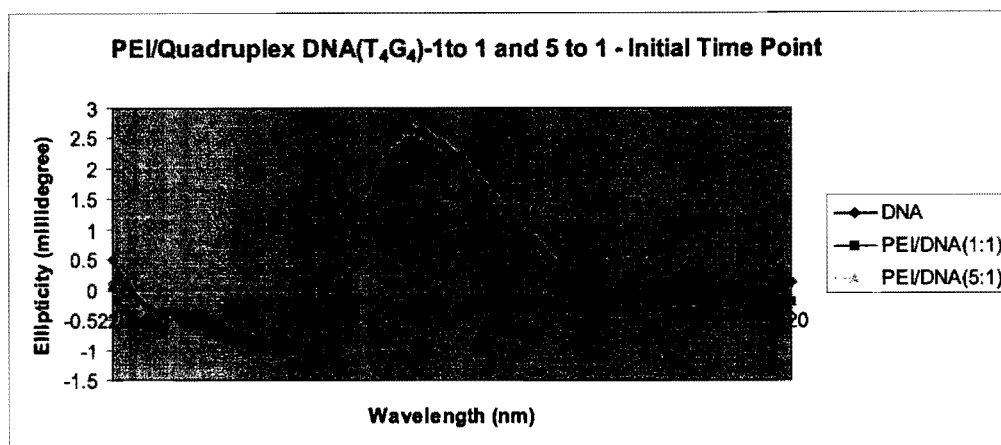


Figure 5.34 shows the CD spectra of the PEI/ T₄G₄ quadruplex DNA mixture (5 to 1 molar ratio in potassium buffer) at different times following addition of PEI to the DNA. We have observed the CD spectrum changing within four hours after addition. The two and half hours spectra showed a negative peak near 260 nm. A negative peak at 260 nm has been associated with an antiparallel structure in the presence of Na⁺ ions.³²⁷ Our T₄G₄ quadruplex DNA without adding the polymer is a parallel quadruplex conformation. In typical CD spectra of G-quadruplex structures, parallel-stranded guanines exhibit a positive peak at 260 nm and a small negative peak at 240 nm.³²⁸ In an antiparallel-stranded of G-quadruplex conformation, guanines have alternating anti

and syn glycosidic conformation along each DNA strand, which generates a positive peak at 290 nm, a negative at 260 nm and a very small negative peak at 240 nm.³²⁹

The time profile of the PEI/quadruplex DNA mixture (5:1) CD spectra is puzzling, especially after four hours, shows that is neither purely parallel or antiparallel – a mixed or hybrid conformation. We tried to shed light on this structural transition of quadruplex DNA induced by PEI. In a search of the literature, we have found that Smargiasso et al has reported the mixed/hybrid of quadruplex DNA in different cations (K^+ , Na^+ and NH_4^+).³³⁰ The hybrid-quadruplexes DNA are the mixtures of parallel and anti-parallel strands in orientation. The DNA in the presence of potassium and ammonium cations mostly existed as mixtures of parallel and anti-parallel orientation. The pure anti-parallel structure was usually observed in the sodium ion (figure 5.35). The Dai research group also discovered a new conformation, mixed hybrid structures, in the human telomeric intermolecular G- quadruplex structure.³²³ Miyoshi and his research team has report the structural transition from antiparallel to parallel of G-quadruplex of d(G₄T₄G₄) induced by calcium ion (figure 5.36).

The CD spectra of PEI/DNA (5 to 1) initial time profile (see Figure 5.34) showed a positive peak at 260 nm and two negative peaks at ~ 240 nm and ~285 nm, still a classic parallel quadruplex conformation. The four hours CD spectra of PEI/quadruplex DNA (5 to 1 ratio) showed two positive peaks at ~ 230 nm and ~ 260 nm and a weak negative peak at ~ 285 nm. In comparing with the typical CD spectra of the parallel and antiparallel strands, the PEI/ (T₄G₄)₄ DNA (5 to 1) existed some peaks in both conformations (230 nm and 260 nm).³³¹

Reviewing these results, all suggest that, most probably, in the high molar ratio of PEI (5 to 1) might induce a structural transition of the G-quadruplex (T_4G_4) DNA from parallel (the original T_4G_4 is a parallel conformation) to another conformation (hybrid or antiparallel) or to a mixture of different structures.

Figure 5.34: CD spectra of the PEI/quadruplex T_4G_4 DNA (5 to 1 molar ratio) Structural Transition Profile As a function of time

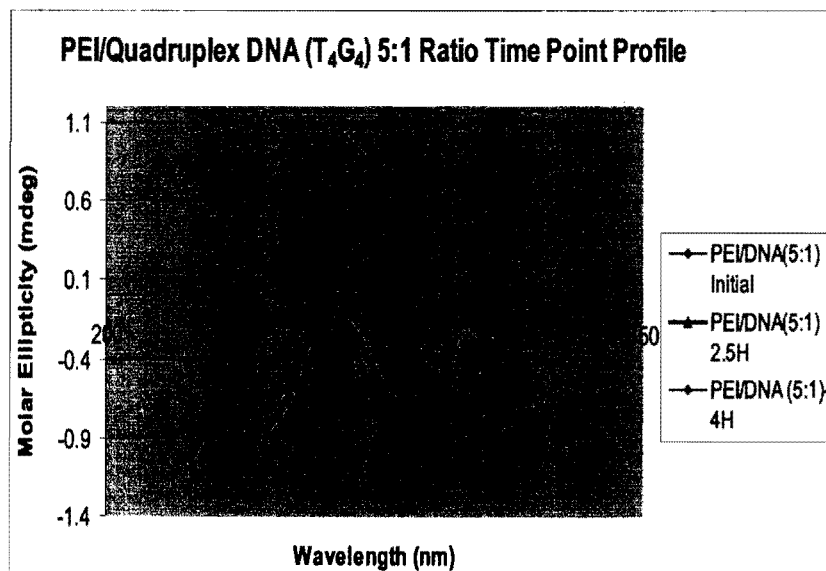


Figure 5.35: CD Spectra of Hybrid G-quadruplex DNA in the presence of the Potassium, Sodium and Ammonium Cation

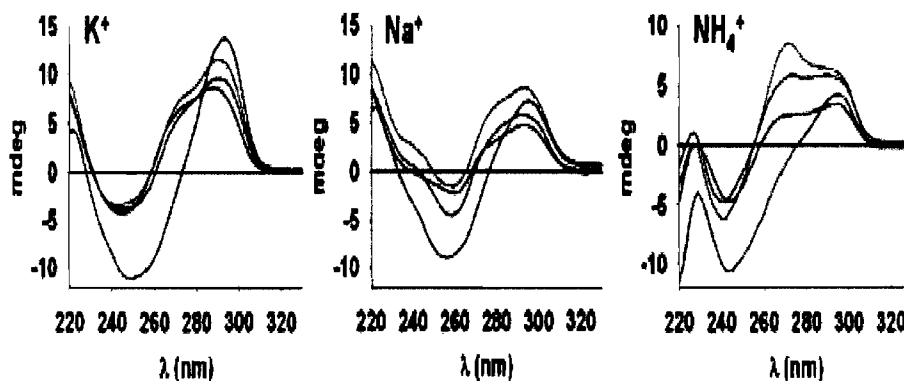
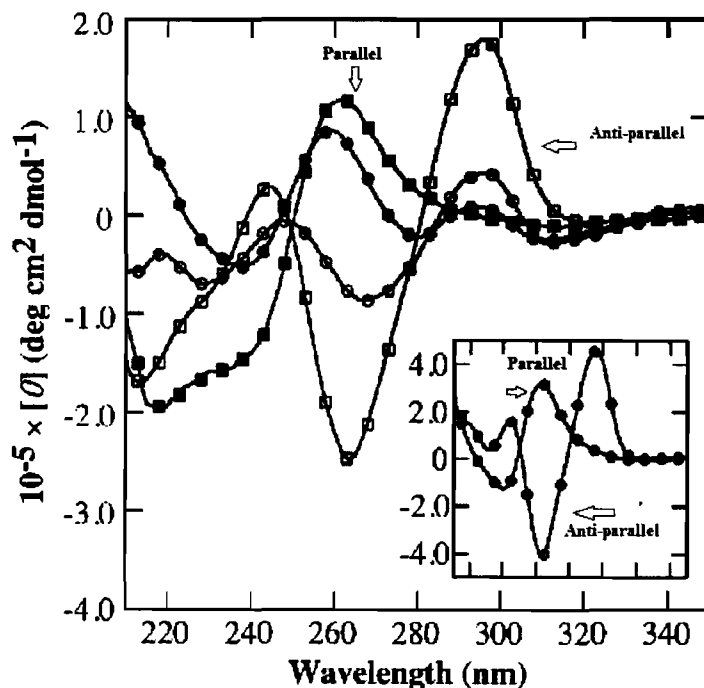


Image adapted from Smargiasso N., et al. *BMC Genomics* 2009, 10(362), 10.1186/1471-2164-10-362.

Figure 5.36: CD Spectra of the Transition from the Antiparallel to the Parallel G-quadruplex.



(\blacksquare): d(G4T4G4), (\bullet): (G3T3G3), (\circ): d[(G4T4)3G4]

Image adapted from Miyoshi D et al. *Nucl. Acids Res.* 2003, 31 (4), 1156-1163

As we assess the NMR and CD results, we cannot conclusively assign the conformation of the G-quadruplex T_4G_4 structures in the presence of PEI at this point. The structural transitions are quite complex, and there are multiple variables: concentration (ratio) of PEI with respect to DNA, time, and temperature. As shown in figure 5.36, the nature of the cation can greatly change the quadruplex structure, however addition of PEI replaces the potassium and any sodium cations with the alkyl ammonium ions of the PEI would induce the conformational change. The structural rearrangements may be occurring slowly but continuously, with equilibration between parallel, mixed 3:1 and antiparallel structures. There is no doubt that the temperature will strongly effect the structural conformation and transition status. All the experimental data reported here provide some information on the structural transition induced by PEI in quadruplex (T_4G_4) DNA, but significant work is required to fully elucidate the solution to this problem.

CHAPTER 6 SUMMARY, CONCLUSION AND FURTHER STUDY

6.1 Summary and Conclusion

The purpose of this study was to discover and examine polymers which bind DNA for nucleic acid research. We were not entirely successful on our original plan (binding – crosslinking – imprinting), but have made significant advances which prepare the way for future work.

We have demonstrated that cross-linking of PEI with isophthalaldehyde occurred both in solution and in bulk. For solution cross-linking, the light scattering results did not show any increase in molecular radii. Instead, there was a trend of a slight decrease in radii, which suggests that the PEI might have “shrunk” through intra-molecular cross-linking. When isophthalaldehyde reacts with two polyethylenimine (PEI) (-NH₂) groups, the branches of the PEI will connect through the isophthalaldehyde.

This intra- molecular cross-linked reaction might slightly decrease the hydrodynamic radius of the PEI because the molecule will become more compact. The light scattering data showed that the PEI molecule did not develop the molecular aggregation behavior up to a concentration of 1.8 M. It can be concluded that intra-molecular cross-links were formed within PEI branched polymers. Furthermore, the data suggested that PEI cross-linking can produce the optimal condensation effect and decrease the molecular radii of the PEI which might improve the biological application of polyethylenimine.

The *In Situ* NMR and UV extraction data also showed that isophthalaldehyde was incorporated into the PEI by chemical cross-linking. This part of the study proves that isophthalaldehyde, a cross-linking agent, was found to be effective in forming

cross-linked with PEI.

Our CD data agreed with the literature that quadruplex DNA (T₄G₄)₄ is a parallel conformation. CD titration results showed that by adding PEI/quadruplex (T₄G₄) DNA complex into quadruplex (T₄G₄) DNA at very low concentration of PEI, the quadruplex DNA still maintains a parallel quadruplex structure. By adding more and more PEI into quadruplex DNA, however, the DNA went through a structural change.

In response to this, we performed the CD melting study to investigate the binding phenomena of the (T₄G₄)₄. However, CD melting did not yield any conclusive data. Other researchers' data indicate that quadruplex (T₄G₄) DNA melts at a very high temperature (closer to 100°C). Therefore, it is difficult to observe conclusive results (melting data was not shown).

As shown in the CD spectra, the initial results of the PEI/ quadruplex (T₄G₄) DNA complexes suggested that PEI might denature quadruplex DNA, and convert it into new structures as a result of strong interactions between the cationic PEI and anionic DNA chains. This impacted the possibility of whether we could template PEI by cross-linking it in the presence of quadruplex DNA. This loss of quadruplex structure questioned our use of the PEI/isophthalaldehyde system for imprinting on quadruplex DNA. It also points to the difficulties of importing any less robust DNA structure into cells using PEI. We then examined other polymers as potential imprinting media.

The finding of other polymers with the capability of more applications in the biomedical field has raised some concerns. We studied the interaction of some cationic and neutral polymers with quadruplex (T₄G₄) DNA. The cationic porphyrin (TMPyP4) was selected as a probe to investigate the interaction of the polymers and quadruplex

(T₄G₄) DNA. TMPyP4 has been reported to have a high affinity to quadruplex DNA due to its similar size with quadruplex DNA. The preliminary polymer screening results showed that the neutral polymers interact with quadruplex DNA without displacing the porphyrin. The porphyrin UV spectrum peak maximum shifts from 422nm to 433 nm remained after adding those polymers.

The polyethylenimine (PEI) binds to quadruplex DNA by electrostatic attraction. The CD and porphyrin UV screening results showed PEI might alter the quadruplex DNA structures. Other researchers have shown that polyvinylpyrrolidone is able to bind to DNA. In contrast to free quadruplex DNA, the polyvinylpyrrolidone (PVP), some changes were observed in ³¹P NMR of quadruplex DNA-binding interaction. By adding a sufficient amount of the compounds, we have observed the ³¹P NMR spectra shifted to a higher frequency field (down field). A slight change of polyvinylpyridine N-oxide (PVNO) was also observed in ³¹P NMR of quadruplex DNA-binding interaction.

Diffusion NMR is a very powerful tool to study mobility of molecules and to characterize mixtures of the complex in the biochemistry fields. Our NMR data from the diffusion experiment has indicated that the poly(N-vinylpyrrolidone) has shown the binding interaction with the quadruplex (T₄G₄) DNA which is consistent with the previous finding. The poly(4-vinylpyridine N-oxide) did show a weak binding interaction with the quadruplex (T₄G₄) DNA.

However, the interaction of the quadruplex DNA with PVNO is still unclear at this moment. Although it is not as well-defined as indicated by the lack of well resolved NMR peak for PVP and PVNO polymers, we still can provide some information for applying these polymers in further studies.

In attempt to better predict the binding interaction for poly(ethylenimine), poly(N-vinylpyrrolidone), and poly(4-vinylpyridine N-oxide) with quadruplex (T₄G₄) DNA; we have conducted the DOSY NMR experiments. The DOSY data verified the same conclusion as the previous NMR studies for these three polymers. Moreover, we have discovered the binding ratio of the PVP and quadruplex DNA, as indicated in the experiment, 1 to 1 binding ratio showed very weak binding or some kinds of interaction. The 5 to 1 ratio showed the better binding affinity and 10:1 ratio was shown many fragment peaks which indicated the conformational changing in quadruplexes DNA.

A 2D NOESY experiment was performed to further investigate the conformational change on binding of the poly (ethylenimine) with quadruplex (T₄G₄) DNA. We therefore conclude that molar ratio of PEI /quadruplex DNA at 5 to 1 has stronger binding interaction than at a 1 to 1 ratio. The PEI/quadruplex DNA structural transition was also investigated by CD; the CD spectra show that PEI will induce the conformational change in quadruplex DNA structures. However, the definitive conformation has yet to be determined by our studies.

A number of challenges still remain unfulfilled in fully understanding the importance of these materials. Further study will continue to develop the suitable functionalized polymers and hope to provide guidance to other researchers and for a better understanding and applying in using these materials in nucleic acid research.

6.2 Suggested Further Studies

Building on these results, further studies in this area will seek to extend the structure-function relationship of quadruplex DNA and its applications. Our research has revealed some preliminary findings about quadruplex T₄G₄ DNA binding to PEI. We hope to find more specific information about the mechanism of the transition steps- does this transition in multiple steps or is it a single step transition? Is there a single PEI induced structure or is there a dynamic equilibrium between a suite of structures? Is the structural alteration by PEI general – will all quadruplex structures be altered – or specific to parallel structures? Can we use the similar sequences with an antiparallel structure to cross-links with PEI and apply this architecture to the imprint techniques. We will evaluate the sequences and structures availability for the improving the binding specificity with G-quadruplex DNA.

The other interests are in the modification of the porphyrin and its derivatives. Based on porphyrin end-stacking property with G-quadruplex, derivative of porphyrins can conjugate with polymers or other small molecules could possible induce quadruplex.

Further improvement will continuously rely on a better understanding of the cellular and *in vivo* barriers in gene transfer. We anticipate that significantly improve the structure specificity will provide new insights into the direction of future research.

REFERENCES

1. Bai, N.; *Health & Medicine*, Dec., **2008**.
2. Ledley, F.D., *Pharm. Res.* **1997**, *13*, 1595–1614.
3. Weir, B.; Zhao, X.; Meyerson, M., *Cancer Cell* **2004**, *6* (5), 433–438.
4. Anson, D.S.; Smith, G.J.; Parsons, D.W., *Curr Gene Ther* **2006**, *6*(2), 161–179.
5. Park, T.G.; Jeong, J.H.; Kim, S.W.; *Adv. Drug Deliv Rev.* **2006**, *58*(4), 467–486.
6. Liu, Z.; Zhang, Z.; Zhou, C.; Jiao, Y., *Progress in Polymer Science*, **2010**, *35* (9), 1144–1162.
7. Kabanov, A.V., *Pharm. Sci. Tech. Today*, **1999**, *2*, 365–372.
8. Nishikawa, M.; Huang, L., *Hum. Gene. Ther.* **2001**, *12*, 861–870.
9. Wong, S.Y.; Pelet, J.M.; Putnam, D., *Prog. Polym. Sci.* **2007**, *32*, 799–837.
10. Smith, A.E., *Annu. Rev. Microbiol* **1995**, *49*, 807–838.
11. Breyer, B.; Jiang, W.; Cheng, H.; Zhou, L.; Paul, R.; Feng, T.; He, T.C., *Curr. Gene Ther.* **2001**, *1*, 149–162.
12. Lee, M.; Kim, S.W., *Pharm. Res.* **2005**, *22*, 1–10.
13. Glover, D.; Lipps, H.J.; Jans, D.A., *Nat. Rev. Genet.*, **2005**, *6*, 299–310.
14. Li, S.; Huang, L., *Gene Ther.* **2000**, *7*, 31–34.
15. Felfner, P.L. *et al.*, *Proc. Natl. Acad. Sci. U.S.A.* **1987**, *84*, 7413–7417.
16. Zelphati, O.; Szoka, C. Jr., *Proc. Natl. Acad. Sci. U.S.A.* **1996**, *93*, 11493–11498.
17. Boussij, O. *et al.*, *Proc. Natl. Acad. Sci., U.S.A.* **1995**, *92*, 7297–7301.
18. Pollard, H. *et al.*, *J. Biol. Chem.* **1998**, *273*, 7507–7511.
19. Brown, M.D.; Schatzlein, A.G.; Uchegbu, I.F., *Int. J. Pharm.* **2001**, *229*, 1–21.
20. Godbey, W.T.; Mikos, A.G. J., *Control Release* **2001**, *72*, 115–125.
21. De Smedt, S.C.; Demeester, J.; Hennink, W.E., *Pharm. Res.* **2000**, *17*, 113–126.
22. Merdan, T.; Kopecek, J.; Kissel, T., *Adv. Drug Del. Rev.* **2002**, *54*, 715–758.

23. Han, H.; Hurley, L.H., *Trends Pharmacol. Sci.* **2000**, *21*, 136-142.
24. Sarder, N. U., *Biote. Mol. Bio. Review* **2007**, *2* (3), 58-67.
25. Arigita, C.; Zuidam, N.J.; Crommelin, D.J.A.; Hennink, W.E., *Pharm. Res.* **1999**, *16*, 1534–1541.
26. Bloomfield, V. A., *Nucleic Acid Science* **1997**, 1-23.
27. Watson, J.D.; Crick, F.H., *Nature* **1953**, *171*(4356), 737-738.
28. Capra, J.A; Paeschke, K.; Singh, M.; Zakian, V. A., *PLoS Comput. Biol.* **2010**, *6* (7), e1000861. doi :10.1371
29. Wang, Y.; Patel, D. J., *Structure* **1993**, *1*, 263-282.
30. Zahler, A.M.; Williamson, J.R.; Cech, T.R.; Prescott, D.M., *Nature* **1991**, *350*, 718-720.
31. Yang, D.; Okamoto, K., *Future Med Chem.* **2010**, *2*(4), 619-646.
32. Neidle, S.; Parkinson, G.N., *Curr.Opin. Struct. Biol.* **2003**, *13*, 275-283.
33. Lundblad, V.; *Proc. Natl.Acad. Sci. USA* **1998**, *95*,8415-8416.
34. Shim, J.W.; Tan, Q.; Gu, L-Q, *Nucl. Acids Res.* **2009**, *37* (3), 972-982.
35. Urraca, J.L.; Hall, A.J.; Moreno-Bondi, M.C.; Sellergren, B. *Angew. Chem. Inter. Ed.* **2006**, *45*, 5158-5161.
36. Miyata, T.; Jige, M.; Nakaminami, T.; Urugami, T., *Proc. Natl. Acad. Sci. USA* **2006**, *103*, 1190-1193.
37. Shi, D.-F. ; Wheelhouse, R.T.; Sun, D.; Hurley, L.H., *J. Med. Chem.* **2001**, *44*, 4509-4523.
38. (a) Mastrobattista, E.; Hennink, W.E., *Nature Materials* **2012**, *11*, 10-12. (b). Castasi, P.; Chen, X.; Moyzis, R.; Bradbury, E.; Gupta, G., *J. Mol. Biol.* **1996**, *264*, 534-545.
39. Jewell, C. M.; Lynn, D. M., *Curr. Opin. Colloid Interface Sci.* **2008**, *13* (6), 395-402.
40. Gao, X.; Kim, K-S; Liu, D., *The AAPS Journal* **2007**, *9* (1), E92-103.
41. Boussif, O.; Lezoualch, F.; Zanta, M.A.; Mergny, M.D.; Scherman, D.; Demeneix, B.; Behr, J.-P., *Proc. Natl. Acad. Sci. USA* **1995**, 7297–7301.

42. Nathan, P. Q.; Pack, D. W., *Biomacromolecules* **2006**, 7(8), 2427–2435.
43. Haq, I.; Trent, J. O.; Chowdhry, B. Z.; Jenkins, T. C., *J. A.C. S.* **1999**, 121 (9), 1768–1779.
44. *Polymers: The Origin and Growth of a Science*, Herbert Morawetz, John Wiley & Sons, **1985**.
45. *Polymers: Chemistry and Physics of Modern Materials*, Cowie, J. M. G, Chapman & Hall, **1991**.
46. Su, J.; Kim, C-J.; Ciftci, K., *Gene Therapy*, **2002**, 9(15), 1031-1036.
47. Mumper, R. J.; Wang, J.; Klakamp, S. L.; Nitta, H.; Anwer, K.; Tagliaferri, F.; Rolland, A. P., *J. Controlled Release* **1998**, 52,191-203.
48. Mumper, R.J. et al. *Pharm Res* **1996**, 13, 701-709.
49. Holt, P.F.; Lindsay, H.; Beck, E.G., *Br. J. Pharmacol.* **1970**, 38(1), 192–201.
50. Walker, G. F.; Fella, C.; Pelisek, J.; Fahrmeir, J.; Boeckle, S.; Ogris, M.; Wagner, E., *Molecular Therapy* **2005**, 11, 418–425.
51. Ogris, M.; Brunner, S.; Schuller, S.; Kircheis, R.; Wagner, E., *Gene Ther.* **1999**, 6 (4), 595–605.
52. Breunig, M.; Lungwitz, U.; Liebl, R.; Fontanari, C.; Klar, J.; Kurtz, A., *J. Gene Med* **2005**, 7 (10), 1287–1298.
53. Lee, H.; Jeong, J. H.; Park, T. G.; *Journal of Controlled Release* **2001**, 76, 183–192.
54. Kircheis, R.; Wightman, L.; Wagner, E., *Adv. Drug Deliver Rev.* **2001**, 53, 341–358.
55. Lemkine, G. F.; Demeneix, B. A., *Curr. Opin. Mol. Ther.* **2001**, 3, 178-182.
56. Lungwitz, U; Breunig, M.; Blunk, T.; Gopferich, A., *Eur. J. Pharm. Biopharm.*, **2005**, 60 (2), 247-266.
57. Hanzlikova, M.; Soininen, P.; Lampela, P.; Mannisto, P. T.; Raasmaja, A, *Plasmid* **2009**, 61(1), 15-21.
58. (a) Abdallah, J. B.; Hassan, A.; Benoist, C.; Goula, D.; Behr, J.-P.; Demeneix, B.A., *Hum. Gene Ther.* **1996**, 7, 1947–1954. (b) Boletta, A.; Benigni, A.; Lutz, J.; Remuzzi, G.; Soria, M.R.; Monaco, L., *Hum. Gene Ther.* **1997**, 8, 243–1251.
59. Von Harpe, A.; Petersen, H.; Li, Y.X.; Kissel, T.; *J. Control Release* **2000**, 69, 309–322.

60. Maruyama, H.; Higuchi, N.; Kameda, S.; Nakamura, G.; Miyazaki, J.; Gejyo, F., *Gene Ther. Mol. Biol.* **2003**, *7*, 221-228.
61. Godbey, W.T.; Wu, K.K.; Hirasaki, G.J.; Mikos, A.G.; *Gene Ther.* **1999**, *6*, 1380–1388.
62. Gosselin, M.A.; Guo, W.; Lee, R.J., *Bioconjugate Chem.* **2001**, *12* (6), 989–994.
63. Lungwitz, U; Breunig, M.; Blunk, T; Göpferich, A., *Eur. J. Pharm. Biopharm.* **2005**, *60*(2), 247-266.
64. Mady, M. M.; Mohammed, W. A.; El-Guendy, N.M.; Elsayed, A.A., *International Journal of Physical Sciences* **2011**, *6*(32), 7328 – 7334.
65. Yanga, T.; Hussaina, A.; Baia, S.; Ikramy, A.; Harashimab, H; Ahsan, F., *J. Control Release* **2006**, *115*, 289-297.
66. Kircheis, R.; Wightman, L.; Schreiber, A.; Robitza, B.; Rössler, V.; Kursa, M.; Wagner, E., *Gene Ther.* **2001**, *8*(1), 28-40.
67. De Smedt, S. C.; Demeester, J.; Hennink, W., *Pharmaceutical Research* **2000**, *17* (2), 113-126.
68. Needham, C.J.; Williams, A.K.; Chew, S.A.; Kasper, F.K.; Mikos, A.G., *Biomacromolecules* **2012**, *13*1429–1437.
69. Huppert J.L.; Balasubramanian, S., *Nucleic Acids Res.* **2005**, *33*, 2908–2916.
70. Sun, H.; Zhou, Q.; Xiang, J.; Tang, Y., *Bioorganic & Medicinal Chemistry Letters* **2009**, *19* (16), 4669-4672.
71. Hershman, S.G.; Chen, Q.; Lee, J.Y.; Kozak, M.L.; Yue, P.; Wang, L. S.; Johnson, F.B., *Nucleic Acids Res.* **2008**, *36*(1), 144-156.
72. Izbicka, E.; Wheelhouse, R.T.; Raymond, E.; Davidson, K.K.; Lawrence, R.A.; Sun, D.; Windle, B.E.; Hurley, L.H.; Von Hoff, D.D., *Cancer Res.* **1999**, *59*, 639–644.
73. Zhang, S.; Zhao, Y.; Zhao, B.; Wang, B., *Bioconjug Chem.* **2010**, *21*(6), 1003-1009.
74. Hu, Q.; Fan, H.; Lou, W.; Wang, Q.; Tang, G., *J. Zhejiang Univ. Sci. B.* **2011**, *12*(9), 720–729.
75. Tang, G.; Guo, H; Alexis, F.; Wang, X.; Zeng, S.; Lim, T.; Ding, J.; Yang, Y.; Wang, S., *J. Gene Med.* **2006**, *8* (6), 736-744.
76. Park, T.G.; Jeong, J.H.; Kim, S.W, *Adv Drug Deliver Rev.* **2006**, *58*, 467–486.

77. Jeong, J.H.; Kim, S. W.; Park, T. G., *Prog. Polym. Sci.* **2007**, *32*, 1239-1274.
78. Choi, Y.H.; Liu, F.; Park, J.S.; Kim, S.W., *J. Control. Release* **1998**, *54*, 39-48.
78. Wei, C.; Han, G.; Jia, G.; Zhou, J.; Li, C., *Biophysical Chem.* **2008**, *137* (1), 19-23.
79. Wei, C.; Jia, G.; Yuan, J.; Feng, Z.; Li, C., *Biochemistry* **2006**, *45*(21), 6681-6691.
80. Munson, B. R.; Fiel, R. J., *Nucleic Acids Research* **1992**, *20* (6), 1315-1319.
81. Lubitz, I.; Borovok, N.; Kotlyar, A., *Biochemistry* **2007**, *46*, 12925 -12929.
82. Wei, C.; Wang, L.; Jia, G.; Zhou, J.; Han, G.; Li, C., *Biophysical Chemistry* **2009**, *143*, 79-84.
83. Wheelhouse, R.T.; Sun, D.; Han, H.; Han, F. X.; Hurley, L. H., *J. Am. Chem. Soc.* **1998**, *120*, 3261-3262.
84. Han, F. X.; Wheelhouse, R. T.; Hurley, L. H., *J. Am. Chem. Soc.* **1999**, *121*, 3561-3570.
85. Kim, M. Y.; Gleason-Guzman, M.; Izbicka, E.; Nishioka, D.; Hurley, L. H., *Cancer Res.*, **2003**, *63*, 3247-3256.
86. Izbicka, E.; Wheelhouse, R. T.; Raymond, E. et al, *Cancer Research* **1999**, *59* (3), 639-644.
87. Garrett, R.H., Grisham. C.M., *Biochemistry* 3rd ed. **2007**, Thomson Brooks/Core, Belmont CA.
88. Horton, R.A.; Moran, L. A.; Scrimgeour, G.; Perry, M.'rawn, D., *Principles of Biochemistry* **2006**, 4/e, ISBN-10:0131453068, Prentice Hall.
89. Bundschuh, R.; Gerland, U., *Eur. Phys. J. E* **19** **2006**, 319-329.
90. Arnott, S.; Chandrasekaran, R.; Selsing, E., Structure and Conformation of Nucleic Acids and Protein- Nucleic Acid Interactions (eds Sundaralingam, M. & Rao, S.T.) **1975**, 477-603.
91. Dahm, R., *Developmental Biol.* **2005**, *278*, 274-288. Friedrich Miescher and the discovery of DNA.
92. Levene, P., *J. Biol. Chem.* **1919**, *40* (2), 415-24.
93. (a) Astbury, W., **1947**. "Nucleic acid". *Symp. SOC. Exp. Bbl*, (66).
 (b) Astbury, W.T.; Bell, F.O., *Quant Bio.* **138**, 6, 109-121

94. Hershey, A.; Chase, M., *J. Gen. Physiol.* **1952**, *36* (1), 39–56.
95. Watson, J.D.; Crick, F.H.C, *Nature* **1953**, *171* (4356), 737–738.
96. Bundschuh, R.; Gerland, U., *Eur. Phys.* **2006**, *19*, 319-329.
97. Khuu, P.; Ho, P.S., *Biochemistry* **2009**, *48*(33), 7824-7832.
98. Richards, FM., *Protein Sci.* **1992**, *1*, 1721-1730.
99. Soyfer, V.N; Potaman, V.N., *Triple-Helical Nucleic Acids* **1995**, Springer Ver., New York, p360.
100. Arnott, S.; Chandrasekaran, R.; Selsing, E., *Structure and Conformation of Nucleic Acids and Protein- Nucleic Acid Interactions* (eds Sundaralingam, M. & Rao, S.T.)**1975**, 477–603.
101. Ghosh, A., Bansal, M., *Acta Crystallogr D Biol. Crystallogr* **2003**, *59* (Pt 4), 620–626.
102. Zhang, H.; Yu, H.; Ren, J.; Qu, X., *Biophysical Journal* **2006**, *90* (9), 3203–3207.
103. Ha, S. C., Lowenhaupt, K.; Rich, A.; Kim, Y.; Kim, K. K., *Nature* **2005**, *437*, 1183-1186.
104. Voet, D.; Voet, J.G, *Biochemistry*, 3rd, **2004**, Chapter, 5, 29
105. Dickerson, et al., *Science* **1982**, *216*, 475-483.
106. Lehninger, A.; Nelson, D.; Cox, M.M., Lehninger, *Principles of Biochemistry* **2004** 4 ed., Chapter 12, Nucleic Acid Structure.
107. Saenger, W., *Principles of Nucleic Acid Structure* **1984**, Springer-Verlag, New York.
108. Wang, AHJ.; Quigley, G.J.; Kolpak, F.J.; Crawford, J.L.; van Boom, J.H.; Van der Marel, G.; Rich, A., **1979**, *Nature (London)* *282* (5740), 680–686.
109. Rich. A., *Ann. NY Acad. Sci.* **1994**, *726*, 1-17.
110. Rich, A.; Zhang S., *Nature* **2003**, *4*, 566-572.
111. Maxim, D. F-K.; Sergei, M.M., *Annu. Rev. Biochem.* **1995**, *64*, 65-95.
112. Wang, E.; Malek, S.; Feigon, J., *Biochemistry* **1992**, *31*, 4838–4846.
113. Radhakrishnan, I.; Patel, D. J., *J. Am. Chem. Soc.* **1992**, *114*(17), 6913–6915.

114. Heo, D.S., *Genetic in Medicine* **2002**, *4*, 52S-55S.
115. Romano, G.; Pacilio, C.; Giordano, A., *The Oncologist* **1998**, *3*(4), 4225-4236.
116. Campbell, N. A.; Brad, W.; Robin, J. H., *Biology: exploring Life*, **2006**, Boston, Massachusetts: Pearson Prentice Hall.
117. Liaw, J.; Chang, S-F.; Hsiao, F-C., *Gene Therapy* **2001**, *8*, 999-1004.
118. Touchefeu, Y.; Harrington, K. J.; Galmiche, J. P.; Vassaux, G., *Aliment Pharmacol Ther.* **2010**, *32*, 953-968.
119. Ledley FD., *Hum. Gene Ther.* **1995**, *6*(9), 1129-1144.
120. Morille, M.; Passirani, C.; Vonarbourg, A.; Clavreul, A.; Benoit, J-P., *Biomaterials* **2008**, *29*, 3477-3496
121. Radler, J.O.; Koltover, I.; Salditt, T.; Safinya, C.R., *Science* **1997**, *275*(5301), 810-814.
122. Editor, Segev; N., Associate Editors: Alfonso; A., Payne; G., Donaldson; J., *Trafficking Inside Cells: Pathways, Mechanisms and Regulation*, Landes Bioscience and Springer Science/Business Media, **2009** Madame Curie Bioscience Database.
123. Burgers, P. M.J, *J. of Biological Chemistry* **2008**, *284* (7), 4041-4045.
124. Das-bradoo; S., Bielinsky; A., *Nature Education* **2010**, *3*(9), 50.
125. Berg, J.M.; Tymoczko, J.L.; Stryer, L.; Clarke, N.D., *Biochemistry* **2002**. W. H. Freeman and Company. ISBN 0-7167-3051-0, Chapter 27: DNA Replication, Recombination, and Repair.
126. Kong, X-P.; Onrust, R.; O'Donnell, M.; Kuriyan, J., *Cell* **1992**, *69*,425-437.
127. (a) Alberts, B.; Johnson, A.; Lewis, J.; Raff, M.; Roberts, K.; Walter, P., *Molecular Biology of the Cell* **2002**, Garland Science. ISBN 0-8153-3218-1, Chapt 5, DNA Replication Mechanisms. (b) Buzzle.com, DNA replication steps.
128. Müller, H.J., *Collecting Net* **1938**, *13*, 181-198.
129. Phan, A.T.; Kuryavyi, V.; Luu, K. N.; Patel, D. J., *Nucleic Acids Res.* **2007**, *35*(19), 6517-6525.
130. Han, H.; Hurley, L.H., *Trends in Pharmacological Sciences* **2000**, *21*(4),136-142.
131. Bodnar, A.G.; Ouellette, M.; Frolkis, M.; Holt, S.E.; Chiu, C.P.; Morin,

- G.B.; Harley, C.B.; Shay, J.W., Lichtsteiner, S.; Wright, W.E., *Science* **1998**, *279*, 349–352.
132. Aubert, G.; Lansdorp, P. M., *Physiol Rev.* **2008**, *88* (2), 557-579.
133. Blackburn; E.H., *Nature Struct. Biol.* **2000**, *7*, 847– 850.
134. Meyne, J.; Ratliff, R.L.; Moyzis, R.K., *PNAS* **1989**, *86* (18), 7049-7053.
135. Moyzis, R.K.; Buckingham, J.M.; Cram, L.S.; Dan, M.; Deaven, L.L.; Jones, M.D.; Meyne, J.; Ratliff, R.L.; Wu, J.-R., *Proc. Natl Acad. Sci. USA* **1988**, *85*, 6622– 6626.
136. Viglasky, V.; Bauer, L.; Tluckova, K.; Javorsky, P., *J. Nuclei Acids* **2010**, *2010*, 1-8.
137. Xu, Y.; Ishizuka, T.; Kurabayashi, K.; Komiyama, M., *Angew. Chem. Int. Ed.* **2009**, *48*, 7833 –7836.
138. Allsopp, R. C.; Morin, G.B.; DePinho, R.; Harley, C.B.; Weissman, I.L., *Blood* **2003**, *102*, 517–520.
139. Grandin, N.; Charbonneau, M., *Biochimie* **2008**, *90*, 41-59.
140. Chakhparonian, M.; Wellinger, R.J., *Trends Genet.* **2003**, *19*, 439-444.
141. Smogorzewska, A.; de Lange, T., *Annu. Rev. Biochem.* **2004**, *73*, 177-208.
142. Viscardi, V.; Clerici, M.; Cartagena-Lirola, H.; Longhese, M.P., *Biochimie* **2005**, *87*, 613-624.
143. Sandell, L. L.; Zakian, V. A., *Cell* **1993**, *75*, 729–739.
144. McClintock, B., *Genetics* **1938**, *23*, 315–376.
145. McClintock, Barbara. A short biographical note: Barbara McClintock **1983**, Nobel Foundation biography.
146. Olovnikov, A.M., *J. Theor. Biol.* **1973**, *41*(1), 181-190.
147. Blackburn, E.H.; Greider, C. W.; Szostak, J.W., *The Nobel Prize in physiology or Medicine* **2009**, Nobel prize.org.
148. Counter, C. M.; Hirte, H. W.; Bacchetti, S.; Harley, C. B., *Proc. Natl. Acad. Sci. U.S.A.*, **1994**, *91*, 2900.
149. Stewart, S. A.; Bertuch, A.A., *Cancer Res.* **2010**, *70*, 7365-7371.
150. Greider, C.W.; Blackburn; E.H., *Cell* **1987**, *51*, 887-898.

151. Blasco, M.A.; *Nat Rev Genet* **2005**, *6*(8), 611-22.
152. Callaway, E., *Nature*, **2010**, doi; 10.1038/news, 2010.635.
153. Funk, W. D.; Wang, C. K., et al., *Exp Cell Res* **2000**, *258*(2), 270-278.
154. Hiyama, E.; Hiyama, K; Yokoyama, T.; Shay, J.W., *Neoplasia*. **2001**, *3*(1), 17–26.
155. Shay, J. W.; Bacchetti, S., *Eur. J. Cancer* **1997**, *33*, 787-791.
156. Akalin, A.; Elmore, L.W.; Forsythe, H.L.; Amaker, B.A.; McCollum, E.D.; Nelson, P.S.; Ware, J.L.; Holt, S.E., *Cancer Res* **2001**, *61*, 4791-4796.
157. Fenton, R. G.; Longo, D.L., *Harrison's Principles of Internal Medicine* **1998**, *69*, Cancer cell biology and Angiogenesis.
158. Willeit, P.; Willeit, J., et al., *JAMA* **2010**, *304*(1), 69-75.
159. Vogelstein, B.; Kinzler, K.W., *Trends Genet.* **1993**, *9*, 138– 141.
160. Shay, J.W.; Wright, W.E.; Werbin, H., *Biochim. Biophys. Acta* **1991**, *1072*, 1–7.
161. Hanahan, D.; Weinberg, R.A., *Cell* **2000**, *100*, 57– 70.
162. Hahn, W.C.; Counter, C.M.; Lundberg, A.S.; Beijersbergen, R.L.; Brooks, M.W.; Weinberg, R.A., *Nature* **1999**, *499*,464– 468.
163. Kim, N. W.; Piatyszek, M. A.; et al., *Science* **1994**, *266* (5193), 2011-2015.
164. Meyerson, M.; Counter, C. M.; Eaton, E. N.; Ellisen, L. W.; Steiner, P.; Caddle, S. D.; Ziaugra, L.; Beijersbergen, R. L.; Davidoff, M. J.; Liu, Q., Bacchetti, S.; Haber, D. A.; Weinberg, R. A., *Cell* **1997**, *90*, 785-795.
165. Fiedler, W.; Dahse, R.; Schlichter, A., *Int. J. Oncol.* **1996**, *9*, 1227-1232.
166. Mehle, C.; Piatyszek, M. A.; Ljungberg, B.; Shay, J. W.; Ross, G., *Oncogene* **1996**, *13*, 161-166.
167. Cong, Y.; Wright, W.E.; Shay, J.W., *Mol. Biol. Rev.* **2002**, *66*, 3408-3425.
168. Raymond, E.; Sun, D.; Chen, S.; Windle, B.; Van Hoff, D. D., *Current Opinin in Biotechnology* **1996**, *7*, 583-591.
169. Saretzki, G., *Cancer Lett.* **2003**, *194*(2), 209-219.
170. Shy, J.W.; Zou, Y.; Hiya, E.,Wright; W.E., *Hum. Mol. Genet.* **2001**, *10*(7), 677-685.

171. Norton, J.C.; Piatyszek, M.A.; Wright, W.E.; Shay, J.W.; Corey, D.R, *Nature Biotechnol.* **1996**, *14*, 615– 619.
172. de Lange, T.; Jacks, T., *Cell* **1999**, *98*, 273– 275.
173. McKenzie, K.E.; Umbricht, C.B.; Sukumar, S., *Mol. Med. Today* **1999**, *5*, 114– 122.
174. White, L.; Wright, W.E.; Shay, J.W., *Trends Biotechnol.* **2001**, *19*, 114– 120.
175. Fossel, M.B., *Cells, Aging, and Human Disease*, Oxford University Press **2004**, ISBN 0-19-514035-4.
176. Sun, D.; Thompson, B.; Cathers, B.E.; et al. *J. Med. Chem.* **1997**, *40*, 2113–2116.
177. Mergny, J.L.; Lacroix, L.; Teulade-Fichou, M-P. et al, *Proc Nat.l Acad. Sci.* **2001**, *98*, 3062–3067.
178. Read, M.A. ; Harrison, J.R.; Romagnoli, B., et al, *PNAS* **2001**, *98*, 4844–4849.
179. Gellert, M.; Li, F.; Lipsett, M. N.; Davies, D.R., *Proc. Natl. Acad. Sci. U.S.A.* **1962**, *48*, 2013-2018.
180. Sannohe, Y.; Sugiyama, H., *Current Protocols in Nucleic Acid Chemistry* **2010**, *40*,17.2.1-17.2.17, Overview of Formation of G-Quadruplex Structures.
181. Sun, D.; Guo, K.; Shin, Y-J., *Nucl. Acids Res.* **2011**, *39* (4), 1256-1265.
182. Fukita, Y.; Mizuta, T-R.; Shirozu, M.; Ozawa, K.; Shimizu, A.; Honjo, T., *J. Biological Chemistry* **1993**, *268*, 17463-17470.
183. Sinden, R.R., *Am. J. Hum. Genet.* **1999**, *64*, 346–353.
184. Burge S.; Parkinson G.N.; Hazel P.; Todd, A.K.; Neidle, S.; *Nucl. Acids Res.* **2006**,*34* (19), 5402-5415.
185. Balasubramanian, S.; Hurley, L. H.; Neidle, S., *Nat. Rev. Drug Discov.* **2011**, *10* (4), 261– 275.
186. Neidle, S.; Balasubramanian, S., *Quadruplex Nucleic Acids* **2006**, Cambridge: RSC.
187. Yang, D.; Okamoto, K., *Future Med. Chem.* **2010**, *2*(4), 619–646.
188. Huppert, J.L., *Chem. Soc. Rev.* **2008**, *37*, 1375-1384.
189. Lipps, H.J.; Rhodes, D, *Trends in Cell Biology* **2009**, *19*(8), 414-422.

190. Schaffitzel, C.; Berger, I.; Postberg, J.; Hanes, J.; Lipps, H.J.; Pluckthun, A., *Proc Natl. Acad. Sci. USA* **2001**, *98*(15), 8572–8577.
191. Yong, Q., Hurley, L. H., *Biochimie*. **2008**, *90*(8), 1149-1171.
192. Mendez, M.A.: *Development and characterization of novel nanomaterials using G- quadruplex DNA building blocks*, ISBN-10: 1244714828, 2011, Pro..Quest, UMI Dissertation Publishing
193. Kaushik, M.; Kaushik, S.; Bansal, A.; Saxena, S.; Kukreti, S., *Curr. Mol. Med.* **2011**, *11*(9), 744-769.
194. Yong, Q.; Hurley, L. H., *Biochimie*. **2008**, *90*(8), 1149-1171.
195. Rachewal, PA.; Brown, T.; Fox, KR., *Biochemistry* **2007**, *46*(11), 3036-3044.
196. Cang, X.; Šponer J.; Cheatham, T.E., *Nucleic Acids Res.* **2011**, *39*(10), 4499–4512.
197. Lee, J.Y.; Yoon, J.; Kihm, H.W.; Kim, D.S., *Biochemistry* **2008**, *47*(11), 3389-3396.
198. Sundquist, W.I; Klug, A., *Nature* **1989**, *342*(6251), 825–829.
199. Burge, S.; Parkinson, G.N.; Hazel, P.; Todd, A.K.; Neidle S, *Nucleic Acids Res.* **2006**, *34*, 5402–5415.
200. Dai, J.X.; Carver, M.; Punchihewa, C.; Jones, R.A.; Yang, D.Z., *Nucl. Acids Res.* **2007**, *35*(15), 4927–4940.
201. Gilbert, D.E.; Feigon J., *Curr. Opin. Struct. Biol.* **1999**, *9*, 305–314.
202. Lane A.N.; Chaires, J.B.; Gray, R.D.; Trent, J.O., *Nucleic Acids Res.* **2008**, *36*, 5482–5515.
203. Jing, N., Marchand, C.; Liu, J.; Mitra, R.; Hogan, M.E.; Pommier, Y., *J. Biol. Chem.* **2000**, *27*, 21460–21467.
204. Miyoshi, D.; Nakao, A.; Sugimoto, N., *Nucleic Acids Res.*, **2003**, *31*, 156–1163.
205. Hazel, P.; Huppert, J.; Balasubramanian, S.; Neidle, S., *J. Am. Chem. Soc.* **2004**, *126*, 16405–16415.
206. Simonsson, T., *Biol. Chem.* **2001**, *382*, 621-628.
207. Cang, X.; Šponer, J.; Cheatham, T. E., *J. Am. Chem. Soc.* **2011**, *133*(36), 14270–14279.
208. Parkinson, G. N.; Lee, M. P. H.; Neidle, S., *Nature*, **2002**, *417*, 6891, 876–880.

209. Wang, Y.; Patel, D.J., *J. Mol. Biol.* **1993**, *234*, 1171 – 1183.
210. Marathias, V. M.; Bolton, P. H., *Biochemistry* **1999**, *38*, 4355-4364.
211. Williamson, J. R.; Raghuraman, M.K.; Cech, T.R., *Cell* **1989**, *59*(5), 871-880.
212. Smith, F.W.; Lau, F.W.; Feigon, J., *Proc. Natl. Acad. Sci. USA* **1994**, *91*, 10546-10550, *Biochemistry*.
213. Rachwal, PA; Findlow, IS.; Werner, JM; Brown, T.; Fox, KR., *Nucl. Acids Res.* **2007**, *35*, 4214-4222.
214. Greene, K.L.; Wang, Y.; Live, D., *J. Biomol. NMR* **1995**, *5*(4), 333-338.
215. Clark, G. R. ; Pytel, P. D.; Squire, C. J., *Nucleic Acids Res.* **2012**, 1–8.
216. Marušič, M. ; Šket, P.; Bauer, L.; Viglasky, V.; Plavec, J., *Nucleic Acids Res.* **2012** *40*(14), 6946–6956.
217. Venczel, E.A.; Sen, D., *Biochemistry* **1993**, *32*, 6220-6228.
218. Bugaut, A.; Balasubramanian, S., *Biochemistry* **2008**, *47*(2), 689-97.
219. Risitano, A.; Fox, K.R., *Nucleic Acids Res.* **2004**, *32*, 2598- 2606.
220. Editor, Neidle S, Authors, Hud, N.V.; Plavec, J., The role of cations in determining quadruplex structure and stability. *Quadruplex Nucleic Acids*, Royal Society of Chemistry, Publishing, Cambridge UK, **2006**, 100–130.
221. Kang, C., Zhang, X., Ratliff, R., Moyzis, R.; Rich, A., *Nature* **1992**, *356*, 126 –131.
222. Miyoshi D; Nakao, A.; Toda, T., Sugimoto, N., *FEBS Lett.* **2001**, *496*(2-3), 128-133.
223. Chen, F.M., *Biophys. J.* **1997**, *73*, 348-356.
224. Chen, F. M., *Biochemistry* **1992**, *31*, 3769-3776.
225. Risitano, Q.; Fox, K.R., *Nucleic Acids Res.* **2004**, *32*(8), 2598-2606.
226. Ross W. S.; Hardin C. C., *J. Am. Chem. Soc.* **1994**, *116* (14), 6070–6080.
227. Rawal, P.; Kummarasetti, V.B.; Ravindran J.; Kumar, N.; Halder, K.; Sharma, R.; Mukerji, M.; Das, S.K.; Chowdhury, S., *Genome Res.* **2006**, *16*, 644–655.
228. Waller, Z.A.; Sewitz, S.A.; Hsu, S.T.; Balasubramanian, S. , *J. Am. Chem. Soc.* **2009** , *131*(35), 12628-12633.
229. Siddiqui-Jain, A.; Grand, C. L.; Bearss, D. J.; Hurley, L. H., *Proc. Natl. Acad. Sci.*

- U.S.A. **2002**, *99*, 11593–11598.
230. Rankin, S.; Reszka, A. P.; Huppert, J.; Zloh, M.; Parkinson, G. N.; Todd, A. K.; Ladame, S.; Balasubramanian, S.; Neidle, S., *J. Am. Chem. Soc.* **2005**, *127*, 10584 – 10589.
231. Maizels, N., *Nat. Struct. Mol. Biol.* **2006**, *13*, 1055–1059.
232. Phan, A. T.; Kuryavyi, V.; Burge, S.; Neidle, S.; Patel, D. J., *J. Am. Chem. Soc.* **2007**, *129*, 4386–4392.
233. Zhao, Y.; Du, Z.; Li, N., *FEBS Lett.* **2007**, *581*, 1951–1956
234. Dai, J.; Dexheimer, T. S.; Chen, D.; Carver, M.; Ambrus, A.; Jones, R. A.; Yang, D., *J. Am. Chem. Soc.* **2006**, *128*, 1096–1098.
235. Viglasky, V., *FEBS J.* **2009**, *276*, 401– 409
236. Gowan, S.M., et al. *Mol. Pharmacol.* **2002**, *61*, 1154–1156.
237. Maizels, N., *Nat. Struct. Mol. Biol.* **2006**, *13*, 1055– 1059.
238. Guo, K.; Pourpak, A.; Beetz-Rogers, K.; Gokhale, V.; Sun, D.; Hurley, L. H., *J. Am. Chem. Soc.* **2007**, *129*, 10220–10228.
239. Bates, P.; Mergny, J.L.; Yang, D., *EMBO Rep.* **2007**, *8*, 1003–1010.
240. Oganessian, L.; Bryan, T.M., *Bio. Essays* **2007**, *29*, 155–165.
241. Oganessian, L.; Moon, I.K.; Bryan, T. M.; Jarstfer, M.B., *EMBO J.* **2006**, *25*, 1148 – 1159.
242. Kumari, S.; Bugaut, A.; Huppert, J.L.; Balasubramanian, S., *Nat. Chem. Biol.* **2007**, *3*, 218–221.
243. Yang, D.Z.; Hurley, L.H., *Nucleoside Nucleotide Nucleic Acids* **2006**, *25* (8), 951–968.
244. Patel, D.J.; Phan, A.T.; Kuryavyi, V., *Nucleic Acids Res.* **2007**, *35*, 7429–7455.
245. Cogoi, S.; Xodo, L. E., *Nucleic Acids Res.* **2006**, *34*, 2536–2549.
246. Sun, D.; Hurley, L.H., *J. Med. Chem.* **2009**, *52*, 2863-2874.
246. Riou, J.F.; Guittat, L.; Mailliet, P.; Laoui, A.; Renou, E., Petitgenet, O., Megnin- Chanet, F.; Helene, C.; Mergny, J.L., *PNAS* **2002**, *99* (5), 2672-2677.

247. Yang, D.; Okamoto, K., *Future Med. Chem.* **2010**, *2*(4), 619–646.
248. Jiang, Y.L.; Liu, Z.P., *Mini Rev. Med. Chem.* **2010**, *10*(8), 726-36.
249. Ou, T.-M.; Lu, Y.-J.; Tan, J.-H.; Huang, Z.-S.; Wong, K.-Y.; Gu, L.-Q., *Chem. Med. Chem.* **2008**, *3*, 690–713.
250. Lusvardi, S.; Murphy, C.T.; Roy, S.; Tanious, F. A.; Sacui, I., *J. Am. Chem. Soc.* **2009**, *131*(51), 18425-18440.
251. Luedtke, N. W., *CHIMIA* **2009**, *63* (3), 134-139.
252. Drewe, W.C.; Nanjunda, R.; Gunaratnam, M.; Beltran, M.; Parkinson, G.N.; Reszka, A.P.; Wilson, W.D.; Neidle, S., *J. Med. Chem.* **2008**, *51*, 7751-7767.
253. Oganessian, L.; Bryan, T. M., *Bioessays* **2007**, *29*, 155-165.
254. Shi, D. F.; Wheelhouse, R. T.; Sun, D. Y.; Hurley, L. H., *J. Med. Chem.* **2001**, *44*, 4509-4523.
255. Grand, C. L.; Han, H.; Munoz, R.M.; Weitman, S.; Von Hoff, L.H.; Hurley, L.H.; Bearss, D. J., *Mol. Cancer Ther.* **2002**, *1*, 565-573.
256. Vicente, M. G., *Curr. Med. Chem.*, **2001**, *1*, 175–194
257. Ding, L.; Balzarini, D.; Schols, D.; Meunier, B.; Clercq, E. *Biochem.Pharmacol.* **1992**, *44*, 1675–1679.
258. Makundan, N.E.; Petho, G.; Dixon, D.W.; Marzilli, L.G., *Inorg. Chem.* **1995**, *34*, 3677-3687.
259. Sehlstedt, U.; Kim, S.K.; Carter, P.; Goodisman, J.; Vollano, J.F.; Norde'n, B.; Dabrowiak, J.C., *Biochemistry* **1994**, *33*, 417– 426.
260. Nagesh, N.; Sharma, V. K.; Kumara. G.; Lewis, E.A., *J. Nucleic Acids* **2012**, *2012*, 1-12.
261. Marzilli, L. G.; Banville, L. D.; Zon, G.; Wilson, W. D. *J. Am. Chem. Soc.* **1986**, *108*, 4188–4192.
262. Fiel, R.J.; Howard, J.C.; Mark, E.H.; Datta Gupta, N., *Nucleic Acids Res.* **1979**, *6*, 3093–3118.
263. Arthanari, H.; Basu, S.; Kawano, T. L. ;Bolton, P. H., *Nucleic Acids Res.* **1998**, *26*, 3724–3728.

264. Fiel, R. J., *J. Biomol. Struct. Dyn.* **1989**, *6*, 1259–1275.
265. Gibbs, E. J.; Tinoco, I. Jr.; Maestre, M. F.; Ellinas, P. A.; Pasternack, R. F., *Biochem. Biophys. Res. Commun.* **1988**, *157*, 350–358.
266. Guliaev, A. B.; Leontis, N. B., *Biochemistry* **1999**, *38*, 15425–15437.
267. Lee, Y.-A.; Lee, S.; Cho, T.-S.; Kim, C.; Han, S. W.; Kim, S. K., *J. Phys. Chem. B.* **2002**, *106*, 11351–11355.
268. Strickland, J. A.; Marzilli, L. G.; Wilson, W. D., *Biopolymers* **1990**, *29*, 1307–1323.
269. Kuroda, R.; Tanaka, H., *J. Chem. Soc. Chem. Commun.* **1994**, *157*, 5–1576.
270. Schneider, H.-J.; Wang, M., *J. Org. Chem.* **1994**, *59*, 7473–7478.
271. Sehlstedt, U.; Kim, S. K.; Carter, P.; Goodisman, J.; Vollano, J. F.; Norde'n, B.; Dabrowiak, J. C., *Biochemistry* **1994**, *33*, 417–426.
272. Pasternack, R. F.; Goldsmith, J. I.; Gibbs, E., J., *Biophys. J.* **1998**, *75*, 1024–1031.
273. Yun, B. H.; Jeon, S. H.; Cho, T.-S.; Yi, S. Y.; Sehlstedt, U.; Kim, S. K., *Biophys. Chem.* **1998**, *70*, 1–10.
274. Lee, S.; Jeon, S. H.; Kim, B.-J.; Han, S. W.; Jang, H. G.; Kim, S. K., *Biophys. Chem.* **2001**, *92*, 35–45.
275. Park, T.; Kim, J. M.; Han, S. W.; Lee, D.-J.; Kim, S. K., *Biochim. Biophys. Acta* **2005**, *1726*, 287–292.
276. Jin, B.; Lee, H. M.; Lee, Y.-A.; Ko, J. H.; Kim, C. Kim, S. K., *J. Am. Chem. Soc.* **2005**, *127*, 2417–2424.
277. Carvlin, M. J.; Datta-Gupta, N.; Fiel, R., *J. Biochem. Biophys. Res. Commun.* **1982**, *108*, 66–73.
278. Carvlin, M. J.; Fiel, R. J., *Nucleic Acids Res.* **1983**, *11*, 6121–6139.
279. Banville, D. L.; Marzilli, J. A.; Strickland, J. A.; Wilson, W. D., *Biopolymers* **1986**, *25*, 1837–1858.
280. Yamashita, T.; Uno, T.; Ishikawa, Y., *Bioorganic & Medicinal Chemistry* **2005**, *13*, 2423–2430.
281. Han, H.; Langley, D.R.; Rangan, A.; Hurley, L. H., *J. Am. Chem. Soc.* **2001**, *123*, 8902–8913

282. Dixon, IM. ; Lopez, F.; Estève, J.P., Tejera, AM.; Blasco, MA; Pratiel, G; Meunier, B., *Chem.biochem.* **2005**, 6(1), 123-132.
283. Yang, D.; Okamoto, K., *Future Med Chem.* **2010**, 2(4), 619–646.
284. Lee, Y.-A.; Kim, J.-O.; Cho, T.-S.; Song, R.; Kim, S. K. *J. Am. Chem. Soc.* **2003**, 125, 8106–8107.
285. Granville, D. J.; McManus, B. M.; Hunt, D. W. *Histol. Histopathol.* **2001**, 16, 309–317.
286. Dalla, V. L; Marciani, M. S., *Curr. Med.Chem.* **2001**, 8(12), 1405-1418.
287. Earnshaw, J.C.; Steer, M.W., *The application of Laser Light Scattering to the Study Of Biological Motion* **1982**, Plenum Press, New York and London.
288. Kerker, M., *The scattering of light and other electromagnetic radiation.* Academic, New York, **1969**.
289. van de Hulst, H.C., *Light scattering by small particles.* John Wiley & Sons, New York, **1957**. (Paperback by Dover Publications, New York, **1981**)
290. Bohren, C.F.; Huffman, D. R., *Absorption and scattering of light by small particles.* John Wiley & Sons, New York, **1983**. (Paperback by Wiley Science Paperback Series, **1998**)
291. Berne, B. J.; Pecora, R, *Dnamic Light Scattering: With Applications to Chemistry, Biology, and Physics.* **1975**, Dover Publications, Inc., Mineola. New York.
292. Kerker, M., *Scattering of Light & Other Electromagnetic Radiation* **1969**, Academic Press Inc.
293. Wyatt Technology, <http://www.wyatt.com>.
294. Edited by Gorenstein, D.G., *Phosphorus-31 NMR Principles and Application* **1984**. Academic Press Inc.
295. Gorenstein, D.G., *Annu. Rev. Biophys. Bioehg.* **1981**, 10, 355-386.
296. Canet, D. and D'ecorps, M., *Applications of Field Gradients in NMR in Dynamics of Solutions and Fluid Mixtures*, Editor, Delpuech, J-J., Wiley, New York, **1995**, 309-343.
297. Packer, K. J., *Diffusion & Flow in Liquids* in *Encyclopedia of Nuclear Magnetic Resonance*. Editor: Grant, D. M.; Harris ,R. K., Wiley, New York, **1996**,

1615-1626.

298. Price, W. S., *Gradient NMR*, in Annual Reports on NMR Spectroscopy. Editor: Webb, G.A. Academic Press, London, **1996**, 51-142.
299. Karger, J.; Ruthven, D. M., *Diffusion in Zeolites and Other Microporous Solids*, Wiley, New York, **1992**.
300. Nose, T., *Annu. Rep. NMR Spectrosc.* **1993**, *27*, 218 – 253.
301. Price, W. S., *Concepts Magn. Reson.* **1997**, *9*, 299 – 336
302. Editor: Young, I. R., *Methods of Magnetic Resonance Imaging and Spectroscopy*. Wiley, Chichester, **2000**.
303. (a) Basser, P. J., *NMR Biomed.* **1995**, *8*, 333–344. (b) Basser, P. J.; Mattiello, J.; Bihan, D. L., *Biophys. J.* **1994**, *66*, 259 – 267.
304. Brand, T.; Cabrita, E. J.; Berge, S., *Progress in nuclear magnetic.* **2005**, *46(4)*, 159-196.
305. Johnson, C. S. Jr., *Diffusion Measurements by Magnetic Field Gradient Methods*, in Encyclopedia of Nuclear Magnetic Resonance. Editor: Grant, D. M. Harris, R. K., Wiley, New York, **1996**, 1626-1644.
306. Hawlicka, E., *Chem. Soc. Rev.* **1995**, *34*, 13743-13750.
307. Hunter, R. J., *Foundations of Colloid Science*, Oxford University Press, Oxford, **1986**.
308. Ernst, R.R.; Bodenhausen, B.; Wokaun, A., *Principles of Nuclear Magnetic Resonances in One or Two Dimensions* **1992**, Oxford University Press.
309. Jones, J. A.; Wilkins, D. K. ; Smith, L. J.; Dobson, C. M. ; *J. Biomol. NMR* **1997**, *10*, 199 – 203.
310. Crank, J., *The Mathematics of Diffusion*, 2nd ed., Clarendon Press, Oxford, **1975**.
311. Cohen, Y.; Avram, L.; Frish, L., *Angew. Chem. Int. Ed.* **2005**, *44*, 520 – 554.
312. De Graaf, R.A., *In vivo NMR spectroscopy: principles and techniques*. John Wiley & Sons Ltd, **2007**.
313. Price, W.S., *Concepts Magn. Reson.* **1997**, *9*, 299-336.
314. Keeler, J., *Understanding NMR Spectroscopy* **2010** (2nd ed.). Wiley ISBN978-0-470-74608-0.

315. Mumenthaler, C.; Braun, W., *J. Mol. Biol.* **1995**, *254*, 465–480.
316. Sherman, R.E., *Analytical Instrumentation 1996*, Cp 31, ISA, ISBN 978-1-55617-581-7, 566-592.
317. Sreerama, N.; Woody, R. W., *Meth. Enzymol.* **2004**, *383*, 318–351.
318. Alder, A.J.; Greenfield, N.J.; Fasman, G.D., *Meth. Enzymology* **1973**, *27* (675), Circular Dichroism and Optical Rotary Dispersion of Proteins and Polypeptides.
319. Woody, R.W.; Berova, N.; Nakanishi, K. (editors), *Circular dichroism and the conformational analysis of Biomolecules*, 2nd, **2000**, Wiley-VCH.
320. Wyatt Technology <http://www.wyatt.com>
321. Wu, et. al. *J. Magn. Reson.* **1995**, *A 115*, 260-264.
322. Utsuno, K.; Uludag, H, *Biophys. J.* **2010**, *99*(1), 201–207.
323. Dai, Z.; Wu, C., *Macromolecules* **2012**, *45* (10), 4346-4353
324. Mady, M.M.; Mohammed, W. A.; El-Guendy, N. M.; Elsayed, A. A., *Romanian J. Biophys.* **2011**, *21* (2), 151–165.
325. Lugo-Ponce, P.; McMillin, D. R., *Coordination Chemistry Reviews* **2000**, *208*, 169–191.
326. Saha, K; Agasti, S.S.; Kim, C.; Li, X.; Rotello, V. M., *Chem. Rev.* **2012**, *112*(5), 2739- 2779.
327. Kypr, J.; Kejnovská, I.; Renčičuk, D.; Vorlíčková, M., *Nucleic Acids Res.* **2009**, *37*(6), 1713–1725.
328. Ambrus, A.; Chen, D.; Dai, J.; Bialis, T.; Jones, R. A.; Yang, D., *Nucleic Acids Res.* **2006***34*(9), 2723-2735.
329. Dai, J.; Carver, M.; Yang, D., *Biochimie.* **2008**, *90*(8), 1172-1183.
330. Smargiasso, N.; Rosu, F., et al, *JACS.* **2008**, *130* (31), 10208–10216.
331. Miyoshi, D.; Nakao, A.; Sugimoto, N., *Nucl. Acids Res.* **2003**, *31*(4), 1156-1163.